Evidence of Late Pleistocene and Holocene Centennial-Scale Drought from Southeastern Massachusetts

By Paige E. Newby

B.A., Brown University, 1982

A.M., Brown University, 2006

A Dissertation Submitted in partial Fulfillment of the

Requirements for the Degree of Doctor of Philosophy

in the Department of Geological Sciences at Brown University

Providence, Rhode Island

May 2010

This dissertation by Paige E. Newby is accepted in its present form

by the Department of Geological Sciences as satisfying the

dissertation requirement for the Doctorate of Philisophy.

Date______________________ ____________________________

Jeffrey Donnelly, Advisor

Recommended to the Graduate School

Date______________________ _____________________________

Timothy Herbert, Reader

Date______________________ _____________________________

Jan Tullis, Reader

Date______________________ _____________________________

James Russell, Reader

Date______________________ _____________________________

Douglas Anderson, Reader

Approved by the Graduate Council

Date______________________ ______________________________

Sheila Bonde, Dean of the Graduate School

CURRICULUM VITAE

1. Name: Paige Elizabeth Newby (Henderson)

   Position: Degree Candidate, PhD.

   Academic Department: Geological Sciences

   Date and Place of Birth: April 17, 1951, Washington D.C.

   Research Expertise: Palynology, Paleoenvironmental Reconstruction

   Marital Status: Married with 6 children, ages 25-36

2. A. Work Address: Department of Geological Sciences

   Brown University, Providence, RI 02912-1846

   Fax: 401-863-2058

   e-mail: Paige_Newby@brown.edu

   B. Home Address: 16 Montague Street, Providence RI 02906

   Telephone: (h) 401-831-0265

   (c) 401-575-3039

3. Education:

   A. B.A. (Honors) Brown University (Anthropology), 1982

   M.A., Brown University, (Environmental Studies), 1992

   PhD., Brown University, (Geology), 2010

4. Work Experience

   2003- Degree Candidate, PhD. Geological Sciences, Brown University

1997- Research Associate, Robert S. Peabody Museum of Archaeology

1992- Senior Research Assistant, Department of Geological Sciences, Brown University, Providence, RI.

1988-1991 Center for Environmental Studies M.A. Program, Brown University, Providence, RI.

1988-1984 Research Assistant, Department of Geological Sciences, Brown University, Providence, RI.

1984 Consultant, Paleobotanical identification and analysis, Rte 4 Project, Rhode Island College, Providence, RI.

1983 Project Archaeologist, Historical Archeology in a Natural Laboratory, Linking the Present to the Past. Parker Woodland, Rhode Island. Grant Support from RI Committee for the Humanities, Brown University, Providence, RI.

1983 Research Assistant, laboratory for Circumpolar Studies, Haffenreffer Museum Bristol, RI. (Undergraduate thesis).

1983 Field Archaeologist, Grant Support from National Science Foundation, Tukuto Lake Site, National Petroleum Reserve, Alaska.

PUBLICATIONS

(in review) Repeated Century-Scale Droughts over the past 13,000 years near the Hudson River watershed, U.S.A. Quaternary Research.

2010 Younger Dryas in the New England-Maritimes. Invited Paper: “Human Respones to the Younger Dryas in the Northern Hemisphere: the New World.” Society for American Archaeology Meetings-April.

2009 Abrupt Climate Change as an Important Agent of Ecological Change in the Northeast U.S. throughout the past 15,000 years. Quaternary Science Reviews.

2009 Evidence of centennial-scale drought from southeastern Massachusetts during the Pleistocene/Holocene transition. Quaternary Science Reviews.

2008 Paleoindians and the Younger Dryas: Changing Landscapes within New England and Maritime Canada. Invited Paper: "Hunter-Gatherer Transitions Through the Younger Dryas: A Global Perspective." Society for American Archaeology Meetings-March.

Post-Glacial Landscape Changes and Paleoamericans in the New England Maritimes Region. Current Research in the Pleistocene.

2007 Early Holocene Landscape Variability in southern New England. Geological Society of America Abstract—March.

2006 Vegetation and water level changes for the Northeast during the 8.2 event. American Geophysical Union Abstract.

2006 Compound-specific isotopic analyses track changes in seasonal precipitation regimes in the Northeastern United States at ca 8200 cal yr BP Quaternary Science Reviews.

2006 Vegetation and water level changes for the northeast during the 8.2 ka event. Association of American Geographers Abstract.

2005 Paleoindian Response to Younger Dryas Climate Change. Quaternary Science Reviews.

2004 Evidence for the Close Climatic control of New England Vegetation History. Ecology.

2002 Parallel climate and vegetation responses to the Early-Holocene collapse of the Laurentide ice sheet. Quaternary Science Reviews.

2002 La sequence et l'adaptation paleoindiennes en Nouvelle-Angleterre et dans les Maritimes. Recherches Amerindiennes au Quebec.

2002 Late-Quaternary Climate History of Western New York State. Bulletin of the Buffalo Society of Natural Sciences, V.37.

2001 700 yr Sedimentary Record of Intense Hurricane Landfalls in Southern New England. GSA Bulletin.

2001 Late-Quaternary Water-Level Variations and Vegetation History at Crooked Pond, Southeastern Massachusetts. Quaternary Research.

2000 Late Quaternary Biomes of Canada and the Eastern US. Journal of Biogeography.

2000 14,000 Years of Sediment, Vegetation and Water Level Changes at the Makepeace Cedar Swamp, Southeastern Massachusetts. Quaternary Research.

1997-1998 Guest Curator, ORIGINS AND ANCESTORS: Investigating New England's Paleo Indians, Peabody Museum at Andover, MA.

1995 Holocene Water-Level Fluctuations in Southeastern New England. GSA Abstract.

1994 11,500 Years of Sediment, Vegetation and Water Level Changes at Makepeace Cedar Swamp, Southeastern Massachusetts. AMQUA Abstract.

1994 Radiocarbon-Dated Pollen and Sediment Records from near the Boylston Street Fishweir Site in Boston, Massachusetts. Quaternary Research.

1994 Pollen and Sediment Records from Walter's Puddle in Central Delaware,in Paleoenvironmental Studies of the Sate Route 1 Corridor: Contexts for Prehistoric Settlement , New Castle and Kent Counties, Delaware. Delaware DOT Archaeology Series No. 114.

1989 Manual for Waste Reduction Planning and Reporting. State of Rhode Island.

1986 Data Recovery, Subsistence, and Contact Period Documentation, Vol. III. Occasional papers in Archaeology, No. 1A. Rhode Island College, Providence, RI.

Dedicated to those still with me

and to those

I lost along the way

TABLE OF CONTENTS

ACKNOWLEDGEMENTS

No one completes a lifelong ambition at age fifty-nine without a long roster of loved ones and friends who deserve thanks. There would be no dissertation without the steadfast support of Jeff Donnelly and my others committee members, Jan Tullis, Doug Anderson, Tim Herbert and Jim Russell. My husband, Vern Henderson, also shines brightly in this process and in my life; such love and full-time support is immeasurable. My grown children, Jessica, Gabriel, Sonam, Alex, Anna and Hope, their two weddings; Anna with Dan, Sandy with Juanita, and two grandchildren, Eden and Walter, also added joy and celebration along the way. My sister, Dr. Rebecca Turner, never failed to offer just the right words, even during her most busy times, and sister Tracie has always been a source of inspiration to me. Thompson Webb III started me on this path many years ago, and ultimately pushed me through the doctorate door. My friends and colleagues from Wyoming, Bryan Shuman and Steve Jackson, and from archaeology, James Bradley and Arthur Spiess, provided support and interesting discourse. Simon, Gabe and Alex kept me afloat. April Martin, William Collins, Phil Leduc and Lynn Carlson did so much, for so long.

I hope that my parents, Robert and Betty Carlin, and in-laws, Donald and Jean Newby and May Henderson are where they know of this milestone. Fannie Goldberg was also a dear friend.

I thank my girlfriends, Audie, Julia and Mary, who gave so much more than lunchtime conversation since 1985. Now onto new projects!

CHAPTER ONE

INTRODUCTION

PAIGE E. NEWBY

BROWN UNIVERSITY, Department of Geological Sciences

On July 2, 1985, a Brown Pollen Laboratory crew and I paddled out onto Houghtons Pond (on the stretch of Route 128, after the end of I-95 and before Braintree), and retrieved ca. 7 m of clay-rich organic lake mud that contained some peat accumulation about 16.5 meters below the modern lake surface. Peat forms at or near the surface, not beneath 9.5 m of water. Disquieted by this intrusion into our quest for "pure" lake mud, we shifted locations after collecting a complete core, and recovered the same sequence. The idea that this enormous deep lake near Boston once may have resembled a large puddle was mesmerizing; different past environments were about ice-sheets and spruce trees, not water. Thus began a long-term pursuit to determine how past changes in moisture have influenced landscapes and human resource procurement in New England, and how they have altered forest composition in concert with changes in temperature at regional and local scales. In the 1980's, it was not clear that lake-level records were obtainable from lakes within temperate regions such as New England, as most lake-level work was done in regions such as (the presently dry) sub-Saharan Africa, where evidence of former high water levels is preserved in above-ground strandlines. Years later, I can place the Houghtons Pond low water level coincident with dry conditions during the earliest Holocene, after 11,600 years ago, at the end of the Younger Dryas Oscillation, during the dramatic change from primarily spruce to white pine trees across the region. Furthermore, the role of moisture remains central to regional prehistory. After the "8.2" event in the North Atlantic region, the subsequent rise in water levels may have prompted human settlements along major waterways and lakes, for resources such as anadromous fish. When humans first arrived in New England around the onset of the Younger Dryas, cool conditions promoted more open landscapes in northern New England and the Canadian Maritimes. New evidence from this work indicates that the Younger Dryas Oscillation was not uniformly wet, and that drier conditions may have also played a role in shifting resources during this 1300 year event. Moisture is critical: humans adapt to changes in temperature, but humans perish or move once an adequate water supply is no longer available. Sometimes they start wars.

In 1985, I contemplated how changing moisture regimes might shift resources for prehistoric populations, or perhaps the populations themselves. Now in 2010, with IPCC (2007) forecasts of changes in total precipitation, intensity, floods, droughts and storminess, I have new motivation for this work. Information about past lake levels provides valuable paleoclimatic data. Lakes respond relatively directly to changes in moisture balance, and high-resolution, regional scale records such as those contained in this work are important for evaluating simulations of past climate.

For New England, temperature-related changes have already been noted. Decreased snow to precipitation ratios (AD 1948-2000), a nine day advancement for the spring ice-out (AD 1850-2000), and earlier flowering dates (AD 1960-2000) are all consistent with warming trends over the last century in observational data and in projections by Atmosphere Ocean General Circulation Models (Hayhoe et al., 2007).

Water resources are also vulnerable to societal needs. Model simulations under warmer-than-present temperatures project more frequent short-term droughts. Unlike the western

United States, New England is sensitive to subtle shifts in the seasonal distribution of precipitation. Chapter 3 shows changes to the local hydrology in the Plymouth-Carver aquifer during the AD 1960s drought, when two years with little to no recharge (AD 1964-1966) lowered groundwater 1.5-3.0 m and stream discharge by 50% (Hansen and Lapham, 1992). Even short-term dry conditions cause disruptions to growing season, biota dependant on annual cycles and other aspects of growth and reproductive cycles.

This work is also motivated by the increased development in and around the Plymouth-Carver aquifer that I have witnessed over the past years. The on-going struggle to maintain water supply and other natural resources is usefully informed by the record of the magnitude and longevity of past lake-level changes. This aquifer is the second largest sole source aquifer (principle supply of drinking water) in Massachusetts. Ironically, the coarse-grained, highly permeable sediments that so greatly enhance the lake-level records in this work also endanger the aquifer because these same surficial sediments enable widespread infiltration of contaminants. Since AD 1971, 40% of agricultural land in southeastern New England has been changed to housing and commercial use, including large tracts of land from the cranberry growing A.D. Makepeace Company. Coupled with a 60% increase in residential, industrial, and commercial properties, the stakes are high to maintain aquifers from saline intrusion, contamination from failing individual sewage disposal systems, and other population-related issues.

Four of the sites in this study, New Long Pond, Rocky Pond, Flax Pond and Round Pond, are from the large, glacial-origin aquifers in southeastern Massachusetts, now imperiled by over-development. Stretching back further in time, records of past changes in moisture conditions across New England show highly different hydroclimate over the last 15,000 years. Reconstructed from sediment cores collected from lakes, these records show broad, millennial-scale patterns of lower-than-modern water levels from 11.0-8.0 ka, moderate levels from 8.0-5 ka and higher-than-modern levels after ca. 3.0 ka (Winkler, 1985; Webb, 1990; Webb et al., 1993; Lavoie and Richard, 2000; Newby et al., 2000; Almquist et al., 2001; Shuman et al., 2001, 2002,2005; Muller et al., 2003; Dieffenbacher-Krall and Nurse, 2005; Shuman and Donnelly, 2006; Newby et al., 2009).

The questions posed by this research begin with reconstructing records of past changes in water level from lake sediments buried beneath the high water levels that presently characterize southern New England. In this work, new techniques are used to refine the records to show highly resolved (centennial-scale) changes in moisture balance from 15.0 ka to present and address the following fundamental questions: What do high-resolution records of changes in lake levels reveal about the natural variability of hydroclimate over the last 15,000 years? Can we attribute any past climatic forcings or feedback mechanisms to these moisture changes? Finally, in anticipation of anthropogenic climate change, can these potential connections between past climate and moisture balance inform us about the future?

Lake Level Reconstructions and Ground Penetrating Radar

The general approach by Digerfeldt (1986) was utilized to reconstruct past lake level fluctuations, in which changes in sediment facies are correlated among multiple cores collected along a transect from the shore toward the center of the lake. Within closed basins such as those in this research, the distribution of sediment at the sediment/water interface is responsive to changes in water level as there is little to no disturbance from stream or river flow. It follows that the distributions of similar sediments across the basin represent changes in the location of sediment facies related to changes in water level.

This multi-core method is greatly enhanced when integrated with two imaging technologies, ground penetrating radar and X-ray fluorescence scanning. Ground penetrating radar records a graphic profile of changes in subsurface facies that reveal the history of sediment accumulation within lakes. Cores are collected in strategic places to optimize sampling of subsurface changes captured in the ground penetrating radar profiles by changes in reflectors.

The images collected from the lakes and the radiographs also enable the correlation of disconformities or changes in facies among cores collected along a transect from the shore toward the center of the lake. Contiguous (one cm^3) grain-size analyses from the sediment cores show changes in the abundance of different fractions within the sediments. An age-model has been added using radiocarbon dates, collected from strategic positions above and below sandy deposits within the cores. Dates which bracket (e.g. dates from above and below sand layers) constrain and track the timing of sand layers deposited within a lake. Together, these techniques and analyses greatly improve the ability to identify changes in water levels over time within a basin, and as shown in this work, provide a powerful methodology for regional correlation with other lakes.

Dissertation Outline

The research in this dissertation reconstructs high-resolution records of past changes in water levels from three ponds in Massachusetts. The water level records between 15.0 and 7.0 ka from Rocky Pond and New Long Pond, in southeastern Massachusetts, are compared with the timing of abrupt climate oscillations in the North Atlantic region during deglaciation, often attributed to meltwater discharges and re-routing events, and possibly linked with meridional overturning circulation. Similarities in the sedimentary records from multiple lakes in southern New England are then examined to determine if they represent regionally coherent changes in hydroclimate during the Holocene (8.0-present). Lastly, the timing of multiple droughts in the water level records between 8.0 and present from New Long Pond (southeastern Massachusetts) and Davis Pond in western Massachusetts are compared with proxy data from the North Atlantic region to identify possible relationships with forcing mechanisms.

Chapter two documents previously unrecognized sub-centennial-to-millennial scale lake-level fluctuations from New Long Pond and Rocky Pond in southeastern Massachusetts from 15.0-7.0 ka. Superimposed on long-term changes in water levels, these century-scale droughts are often concomitant with abrupt climate oscillations recorded in ice core data, and are associated with freshwater influx and subsequent reductions in meridional overturning circulation in the North Altlantic region. A concomittant rise in the abundance of percent siliciclastic material in the sediments from New Long Pond during the AD 1960’s drought in the Northeast correlates with the timing of low sea surface temperatures off the eastern seaboard, and may represent a modern analog for the late-Pleistocene/Early Holocene correspondence between cool North Atlantic conditions and increases in percent siliciclastic material.

Chapter three reports on the lake-level record from Davis Pond, in western Massachusetts. Prior to this work, no similar long-term moisture records were available from basins in western Massachusetts, and the record from Davis Pond also provides a contrast to the hydroclimatic records reconstructed from the lakes in southeastern Massachusetts. In addition, the Davis Pond record provides information about pre-historic droughts from a region that presently supplies water to the heavily-populated area in and around New York City. From a transect containing six cores, evidence is presented for eleven lowstand, paleoshoreline deposits from 13.4-0.6 ka, many of which contain indications of short-term individual event layers. The main conclusion from this chapter is that sub-centennial-to-millennial scale lake-level fluctuations similar to those recorded in New Long Pond are also recorded at Davis Pond, and other sites with high resolution in southern Canada and New Jersey. In particular, a pattern of possible changes in the frequency of sub-millennial scale hydrologic change over the past 8000 years appears consistent among these lakes.

Chapter four focuses on the Holocene-age interval in two separate analyses. First, individual cores from New Long Pond and Davis Pond, and ground penetrating radar data from these and two additional lakes, are used to examine evidence for synchronous hydroclimatic change across southern New England. Establishing a regionally coherent pattern of synchronous changes in water levels among lakes is the cornerstone for inferring underlying climatic processes. In particular, the Holocene-age hydroclimatic records from Davis Pond and New Long Pond both show an increase in the frequency of drought between ca. 6.0 and 2.0 ka. If this pattern is regionally robust, regionally drier-than-modern conditions may have prevailed during the mid-Holocene in southern New England. Furthermore, changes in hydroclimatic may also be examined for the intervals corresponding to the Medieval Climate Anomaly and Little Ice Age. Regionally focused work in the drought-prone American Southwest has revealed prolonged aridity coincident with the Medieval Warm Period, which was accompanied by climate variability similar to that of today. Few detailed moisture histories exist for New England for the last 2000 years, however, as it is generally supposed that New England has always had an abundant water supply.

In the second analysis, I relate broad-scale changes in the North Atlantic region to the timing for individual and collective trends among droughts during the Holocene. Here, proxies associated with past atmospheric circulation and ocean temperatures/states are explored as potential forcing mechanisms for variations in New England hydroclimate history. Other mechanisms also may force droughts, including changes in seasonal insolation, and perhaps as early as 6.0 ka, changes in sea-surface temperatures in the Pacific Ocean region. The influence of mid-continent aridity on southern New England during the mid-Holocene may also have played a role. Our records also indicate drought conditions during the Roman Warm Period and Medieval Climate Anomaly, and may be related to warm temperatures. The transition to the Little Ice Age shows a change to wet condition until the early 20^{th} century.

References

Almquist, H., Dieffenbacher-Krall, A.C., Brown, R., Sanger, D., 2001. An 8000-yr holocene record of lake-levels at Mansell Pond, Central Maine, USA. The Holocene 11, 189–201.

Dieffenbacher-Krall, A.C., Nurse, A.M., 2005. Late-glacial and Holocene record of lake levels of Mathews Pond and Whitehead Lake, northern Maine. Journal of Paleolimnology 34, 283–310.

Digerfeldt, G., 1986. Studies on past lake-level fluctuations. In: Berglund, B.E., (Ed.), Handbook of Holocene palaeoecology and palaeohydrology. John Wiley and Sons, Chichester, UK, pp. 127–142.

Hansen, B.P., Lapham, W.W., 1992. Geohydrology and Simulated Groundwater Flow, Plymouth–Carver aquifer, Southeastern Massachusetts. United States Geological Survey Water Resources Investigation Report 90– 4204, Marlborough, Massachusetts.

Hayhoe, K., Wake, C.P., Huntington, T.G., Luo, L., Schwartz, M.D., Sheffield, J., Wood, E., Anderson, B., Bradbury, J., DeGaetano, A., Troy, T.J., Wolfe, D., 2007. Past and future changes in climate and hydrological indicators in the US Northeast. Climate Dynamics 28, 381-407.

IPCC, 2007. Climate Change 2007: Synthesis Report. Contribution of Working Groups I, II and III to the Fourth Assessment Report of the Intergovernmental Panel on Climate Change, Core Writing Team, Pachauri, R.K and Reisinger, A., (Eds.), IPCC, Geneva, Switzerland.

Lavoie, M., Richard, P.J.H., 2000. Postglacial water-level changes of a small lake in southern Quebec, Canada. The Holocene 10, 621– 634.

Muller, S.D., Richard, P.J.H., Guiot, J., de Beaulieu, J.-L., Fortin, D., 2003. Post-glacial climate in the Saint Laurence lowlands, southern Quebec: pollen and lake-level evidence. Palaeogeography, Palaeoclimatology, Palaeoecology 193, 51–72.

Newby, P., Killoran, P., Waldorf, M., Shuman, B., Webb III, T., Webb, R., 2000. 14,000 years of sediment, vegetation and water level changes at the Makepeace Cedar Swamp, southeastern Massachusetts. Quaternary Research 53, 352–368.

Newby, P.E., Donnelly, J.P., Shuman, B.N., and MacDonald, D., 2009. Evidence of centennial-scale drought from southeastern Massachusetts during the Pleistocene/Holocene transition. Quaternary Science Reviews 28**,** 1675-1692.

Shuman, B., Bartlein, P., Logar, N., Newby, P., Webb III, T., 2002. Parallel Climate and Vegetation Responses to the Early-Holocene Collapse of the Laurentide Ice-Sheet. Quaternary Science Reviews 21, 1793–1805.

Shuman, B., Bravo, J., Kaye, J., Lynch, J.A., Newby, P., Webb III, T., 2001. Late-Quaternary Water-Level Variations and Vegetation History at Crooked Pond, Southeastern Massachusetts. Quaternary Research 56, 401–410.

Shuman, B., Donnelly, J.D., 2006. The influence of seasonal precipitation and temperature regimes on lake levels in the northeastern United States during the Holocene. Quaternary Research 65, 44–56.

Shuman, B., Newby, P., Donnelly, J., Tarbox, A., Webb III, T., 2005. A record of late-Quaternary moisture-balance change and vegetation response in the White Mountains, New Hampshire. Annals of the American Association of Geographers 95, 237– 248.

Webb, R. S., 1990. Late-Quaternary Lake-Level Changes in the Northeastern United States. Ph.D. Thesis, Brown University, Providence, RI.

Webb, R.S., Anderson, K.H., Webb III, T., 1993. Pollen response-surface estimates of late-Quaternary changes in the moisture balance of the northeastern United States. Quaternary Research 40, 213–227.

Winkler, M.G., 1985. A 12,000-year history of vegetation and climate for Cape Cod, Massachusetts. Quaternary Research 23, 235–250.

CHAPTER TWO

EVIDENCE OF CENTENNIAL-SCALE DROUGHT FROM SOUTHEASTERN MASSACHUSETTS DURING THE PLEISTOCENE/HOLOCENE TRANSITION

PAIGE E. NEWBY[a]

JEFFREY P. DONNELLY[b]

BRYAN N. SHUMAN[c]

DANA MACDONALD[a]

[a] **BROWN UNIVERSITY,** *Department of Geological Sciences*

[b] **WOODS HOLE OCEANOGRAPHIC INSTITUTE,**

Department of Geology and Geophysics

[c] **UNIVERSITY OF WYOMING,** *Department of Geology and Geophysics*

Published in:

Quaternary Science Reviews, 28: 1675-1692

Abstract

A principle method for studying past hydroclimatic change is the reconstruction of paleo-lake levels. Here, we provide high-resolution lake-level records from New Long Pond and Rocky Pond in southeastern Massachusetts, which each contain evidence for multiple, sub-centennial-to-millennial scale low stands during the transition between the late-Pleistocene (15.0 ka) and middle Holocene (ca. 7.0 ka). Data from New Long Pond also demonstrate sedimentary evidence for a drop in water levels in the early to mid AD 20th century, when long-term trends in instrumental data show lower-than-average precipitation in the northeastern United States. Local data show the most precipitous declines in precipitation and groundwater levels are concurrent with the most severe drought in the AD 1960s, which occurred during a period of low sea-surface temperatures in the western North Atlantic. Ground penetrating radar and sediment core data indicate five intervals with numerous paleo-shoreline deposits between ca. 15.0 and 7.0 ka, similar to the layer deposited in the AD 1960s. Many of the intervals of low lake levels coincide with proposed meltwater release events or abrupt climate oscillations in the circum North Atlantic. For example, we document at least three low stands during the Younger Dryas (12.9-11.6 ka) and in association with the "9.2" and "8.2" ka events. The combined evidence of, 1) concurrent paleo-droughts in southeastern New England with documented North Atlantic abrupt cooling events, and 2) recent drought with the modern association of low sea-surface temperatures, indicates that freshening and cooling of the western North Atlantic is a viable mechanism for decreasing moisture within the region. Large-scale changes in seasonality and ice sheet extent also may have increased the

susceptibility of the northeast to dry conditions triggered by changes in the North Atlantic.

1. Introduction

Understanding the hydroclimatic response to abrupt temperature oscillations in the North Atlantic region during deglaciation can provide important clues regarding the character of centennial-to-millennial climate variations and future climate responses to similar forcing. High-resolution paleohydrologic records are needed, however, to distinguish the hydroclimatic impacts of monotonic changes in climatic boundary conditions (e.g., insolation, ice-sheet volume, atmospheric CO_2) from those of sub-centennial-to-millennial-scale temperature oscillations, such as the ones occurring in the circum North Atlantic region at the Pleistocene/Holocene transition. These abrupt cooling events, such as the Intra-Alleröd Cold Period (IACP), Younger Dryas Chronozone (YD), Preboreal Oscillation (PBO), and the "9.2 ka" and the "8.2 ka" events, have often been attributed to meltwater discharges or rerouting events (Barber et al., 1999; Clark et al., 2001; Teller et al., 2002; Donnelly et al., 2005; Alley, 2007; Fleitmann et al., 2008), which may be linked with changes in meridional overturning circulation (Broecker et al., 1989; Clark et al., 2002; McManus et al., 2004; Broecker, 2006; Alley, 2007).

These abrupt climate oscillations may have also affected the hydroclimates of regions near the North Atlantic such as the northeastern United States (e.g., Kirby et al., 2002; Hou et al., 2006). However, past combinations of ice discharge, location, magnitude and timing of freshwater influx, longevity of events, the precondition of the North Atlantic, as well as slow changes in synoptic climatic patterns associated with the state of global boundary conditions, likely led to significant differences in the nature of the impact of these events (Fisher et al., 2002; Ellis et al., 2006; Meissner and Clark, 2006; Stanford et al., 2006; Came et al., 2007; Marshall et al., 2007; Bradley and England, 2008; Kleiven et al., 2008).

Climate-model experiments have produced similar temperature responses to perturbations in the modern North Atlantic, although the hydroclimatic responses have varied (e.g. Rahmstorf, 1995; LeGrande et al., 2006; Wiersma and Renssen, 2006). Furthermore, documented historic changes in sea-surface temperature gradients in the North Atlantic, perhaps from cold, freshwater outflow from the Labrador Sea, are associated with the most severe drought on record in adjacent regions during the AD 1960s (Namias, 1966; Wandle, 1991).

To examine if there were hydrological responses to abrupt climate oscillations during deglaciation, we developed high-resolution, lake-level records from New Long Pond (41.85°N, 70.71°W) and Rocky Pond (41.89°N, 70.69°W), in southeastern Massachusetts (Fig. 1) from ca. 15.0 ka into the Holocene (ca. 7.0 ka). Both New Long Pond and Rocky Pond are located in the Plymouth–Carver aquifer, where previous studies (Newby et al., 2000; Shuman et al., 2001) have shown that in the past 15,000 years water levels were lowest between 11.0 and 8.0 ka, then rose, but were low again from ca. 5.4 to 3.0 ka, with the wettest conditions of the Holocene during the last 2000 years. These data match well with patterns observed in New Hampshire (Shuman et al., 2005) and Quebec (Lavoie and

Richard, 2000; Muller et al., 2003) but few lake-level records from the northeastern United States (Winkler, 1985; Harrison, 1989; Webb, 1990; T. Webb et al., 1993; Almquist et al., 2001; Dieffenbacker-Krall and Nurse, 2005; Shuman and Donnelly, 2006) were examined at sufficient resolution to capture short-term, high-frequency changes in water levels.

Previous work at New Long Pond, from a single sediment core, documented early and mid-Holocene low stands using a combination of reflectors in ground penetrating radar profiles and visible sand layers in sediment cores (Shuman and Donnelly, 2006), but the high-resolution record of subsurface reflectors evident from a ground penetrating radar survey at the basin was unexplored. Here, we develop this paleohydrologic record from New Long Pond and an additional high-resolution record from nearby Rocky Pond, using sedimentary evidence of past lake-level changes and the multiple-core approach advocated by Digerfeldt (1986), supplemented with sub-surface geophysical data (i.e., ground penetrating radar). Reflectors in the ground penetrating radar profiles correlate to sand layers deposited symmetrically around the basin within the finer grained lacustrine sediment. We infer that these sand layers represent paleo-shorelines from past low water levels in southeastern Massachusetts. These inferred lake-level changes reveal that higher-frequency variations in drought occurred over the last 15,000 years than previously documented (e.g. Newby et al., 2000; Shuman and Donnelly, 2006; Shuman et al., 2001). Finally, we examine the timing of low stands between 15.0 and 7.0 ka to determine if sub-millennial scale drought may have been related to abrupt climate change events, potentially forced by meltwater routing and discharge events.

2. The Plymouth Carver Aquifer, Site Description, and Climate

As shown in previous work (Newby et al., 2000; Shuman et al., 2001, Shuman and Donnelly, 2006), the geology and geomorphology of the previously glaciated Atlantic coastal plain that contains the Plymouth–Carver aquifer in southeastern Massachusetts is ideal for obtaining high-quality paleo-records of changing water levels (Fig. 1). New Long Pond and Rocky Pond are two of the numerous kettle ponds that dot the predominately sandy outwash plains and moraines within this aquifer; few of these basins have surface inlets or outlets (Fig. 2; Hansen and Lapham, 1992). The topography of the aquifer is flat-to-gently sloping, ranging from sea level to 76 m (Fig. 2). Precambrian-age granitic bedrock, which does not contain any carbonates, underlies the aquifer (Hansen and Lapham, 1992; Robinson and Kapo, 2003). Unconsolidated, stratified glacial deposits compose most of the 3.63×10^2 km^2 aquifer (Hansen and Lapham, 1992). These saturated deposits vary in thickness between 6 and 60 m, depending on the altitude of the bedrock surface, which ranges from ca. 30 m above to 60 m below sea level across the aquifer (Hansen and Lapham, 1992). Infiltration of precipitation into the permeable, primarily sand-and-gravel substrate supplies nearly all water to the aquifer. Groundwater discharges to streams, ponds, wetlands, bogs and the ocean (Hansen and Lapham, 1992). During deglaciation the Laurentide ice sheet was north of the aquifer after ca. 18.0 ka, and the area did not sustain longstanding pro-glacial lakes (Larson, 1982; Ridge, 2003).

New Long Pond (6.5 ha) and Rocky Pond (8.1 ha) are less than 4 km apart, within separate northeast-to-southwest alignments of kettle ponds (Fig. 2). Both ponds have small watersheds (<40 and < 60 ha respectively) and intersect the water table with no interference from streams or rivers. At present, New Long Pond is shallow with a maximum water depth of less than 2 m and modern groundwater flow from the north to the south. Rocky Pond has a maximum depth of ca. 5 m with modern groundwater flow from the northeast to the southwest (Hansen and Lapham, 1992). New Long Pond is 30.2 m above sea level and Rocky Pond is 32.6 m above sea level; the surface bedrock is approximately at modern sea level beneath both basins.

Within the area of New Long Pond and Rocky Pond, the aquifer is unconfined, and the water table rises and falls in response to changes in recharge and discharge, which fluctuates seasonally and over the long term (Hansen and Lapham, 1992; Shuman and Donnelly, 2006). Modern data analyzed by Hansen and Lapham (1992) show water storage is greatest in late winter and early spring when recharge exceeds discharge. Increased rates of evapotranspiration and slightly reduced rates of precipitation during the growing season decrease net recharge and aquifer storage. During late fall and early winter, when precipitation increases and evapotranspiration decreases, recharge is equal to or slightly greater than discharge. Modeled simulations of modern and past changes within the aquifer are detailed in Hansen and Lapham (1992) and Shuman and Donnelly (2006).

Local, instrumental climate records (1891-2000) show an annual mean temperature of 9 ^{o}C, with warm summers (mean July temperature 21 ^{o}C) and cold winters (mean January temperature -4 ^{o}C; (www.bluehills.org/climate.html). The annual precipitation averages ca. 1280 mm, with a seasonal average of 520 mm from March to August and 640 mm from September to February (http://cdiac.ornl.gov/r3d/ushcn/ushcn.html#TOP).

The modern Pitch Pine (*Pinus rigida*)-Oak (*Quercus*) Forest/Woodland dominates the aquifer (Swain and Kearsley, 2001), with pitch pine, white pine (*P. strobus*), northern red, white and scrub oaks (*Quercus rubra, Q. alba, Q. ilicifolia*) and some red maple (*Acer rubrum*) forming the canopy. Shrub borders of blueberry (*Vaccinium* sp.) dominate the understory, with sweet pepperbush (*Clethra alnifolia*) and green briar (*Smilax rotundifolia*) also present. The composition of aquatic and herbaceous plants varies with long and short-term changes in the water level. Presently at both basins, high water levels limit the encroachment of trees and shrubs and low water levels expose the shore, particularly in late summer. This is evident in the photograph (Fig. 3), where herbaceous plants become abundant on the highest level of the flooded sandy shoreline. During prolonged drought, the expanded shoreline may contain, among other plants, goldentop (*Euthamia* spp.), rush (*Juncus* spp.) and beaksedge (*Rhynchospora* spp). During wet intervals, spike-sedge (*Eleocharis* spp.) and pipewort (*Eriocaulon* spp.) may be present. The understory, herbaceous and aquatic vegetation at Rocky Pond include the shrubs sweet pepperbush (*Clethra alterniflora*) and highbush blueberry (*Vaccinium corymbosum*), which surround the sandy/shallow water shore, in which pipewort (*Eriocaulon* spp.*)* and watershield (*Brasenia schreberii*) are present. Within the pond, the emergent bayonet rush (*Juncas militaris*) and submerged aquatic plants include bladderwort (*Utricularia* spp.), hornwort (*Ceratophyllum* spp.) and water milfoil (*Myriophyllum* spp.) At New Long Pond, the shrubs are dominated by highbush blueberry, steeplebush (*Spirea tomentosa*) and leatherleaf (*Chamaedaphne calyculata*). The sandy shore includes switch grass (*Panicum* spp.), rush (*Juncus* spp), sedge (*Cyperaceae* spp), flat-top goldentop (*Euthamia graminifolia*) and little bluestem (*Schizachyrium scoparium*), with the pond containing the emergent Robbins' spikerush (*Eleocharis robbinsii*) and abundant pondweed (*Potamogeton*).

3. Methods

3.1. Field Methods

Ground penetrating radar profiles provide continuous records of facies changes that record the history of sediment accumulation within lakes. Changes in subsurface materials create boundaries with different dielectric properties, which are delineated as "reflectors", so compositional changes can be tracked across the basin. We used a GSSI SIR-2000 ground penetrating radar system and collected multiple transects of data continuously across both lakes by floating a 200-MHz antenna in an inflatable raft. At New Long Pond we targeted our coring along the same west-to-east, 175 m transect (T-1) used by Shuman and Donnelly (2006), from which we collected a total of 13 vibra-cores (7.5-cm diameter) (Fig. 2). At Rocky Pond seven cores were collected from the north-to-south, 360 m transect (T-1). We used the lake's acronym (New Long Pond NLP; Rocky Pond RP) with its distance from the shore (west at New Long Pond and north at Rocky Pond) to label each core. Our focus in this study is the 13 cores from New Long Pond, and two shoreward cores, RP96 and RP110, from Rocky Pond.

3.2 Laboratory Analyzes

The cores were first split in half in the lab, then the archive half was scanned on the X-ray Fluorescence (XRF) scanner at Woods Hole Oceanographic Institution, Massachusetts. Digital photos ("opticals") of the sediment cores (50 μm resolution) were collected, followed by radiographic imaging (lighter is denser) (200 μm resolution) and high-resolution elemental analysis (1000 μm resolution).

Contiguous 1-cm samples for loss-on-ignition analysis were used to estimate the percentage organic matter composition of the sediment samples (Dean, 1974). Percent siliciclastic coarse fraction was determined by screening the residual combusted sediment from each loss-on-ignition sample to extract the sand (>63 μm) content, and then calculating the ratio of sand to total dry sediment. The loss-on-ignition data and percent siliciclastic coarse fraction from NLP43 and percent siliciclastic coarse fraction from RP110 are shown here.

3.3 Dating

We obtained fifty-one accelerator mass spectrometry (AMS) radiocarbon dates for New Long Pond and seventeen dates from Rocky Pond (Table 1). For both sites, intervals for radiocarbon samples were selected to bracket changes in lithology and to corroborate the timing for changes in shoreline features from different points in the basins. Sediment samples ($\leq$ 2 cc) were screened and like-materials, such as similar stems, leaf fragments, or rootlets, were selected, briefly sonicated to remove non-organic materials and fine grained organics, dried at 105^{o} C and then weighed before submitting to the National

Ocean Sciences Accelerator Mass Spectrometer (NOSAMS) Facility (Table 1). Few identifiable organics macrofossils or plant fragments with diagnostic features were present in the cores.

We calibrated all but one date using CALIB v5.0.2, and then used the median age and the maximum and minimum ages of the 2σ range to represent the age span for each date (Reimer et al., 2004a). A single "post-bomb" date (>AD 1950) was calibrated using CALIbomb (Reimer et al., 2004b), with the northern hemisphere zone 1 (NH_zone 1; southern boundary at 40°N) data set (Hua and Barbetti, 2004).

The ^{137}Cs and ^{210}Pb activity as well as Pb pollution in recent sediments from NLP 43 were used to provide stratigraphic ages (e.g. Donnelly et al., 2001; Donnelly and Bertness, 2001). Measurements for ^{137}Cs and ^{210}Pb were made using a high-resolution gamma detector. Approximately 2.0 to 5.0 g of powdered sediment samples were placed in 2.54 cm diameter plastic jars and counted on a Canberra GCW4023S coaxial germanium well detector for 24 to 48 hours. ^{137}Cs is an anthropogenic radionuclide that was released to the environment beginning in the early 1950s, the onset of atmospheric nuclear weapons testing, with fallout reaching a maximum in AD 1963. Relative Pb levels were determined using the above mentioned scanning XRF analysis.

3.4 Methods for Reconstructing Changes in Water Level

Digerfeldt (1986) determined past lake-level fluctuations using unconformities and/or changes in facies, as well as macrofossil and pollen analyses. These data were correlated among cores collected along transects from the shore toward the center of the basin. With this method, the magnitude of past lake-level declines are determined using the depth of unconformities located near shore in lacustrine sediments. Within the Plymouth–Carver aquifer, the small fetch limits the exposure of the basins to the potential impact wind may have on sediment accumulation. In previous studies, Newby et al., (2000), Shuman et al. (2001), and Shuman and Donnelly (2006) inferred that correlations among sand layers within individual basins revealed paleo-shorelines deposited during low water levels, and that these patterns of past lake-level changes can be replicated among basins. In these studies, a lack of evidence for sub-aerial exposure (e.g. soil development, sediment oxidation) within the cores indicates that water levels did not fall below the level of the unconformities. Similarly, water levels were not significantly higher than the unconformities because wave energy in shallow water is needed to account for associated sand deposits.

Our addition of ground penetrating radar records greatly enhances the general approach introduced by Digerfeldt (1986) in that they allow for mapping lithological boundaries continuously across the basin. Multiple ground penetrating radar profiles and cores from New Long Pond and Rocky Pond reveal that the sand layers, which fine, become thin and sometimes “pinch-out” toward the center of the basins, are deposited around the margin of the lakes.

These continuous sand units around the periphery of the basins, even portions of the basin that are separated from an adjacent sub-basin by a low elevation sill with effectively no watershed, indicate that basin-wide fluctuations in water level are likely the only viable mechanism for the deposition of these layers. The basin-wide deposition of these sand layers is not what would be caused by run-off events where flow is concentrated and deposition would be localized. While fires, wind-throw events, human modifications, and other disturbances to the landscape may increase the exposure of the siliciclastic component of sediments in the watershed, limited surface runoff would confine any deposition to small areas. For example, during large precipitation events we observed surface runoff along the road at the western margin of New Long Pond (see Fig. 2). This surface flow discharged into the western corner of New Long Pond and deposited a small (50 m^2) localized delta, but did not result in siliciclastic deposition in other portions of the basin. Given the highly permeable substrate and small, low-relief catchments, runoff events such as this were likely rare or nonexistent prior to road building.

Other processes such as eolian transport and ice rafting are potential mechanisms for transporting siliciclastic material to the basin. However, the continuity and distribution of the layers is inconsistent with localized ice rafted debris deposition and the large grain sizes present in the deposits indicate non-eolian transport. Thus we infer that continuous and widespread sand layers that can be mapped around the basin and thin toward the center of the basin reflect lake-level low stands.

To reconstruct changes in water levels for New Long Pond and Rocky Pond, we plotted each cores distance from shore (co-located with ground penetrating radar data). The presence of sand layers was determined by visible inspection and in select cores by sieving the loss-on-ignition ash. As coarse-grained layers correlate well with dense layers (lighter) in the radiography (see Figs. 6 and 9), we used the radiographic images from the remaining cores to map sand units across the basins. In many cases, we cross checked that the dense layers in the radiographic images were coarse grained by additional sieving of discrete samples. We combined these data and the ground penetrating radar profile (T-1) for New Long Pond to map the lithologic boundaries along the transect (Fig. 4B). The limited number of cores extracted from Rocky Pond prevented the same sort of mapping across the entire basin at this site. However, the same procedure was performed to interpret the ground penetrating radar data from Rocky Pond and the core data from RP96 and RP110 (Figs. 8-10).

4. Results

4.1. New Long Pond

New ground penetrating radar data from New Long Pond confirmed the same two low stands (Fig. 4A, 1 and 2) shown by Shuman and Donnelly (2006) and the finer scale variability indicated by multiple additional reflectors (Fig. 4A). The compilation of 13 cores along transect also showed numerous sand units, which correlated well with reflectors in the ground penetrating radar profile (Fig. 4B).

The lacustrine sequence begins with low-organic silt (<20%) deposited over glacially derived sand and gravel followed by a transition to peaty silt (>60% organic; Fig. 5). This peaty silt was recovered in the uppermost sediments of each core and is a matrix of predominantly in situ rootlets and plant detritus containing organic-rich silt. Peaty silt is currently being deposited subaqueously and predominantly by the growth of shallow aquatic vegetation and algal remains. We infer the fine rootlets that comprise the bulk of the macroscopic material record a growing surface over time, similar to the way terrestrial and intertidal peats accumulate.

These lacustrine sediments are interrupted by five major sand units (I to V), which originate near shore and often break apart into smaller layers as they extend basinward (Fig. 4B). Unit I occurs in the deepest portion of the basin and is evident as a single sand layer at the base of NLP80 and NLP113, which splits into multiple sand layers in NLP101. Above this, the Unit II sand layers emerge from the shoreward sand body between NLP31 and NLP43 on the western side of the basin and beyond NLP131 from the eastern side of the basin. The Unit III and Unit IV sand layers extend across the basin and Unit IV separates into multiple sand layers between NLP43 and NLP131. Uppermost Unit V is a series of at least seven sand layers, which merge into single units at both shores. One additional recent sand layer is present within the upper 10 cm of the sequence.

Before ca 14.5 ka the earliest low stands recorded in the basin (Unit I) are inferred from the single sand layer in NLP80 and NLP113 (Fig. 4B, a). This single sand layer breaks apart into multiple thin sand lenses in NLP101 (Fig. 4B, b). The earliest New Long Pond, before 14.5 ka (as indicated by the radiocarbon ages below Unit II in NLP43 and NLP53; Fig. 4B), may have been smaller than present, although early, fine-grained lacustrine sediments shoreward of NLP43 and NLP113 could have eroded over time (Fig. 4B, x_1). Silt deposited above Unit I indicates that an interval of high water levels followed this low stand (Fig. 4B, x_2).

Unit II sand extends basinward from both shores, at NLP31 on the western side and just beyond NLP131 on the eastern side (Fig. 4B, c). A radiocarbon age of 14.5 ka at the base of NLP43 and two radiocarbon ages in NLP53 above (13.7 ka) and below (14.4 ka) this unit (Figs. 4B and 6) constrain the timing for this low water level. Silt deposited above Unit II, after 13.7 ka, indicates that water levels rose and remained high until ca. 13.0 ka (Fig. 4B, x_3; see radiocarbon ages in NLP43 (12.9 ka), NLP65 (13.0 ka), and NLP161 (12.8 ka) also in Fig. 5).

The Unit III sand layer occurs across the basin, thinning toward the center of the lake. Four radiocarbon dates immediately below this unit provide an estimate for the beginning of this low stand at ca. 12.9 ka at the beginning of the YD (Fig. 4B, d; two samples from NLP43 date to 12.8 and 12.9 ka, 13.0 ka in NLP65, and 12.8 ka in NLP161). A radiocarbon date above this sand layer in NLP 65 of 13.6 ka appears to be too old and the material dated was likely reworked (Fig. 4B). The extension from the shoreward sand body of Unit III toward the middle of the basin marks a drawdown in which the lake may have dried out and/or at least lowered ca. 6.0 $\pm$ 1.0 m below modern water.

Radiocarbon-dated macrofossils embedded within silt in NLP31 above Unit III indicate at least a brief mid-YD high stand ca. 12.0 ka (Fig. 4B, x_4). To achieve lacustrine deposition this close to the modern shore, water levels had to rise at least 3 m (below the modern water level) after the low stand at 12.9 ka. Further offshore, the accumulation of silt until 10.4 ka (see radiocarbon ages in NLP65 and NLP43) also indicates relatively high water levels until this time (Fig. 4B, x_5).

After 10.4 ka, the two uppermost sand units, Unit IV and V (Fig. 4B), correspond with two prominent ground penetrating radar reflectors across the basin that date to the early and the mid-Holocene low stands (Fig. 4A; unconformity 1 and 2, Shuman and Donnelly, 2006). Both the Unit IV and V sand layers originate from shoreward bodies of sand (e.g., NLP23 and 27; Fig. 4B, e). Beyond NLP43, toward the deeper portion of the basin, Unit IV splits into layers of sand interbedded with silt (Fig. 3B, f). Peaty silt begins to accumulate above the Unit IV sand layers (Fig. 4B, x_6). Radiocarbon dates from just above Unit IV in NLP65 and NLP43 at 9.0 ka and 8.9 ka, respectively, constrain the age of the termination of this series of low stands (Figs. 4B and 5).

Above the transition from Unit IV to peaty silt, two small, thin sand layers extend basinward from either shore (Fig. 4B, g and h). Radiocarbon dates from NLP65, NLP43 and NLP31 indicate that the lower of these sand layers was deposited ca. 8.4 ka (Fig. 4B). In NLP31, a radiocarbon date from material just above this sand layer indicates lacustrine deposition in the shoreward cores initiated by 8.2 ka (Fig. 4B, x_7). This lower sand layer (Fig. 4B, g) is evidence of an abrupt, short-term drawdown at New Long Pond coincident with the timing of the “8.2 ka” event in the North Atlantic (Alley et al., 1997).

Radiocarbon dates from NLP31 bracket the upper of these sand layers and constrain its age to ca. 7.5 to 7.2 ka (Fig. 4B, h).

Near the top of the sequence, Unit V extends into the basin, splitting into multiple thin sand lenses (Fig. 4B, i). Radiocarbon dates from NLP31, NLP43 and NLP65 indicate that Unit V was deposited after ca 6.0 ka (Fig. 4B, x_8). The uppermost sand layer of Unit V, within the upper 10 cm of the sediment record, dates to the AD 20th century (Fig. 4B, j). In NLP43, this sand layer occurs above the onset of Pb (Int) pollution associated with the industrial revolution (ca. AD 1875; Fig. 7). The supported ^{210}Pb profile also indicates that this coarse layer was deposited in the last 150 years as the ^{210}Pb activity is above background levels in the upper 11 cm. In addition, the peak in ^{137}Cs activity, related to the height of atmospheric nuclear weapons testing in AD 1963, corresponds with the peak in coarse fraction associated with this layer. A post bomb radiocarbon age also dates this interval to the early AD 1960s. Extrapolating the sedimentation rate between the Pb rise and ^{137}Cs peak (5.68 mm/yr) to the beginning of the rise in coarse fraction suggests this modern drought layer likely began to be deposited in the early AD 20th century (Fig. 7).

4.2. Rocky Pond

At Rocky Pond, the ground penetrating radar profile from T-1 reveals a sequence of reflectors evident within the other profiles (not shown) collected at the basin (Fig. 8). The lowermost, sub-horizontal reflectors are well-defined and some “pinch-out” and then reappear on the other side of the basin (Fig. 8). Above these, a condensed series of reflectors just below the sediment water interface extends across the basin (Fig. 8).

The enlarged section of the ground penetrating radar profile shows the association between these reflectors and the four uppermost sand units (II-V) at New Long Pond (Fig. 9). The optical from RP96 shows the sedimentary sequence at Rocky Pond, which is silt interrupted by multiple, well-sorted, sand lenses and sand mixed with silt to the top of the core (Fig. 9). The silt becomes more organic rich near the top of the core. The radiograph displays these sedimentary transitions as light (dense) layers (Fig. 9).

At Rocky Pond, Unit II, from ca.15.3 to 14.5 ka, and is represented by at least two sand layers in RP110 (Fig. 10). The other three units are all found in both RP96 and RP110: Unit III, dating to ca. 12.9 to 12.6 ka is represented by a thick sand layer in RP96 and in RP110 by at least one pronounced sand interval in RP110. Unit IV consists of a package of sand layers in RP96 dating from ca. 10.5 to 9.0 ka, with the thickest unit dating to between 10.7 to 10.3 ka (Fig. 10). Four additional thinner layers in this unit (IV) of RP96 were deposited between 10.3 and 9.0 ka. In RP110, Unit IV splits into at least 14 thin sand layers; one of these sand layers near the base of the unit is slightly thicker. Immediately above Unit IV, two sand layers are present in RP96 that date to ca. 8.4 and 7.2 ka, respectively (Fig. 10). The uppermost Unit V was deposited after 6.1 ka, and likely corresponds to the condensed set of ground penetrating radar reflectors just below the sediment water interface (Figs. 8 and 9). This complex unit, with cross cutting reflectors and slow sedimentation rates in this upper part of the sequence (ca. 12.0 cm/10^3 yr), make it difficult to differentiate and map individual strata. Hence, we did not attempt to try and unravel the late Holocene portion of the record.

Above the glacial material, the earliest silt is interrupted by two intervals in RP110 (Unit II) containing $\geq$ 25% coarse fraction (Fig. 10). We infer these deposits represent two low stands before ca. 14.4 ka, when, relative to the modern, the basin was a smaller and deeply configured pond, ca. 9.8 $\pm$ 1 m below modern water. By about 14.0 ka, water levels rose toward the modern shore and remained high until ca. 13.0 ka (Fig. 10, x_1). We do not know how far the basin expanded beyond the location of RP96 toward the modern shore, however, the transition to a larger-than-previous lake by ca. 14.0 ka is marked by the accumulation of silt in both cores.

At the beginning of the YD (12.9 ka), a thick (40 cm), coarse sand layer above the silt in RP96 Unit III (Fig. 10) indicates that water levels dropped ca. 2.5 m during a brief drawdown. During this low stand, a thin interval of silt, deposited midway within the sand in RP96 Unit III (Fig. 10, x_2) indicates a rapid rise, then drop in water levels, which remained low until after ca. 12.6 ka (Fig. 10). These sand layers correspond to three individual sand layers in RP110 deposited between about 13.1 and 12.4 ka (Fig. 10). A radiocarbon age from the silt just above the uppermost sand layer in RP110 dates the subsequent rise in lake levels between 12.6 and 12.0 ka (Fig. 10, x_3). During this highstand, percent coarse fraction remains less ca. 10% in RP110 (Fig. 10), and only 30 cm of sediment accumulated in RP96 and about 1 m accumulated in RP110.

In Unit IV, a thick sand layer in RP96, deposited ca. 10.5 to 10.3 ka, may correlate with a prominent sand layer in RP110, which has the peak value (95%) for coarse fraction in the core (Fig. 10). Thus, this low water level likely extended far into the pond. After this low stand, multiple sand layers in RP96 and RP110 indicate additional low stands during Unit IV.

Between ca. 9.0 and 7.0 ka, two sand layers in RP96 document low stands, radiocarbon dated at ca. 8.2 ka and 7.2 ka (Fig. 10). In RP110, percent coarse fraction increases after ca. 9.0 ka and a sand layer deposited below sediments radiocarbon dated to ca. 8.2 ka mark the end of this trend (Fig. 10). An additional sand layer in RP110 occurs just above the sediments dated to 8.2 ka and a radiocarbon date of 7.2 ka above the sand layer constrains the timing for its deposition. However, since the upper date is ca. 30 cm above the sand layer, the age of deposition is not tightly bracketed.

5. Discussion

5.1. Water-level history from 15.0 to 7.0 ka

Maps of millennial-scale patterns for water-level changes in the northeastern United States show dry conditions during the early Holocene (10.0 to 8.0 ka) and intermediate conditions during the early to middle Holocene (after 7.0 ka; Shuman et al., 2002.) Prior to the present study, however, sub-millennial scale variations had not been methodically examined. As a result the moisture record for the 8000 years from 15.0 to 7.0 ka was not well resolved (Winkler, 1985; Harrison, 1989; R.S. Webb et al., 1993; T. Webb et al., 1993). Later studies, some of which use multiple cores to reconstruct lake levels, e.g. Crooked Pond (Shuman et al., 2001) and Makepeace Cedar Swamp (Newby et al., 2000) in southeastern Massachusetts, Mansell Pond (Almquist et al., 2001) and Mathews Pond/Whitehead Lake (Dieffenbacker-Krall and Nurse, 2005) in Maine, Echo Lake in

New Hampshire (Shuman et al., 2005), Albion Lake (Lavoie and Richard, 2000) and Lac Hertel (Muller et al., 2003) in Quebec, hint at high-resolution water-level changes, but lack temporal control and stratigraphic resolution.

The data presented here augment these previous works by documenting reproducible, high-resolution variations in water levels for southeastern New England: five major sand units (I-V) are evident at New Long Pond and four of them (II – V) are also recorded at Rocky Pond. In light of the evidence of higher frequency water-level fluctuations documented here it is necessary to re-examine previous data from the Plymouth–Carver aquifer.

Previous work within the Plymouth–Carver aquifer shows that early water levels were high (Newby et al., 2000; Shuman et al., 2001), but these records do not extend ca. >14.0 ka. Between 15.0 and 13.7 ka, we have documented two intervals with low water (I-II) at New Long Pond and one interval with low water (II) at Rocky Pond. Before 14.5 ka, accumulating lacustrine sediments were interrupted by as many as four paleo-shorelines (Unit I) at New Long Pond. Evidence for these low stands may be present in deeper portions of the Rocky Pond basin, where the sediment record exceeds 11.0 m and cannot be resolved by existing ground penetrating radar data (see Figure 8). Between 14.4 and 13.7 ka, one additional low stand is recorded at New Long Pond, with two low stands at Rocky Pond (Unit II).

Multiple low stands (Unit III) at New Long Pond and (at least) three low stands at Rocky Pond document intermittently dry conditions in southeastern Massachusetts during the YD. The onset of the Unit III low stand and the YD are more or less synchronous at ca. 12.9 ka. Other studies have inferred moist conditions with cooling during the YD (Levesque et al., 1997; Shemesh and Peteet, 1998; Huang et al., 2002). Consistent with this interpretation, Shuman et al. (2001) initially inferred relatively high-water levels because YD-related pollen sequences were present in deep and littoral cores at Crooked Pond. The rates of sediment accumulation associated with these pollen sequences, however, range between 12.5 to 5.0 cm/10^3yrs, and are near or below Webb and Webb's (1988) threshold for 'non-constant' accumulation (10 cm/10^3yrs). These slow sedimentation rates likely indicate winnowing or non-accumulation associated with shallow conditions. In combination with our inference of intermittently wet and dry conditions during the YD, the data from Crooked Pond are consistent with wet conditions during a portion but not the entire YD.

Between 11.0 and 8.0 ka, bracketing radiocarbon dates and pollen data from deep and shoreward cores at Makepeace Cedar Swamp and Crooked Pond show dry conditions, which correlate with the timing for increased white pine populations (Newby et al., 2000; Shuman et al., 2001). At Makepeace Cedar Swamp, open water at ca. 10.6 ka changed to peat, and then dried completely after ca. 8.5 ka (Newby et al., 2000). At Crooked Pond, sand layers within each of three shoreward cores constrained the timing for the low water interval from ca. 11.2 to 8.0 ka, with the maximum lowering from ca. 10.2 to 9.0 ka. At New Long Pond, at least four low stands (Unit IV) are associated with this interval, while at Rocky Pond (Unit IV), at least 14 sand layers in RP110 indicate highly variable water levels during the earliest Holocene. Radiocarbon dates from New Long Pond and Rocky Pond constrain the timing for this interval to ca. 10.4 to 9.0 ka, which corresponds well with the time of maximum lowering at Crooked Pond.

A low stand before ca. 8.4 ka at New Long Pond and before ca. 8.2 ka at Rocky Pond is approximately at the same time as the "8.2 ka" event (Alley et al., 1997). In addition, two radiocarbon dates that bracket a sand layer in NLP31 and a radiocarbon date just below a sand layer in RP96 both point to an additional low stand at ca. 7.2 ka. Slow rates of sediment accumulation mark this event in the data for Crooked Pond: water levels rose slowly before 9.0 ka, and then rose even more slowly after 9.0 ka, taking ca. 1000 years to begin fine-grained deposition 10 m closer to the shore (at ca. 7.7 ka). At Makepeace Cedar Swamp, a ca. 500-yr hiatus from ca. 8.5 to 8.0 ka overlaps the timing for the "8.2 ka" event (Newby et al., 2000). After ca. 8.0 ka, a radiocarbon age of 7.2 ka marks the peak value for grass pollen percentages (60%) and a corresponding, sharp fall and rise in percent organic matter (75-50%) before water levels lowered at 5.6 ka.

Evidence for sub-centennial scale changes in vegetation in concert with abrupt climate oscillations in the North Atlantic, such as the "8.2ka" event, show varying responses, which may relate to local vegetation and conditions at different lakes, changes in pollen productivity or representation, and/or differences in elevation, topography and soil type. Dry conditions during the early Holocene associated with abundant white pine pollen, and during the mid-Holocene associated with the regional decline in hemlock pollen and a possible pathogen, indicate that changes in hydroclimate have the potential to strongly impact regional and local vegetation (see Shuman et al., 2009).

5.2 Instrumental Data and the Sedimentary Record of Drought

The uppermost sand layer at New Long Pond dates to the AD 20th century with the peak in coarse fraction dating to ca. AD 1960s, which correlates with the timing for the most extreme drought in the historical record (AD 1961-1969) in the northeastern United States (Wandle, 1991). The duration and severity of this drought had substantial consequences for water supplies and agriculture across the region and in southeastern Massachusetts. Water levels were sufficiently low during this event to invoke state intervention to maintain supply to the cranberry industry (Wandle, 1991). Data from a groundwater monitoring well near New Long Pond (ca. 8.0 km; Fig. 1) and Rocky Pond (ca. 4.2 km) show groundwater elevations below the long term average elevation (36.9 m above sea level) over several different intervals (http://ma.water.usgs.gov/water/water_g.htm; Fig. 11B). Hansen and Lapham (1992) identified two periods of pronounced low ground water elevations from these well data (1964 to 1965 and 1980 to 1981; Fig. 11B), which they to related to large precipitation deficits within the Plymouth–Carver aquifer in 1964 (266.7 mm), in 1965 (558.8 mm) and in 1980 (279.4 mm).

At the broader scale, the precipitation anomaly record, averaged from the three closest stations to the sites (Fig. 1; New Bedford, Taunton, and Plymouth; Karl et al., 1990), shows a negative AD 20th century precipitation anomaly between ca. AD 1920 and 1950

(Fig. 11C). During this time, the values for the running average were as low as ca. 200 mm below the mean (Fig. 11C). The AD 1960's drought is recorded as a ca. ten-yr anomaly in the running average, during which time values dropped ca. 250 mm below the mean (Fig. 11C). From ca. AD 1969 to 2005, the running average in the precipitation record does not drop below the mean, however, two precipitation lows are evident in AD 1980 and 1990 (Fig. 11C).

In concert with fluctuations in moisture availability recorded in historic well and precipitation data, the sedimentary record from New Long Pond shows a steady rise in coarse fraction from 2 to 6% during the ca. AD 1920 to 1950 precipitation anomaly. The peak value in coarse fraction of 14% for the historic record dates to the AD 1960s. Percent coarse fraction then drops, rises to 6% at ca. AD 1980s, and then declines to 3% by the top-most sample in the record (Fig. 11A). Though the relatively low resolution of the sediment archive likely prevents distinguishing individual short-term droughts (subdecadal scale), the site appears to be able to record multi-decadal to centennial-scale droughts. This modern analog provides a useful estimate of the minimum sensitivity of the site to past drought. As most of the early (between 15.0 and 7.0 ka) sand layers mapped at New Long Pond are more substantial than this modern analog, these deposits potentially represent more severe droughts that may have lasted many decades or even centuries. Changes in vegetation and basin infilling over time, however, can alter how lakes record low moisture intervals of varying magnitudes. Further, the uncertainty of the radiocarbon ages and potential for erosion of the previous lake bottom by subsequent low stands limits our ability to constrain the duration of these droughts.

Sea-surface temperatures from AD 1860 to 2007 off New England (39-40ºN; 65-66ºW; HadSSTs from Rayner et al., 2003) confirm the low sea-surface temperatures that Namias (1966) linked with this drought (Fig. 11D). The converging lines of evidence, among sediments, well data, precipitation and sea-surface temperature, link the deposition of sand-rich sediment at New Long Pond with documented drought conditions, potentially associated with cool ocean temperatures that may have diverted moisture-laden air masses (Namais, 1966). The AD 1960s drought was also likely preconditioned by the long-term decrease in precipitation recorded in the running average of the precipitation record (Fig. 11C). While some droughts are related to other forcing mechanisms (e.g. 1980 to 1981), cold sea-surface temperature anomalies in the western North Atlantic appear to be one viable mechanism for causing severe drought in the region.

5.3. Potential forcing mechanisms for paleo-hydrologic variability

Late Quaternary changes in climate are primarily the combined result of external (orbital) and internal (ice sheet) forcing (COHMAP members, 1988) and these monotonic forcing mechanisms have been proposed to account for millennial-scale trends in moisture variability during the late Pleistocene and early Holocene. During the Late Pleistocene, the formation of steep thermal gradients south of the Laurentide ice sheet likely concentrated precipitation in latitudinal bands as the ice mass retreated northward (Webb, 1990). As the Laurentide ice sheet moved northward after ca. 11.0 ka, the millennial-scale pattern of low-water levels in the northeastern United States may have resulted from increased evaporation due to warm temperatures and high summer insolation (COHMAP members, 1988). The high-frequency fluctuations in water levels recorded at

New Long Pond and Rocky Pond, however, indicate more variability in regional climate during the Pleistocene/Holocene transition than expected from these long-term changes in climatic boundary conditions. Other mechanisms are needed to explain these high-resolution changes in regional hydrology.

Multiple lines of evidence, including records from Greenland ice cores (Stuiver and Grootes, 2000; Rasmussen et al., 2006), North Atlantic sediments (Keigwin et al., 2005; Ellis et al., 2006; Came et al., 2007; Kleiven et al., 2008), and lake records from Europe (Magny and Begeot, 2004; Veski et al., 2004; Marshall et al., 2007) and North America (Mott et al., 1986; Peteet et al., 1990; Levesque et al., 1993; Yu and Eicher, 1998, 2001; Yu and Wright, 2001; Li et al., 2006) indicate that the Late Pleistocene and Early Holocene climate experienced centennial-scale variability and included abrupt changes. The Oldest Dryas (OD; >14.5 ka), Older Dryas (14.1 to 13.9 ka), IACP (13.35 ka), YD (12.9 to 11.6 ka), PBO (11.2 to 11.0 ka), "9.2" and "8.2" ka events are familiar oscillations identified in ice cores, which are characterized by abrupt changes in ^{18}O and other proxies during the last deglaciation and into the early Holocene (Johnsen et al., 1992; Alley et al., 1997; Barber et al., 1999; Stuiver and Grootes, 2000; Fisher et al., 2002; Stanford et al., 2006; Fleitmann et al., 2008).

Variations in solar output have been suggested as a possible mechanism for forcing some of these ^{18}O isotopic excursions (van Geel et al., 1999; Bond et al., 2001). Rohling and Pälike (2005), for example, suggest that the "8.2 ka" event was a local circum North Atlantic expression of a widespread climatic deterioration between 8.5 and 8.0 ka, linked to fluctuations in solar output. However, many of these abrupt oscillations in climate at the Pleistocene/Holocene transition have been linked with freshwater outbursts and reroutings into oceans that are believed to have altered meridional overturning circulation, which strongly influences temperatures in the North Atlantic region (McManus et al., 2004; Broecker 2006; Alley, 2007).

The earliest low stand intervals, before ca. 14.5 ka at New Long Pond (Unit I), are well represented in the sediment cores by several sand layers, but there is no precise radiometric control for this portion of the basin. The Rocky Pond record recovered to date apparently does not extend back in time far enough to capture this interval. However, water levels at New Long and Rocky Ponds were relatively high as conditions sharply warmed with the onset of the Bølling ca. 14.6 ka (Björck et al., 1998) as both were accumulating silt at this time.

The abrupt change to cold conditions associated with the Older Dryas ca. 14.1 to 13.9 ka, (Björck et al., 1998; Rasmussen et al., 2007) fits well with the timing of two increases in coarse fraction at New Long Pond and Rocky Pond (Unit II; Fig. 12). Both low-stand sand layers at Rocky Pond rise and fall slightly before those at New Long Pond but are within the uncertainties of our age models and occur within ca. 400 years at each basin. A sand layer in NLP53, emplaced between 14.4 and 13.7 ka (Fig. 6), is particularly coincident with the Older Dryas oscillation. High resolution data from marine sediments south of Greenland show slightly weakened meriodional overturning circulation in association with the Older Dryas (Stanford et al., 2006). Clark et al. (2001) propose two rerouting events at this time (R5 and R6) that may have played a role in forcing the Older Dryas, and potentially drought in southeastern New England that caused the Unit II low stand.

No significant sand layers are present at either New Long Pond or Rocky Pond at the IACP event, likely associated with a catastrophic, brief (ca.< 300 yr) release of freshwater down the Hudson River Valley into New Island Sound ca. 13.35 ka (Donnelly et al., 2005) or the brief ^{18}O isotopic excursion at ca. 13.6 ka in the NGRIP ice core record (Fig. 12). Thus, no documented evidence of droughts appears related to these short-lived climate excursions in southeastern New England.

The onset of a brief, centennial-scale drought at 12.9 ka is coincident with the onset of the YD (Fig. 12). The YD-related increase in percent coarse fraction at New Long Pond (Unit III) peak around 12.6 ka, after the abrupt onset of cold conditions across the circum North Atlantic (Ruddiman and McIntyre, 1981; Rind et al., 1986; Rasmussen et al., 2007). Three additional rises and falls in percent coarse fraction during the YD are recorded at New Long Pond (between ca. 12.1 and 11.6 ka). At Rocky Pond, three increases in percent coarse fraction are present during the YD (Unit III; Fig. 12). We infer these low stands accompanied the cold YD before ca. 12.2 ka at Rocky Pond, after which, water levels were high until 11.6 ka, based on the relatively low values for coarse fraction (Fig. 12).

The change from warm to glacial-like conditions recorded in marine and terrestrial records associated with the YD have been postulated to be linked with a catastrophic discharge from Lake Agassiz to the Atlantic Ocean (Ruddiman and McIntyre, 1981; Broecker et al., 1985; Mott et al., 1986; Rind et al., 1986; Peteet et al., 1990; Alley et al., 1993; Clark et al., 2001; Teller and Leverington, 2004). Teller and Leverington (2004) associated a major rerouting of Lake Agassiz meltwater from the southward drainage to the Gulf of Mexico to an eastward drainage into Lake Superior, then through the St. Lawrence River to the Atlantic Ocean with the onset of the YD (Fig. 12, R3 of Clark et al., 2001, also see Licciardi et al., 1999). At this same time Atlantic meridional overturning circulation declines (McManus et al., 2004; Stanford et al., 2006). This meltwater-meriodional overturning circulation connection as the key-triggering mechanism for the YD is called to question by a lack of deeply incised drainage channels associated with Lake Agassiz drainage (Lowell et al., 2005; Teller et al., 2005), and an alternative hypothesis that proposes an atmospheric explosion of extra-terrestrial objects as the trigger for the YD (Firestone et al., 2007; Kennett et al., 2009). However, Broecker's (2006) review lends continued support for a meltwater conduit – meriodional overturning circulation connection for the YD, but notes the location for this discharge remains problematic. Freshwater discharge from other smaller lakes, such as those in the modern Great Lakes basins, may have played a role in triggering the YD as the Saint Lawrence River valley opened as a conduit for freshwater at ca. 13.0 ka (Donnelly et al., 2005; Richard and Occhietti, 2005).

Just before 11.0 ka, NLP43 records a rise in percent coarse fraction that is only evident in this shoreward core (Fig. 12). There is little evidence of sand being deposited at Rocky Pond, but given radiocarbon uncertainties, it is possible that one of the sand layers at the base of Unit IV at RP110 could correlate with this event in NLP43 (Fig.10). A thin sand layer just below Unit IV in RP96 may also date to this time (Fig. 10). Given our current age model, the coarse fraction in RP110 is unchanged from the low values that began after the rise in water levels after ca. 12.2 ka. The brief PBO began shortly after the end of the YD (11.6 ka). The NGRIP ^{18}O data, however, reveals two oscillations to more negative values, at ca. 11.4 and 11.0 ka, potentially timed with this event (Fig. 12). Fisher et al. (2002) suggest the PBO was a short-lived discharge from Lake Agassiz into the Arctic Ocean centered around 11.3 ka, based on radiocarbon ages obtained from flood and delta deposits near ancient spillways (also see Teller and Leverington, 2004). Hald and Hagen (1998) found evidence, however, for a two-stage freshwater discharge, at ca. 11.3 and 11.0 ka, from a core collected in the Norwegian Sea, which fits well with the two NGRIP ^{18}O oscillations (Fig. 12). The rise in values for percent coarse fraction at New Long Pond at ca. 11.0 ka are closer to the timing for the later ^{18}O isotopic excursion.

At approximately 10.5 ka, percent coarse fraction at Rocky Pond began to rise and fluctuate and marks the bottom of Unit IV (Fig. 12). The lowermost sand layer in New Long Pond extends across the basin and dates to between 10.4 and 10.2 ka (Fig. 4B). After a brief return to silt and higher water levels, at least three more sand layers were deposited across New Long Pond between 10.2 and 9.0 ka. In NLP43, a large sand layer represents this interval (Fig. 4B). The record from RP110 is much better resolved and shows numerous (14) sand layers in this interval (Unit IV; Fig 10). Teller and Leverington (2004) identified at least 12 abrupt discharge events (Fig. 12, R2 of Clark et al., 2001) at Lake Agassiz between 10.6 and 8.4 ka. Three ^{18}O isotopic oscillations from GISP and GISP2 (YD, PBO and "8.2ka") were correlated with the timing for discharge events and subsequent changes to meridional overturning circulation (Teller and Leverington, 2004). Further links among Lake Agassiz outbursts and these isotopic records were less clear because of differences between the age models for GISP and GISP2 and uncertainty in the ages for the discharge events from Lake Agassiz.

At ca. 9.2 ka, percent coarse fraction at New Long Pond remains high except for a single drop within the radiocarbon uncertainty at ca. 9.2 ka (Fig. 12). Percent coarse fraction at Rocky Pond show as many as four rises and falls (Fig. 12). The NGRIP ice core record shows two oscillations between ca. 9.3 and 8.9 ka, which correlate with freshwater discharges to the circum North Atlantic (Came et al., 2007; Fleitmann et al., 2008).

Both New Long Pond and Rocky Pond provide evidence of a short-lived water-level drop around 8.4 ka (Fig. 12). The timing of this drawdown is consistent with the "8.2 ka" event likely associated with the final drainage of Lake Agassiz (Barber et al., 1999; Teller and Leverington, 2004). The "8.2 ka" event is a well-documented example of a change from warm-to-cold and back to warm conditions for the Holocene and took place when warm conditions had prevailed in the circum North Atlantic for ca. 3000 years (Alley et al., 1997; Alley and Ágústsdóttir, 2005). Alley et al. (1997) estimate a rapid drop in temperature from around 0 to -5^0C for central Greenland.

Modeling results, related to the impact of different freshwater release scenarios for the "8.2 ka" event, indicate that the amount of water released is the "decisive factor in the response of the ocean" (Wiersma et al., 2006). Further model simulations that also include parameters for the YD, PBO and "8.2 ka" event indicate that routing events (long-term, low amplitude) have more potential to impact meridional overturning circulation than short-term floods (Meissner and Clark, 2006). Thus, the specific mechanisms and the scale at which different forcings may have impacted the local paleohydrology are not yet clear.

At ca. 7.2 ka, increases in percent coarse fraction in RP110 are less prominent than those in NLP43 (Fig. 12). Meltwater events have not been documented for this interval and the NGRIP ice core data show only small oscillations at the time (Fig. 12). However, based on Alley's (2000, 2004) temperature reconstruction from GISP2 ice core data, the timing for this sand layer at New Long Pond correlates with a cool interval in the North Atlantic. Sediment records from Lough Inchiquin in Ireland (Diefendorf et al., 2006) and from Seneca Lake in New York (Guiles-Ellis et al., 2004) also document changes at ca. 7.2 ka.

6. Conclusion

We have documented evidence of previously unrecognized water-level fluctuations on sub-millennial time-scales in southeastern Massachusetts between 15.0 and 7.0 ka. For this interval, we have defined four units that each contain evidence of multiple centennial-scale droughts (Unit I - >14.5 ka; Unit II – 14.4-13.7 ka; Unit III – 12.9-11.2 ka; Unit IV – 10.4-9.0 ka). In addition, sand layer deposits that date to 8.4 and 7.2 ka provide evidence of further severe drought. The concurrent timing of sand-layer emplacement at New Long and Rocky Ponds indicates a coherent response to climate forcing, rather than site-specific, small-scale processes. In addition, our reconstruction documents the sensitivity of the stratigraphic record at New Long Pond to brief events, such as the multi-decadal decrease in precipitation in the mid 20th century, which culminated in the AD 1960s drought. Monotonic changes in isolation and ice-sheet extent, related rising temperatures, and changes in the seasonality of precipitation likely contributed to dry conditions in the early Holocene. However, other mechanisms, such as abrupt oceanic responses to meltwater, may be necessary to explain the centennial-scale droughts that we have documented.

Our evidence of century-scale droughts in southeastern New England is often concomitant with abrupt climate oscillations documented in ice core data and elsewhere (such as the Older Dryas, YD and “9.2” and “8.2 ” ka events), and many large and rapid releases of impounded meltwater and reroutings from the wasting Laurentide ice sheet. These meltwater pulses may have inhibited meridional overturning circulation and resulted in low sea-surface temperatures off eastern North America. Further, the historic link between low sea-surface temperatures and drought in the region in the AD 1960s suggests that meltwater-induced cooling of the North Atlantic may be a viable mechanism for forcing paleo-droughts. However, some climate oscillations likely forced by meltwater release (e.g., IACP) apparently did not result in drought documented in our data.

Changes in meridional overturning circulation and abrupt climate changes appear linked, but the character of meltwater discharge (volume, duration, locations) and its impact on the climate system remains poorly understood. Given the entangled and complex climatic role of freshwater influxes to the North Atlantic, the close coupling between meltwater discharge and rerouting and the timing of inferred sub-millennial droughts in southeastern New England between 11.0 and 8.4 ka is striking. The combination of long-term forcing from the diminishing influence of the Laurentide ice sheet and the large summer insolation anomalies may have made the climate system sensitive to tripping the northeastern United States into a drought in response to meltwater releases at the Pleistocene/Holocene transition. Gaining a better understanding of the potential link between drought in southeastern New England and ice/ocean dynamics is important as current and future climate change may make the region more susceptible to severe drought. Given that climate models indicate continued freshening of the North Atlantic in the next century (IPCC, 2007) and that recent instrumental data already show increased freshwater input in the north latitude oceans, we need to consider how this potentially will impact drought frequency and intensity in the region.

7. Acknowledgments

The National Science Foundation (NSF-ESH 0602408 to Shuman and Donnelly) and the Woods Hole Oceanographic Institution, Ocean and Climate Change Institute (to Donnelly) funded this research. Many people contributed to the laboratory and field work of this project: J. Berman, K. Boldt, W. D'Andrea, Z. Fjeldheim, M. Gomes, A. and H. Henderson, J. Hou, Z. Klaus, S. LaRose, G. and A. Newby, R. Sorell, J. Tierney, M. Toomey, N. Trenholm, T. Webb III, and J. Woodruff. We thank Sarah Haggerty, Tara Huguenin, Sarah Maier and the expertise of the Natural Heritage and Endangered Species Program (Massachusetts Division of Fisheries and Wildlife/Natural Heritage network), Westborough, Massachusetts for plant identifications. Finally, we kindly thank our two reviewers for their time and comprehensive comments, which greatly improved this manuscript.

8. References

Alley, R.B., 2000. Ice-core evidence of abrupt climate changes. Proceedings of the National Academy of Sciences 97, 4, 1331–1334.

Alley, R.B., 2004. GISP2 Ice Core Temperature and Accumulation Data. IGBP PAGES /World Data Center for Paleoclimatology Data Contribution Series #2004-013. NOAA/NGDC Paleoclimatology Program, Boulder CO, USA.

Alley, R.B., 2007. Wally was Right: Predictive Ability of the North Atlantic "Conveyor Belt" Hypothesis for Abrupt Climate Change. Annual Review of Earth and Planetary Sciences 35, 241–272.

Alley, R.B., Ágústsdóttir, A.M., 2005. The 8k event: cause and consequences of a major Holocene abrupt climate change. Quaternary Science Review 24, 1123–149.

Alley, R.B., Mayewski, P., Sowers, T., Stuiver, M., Taylor, K., Clark, P., 1997. Holocene climatic instability: a prominent, widespread event 8200 yr ago. Geology, 25 483–486.

Alley, R.B., Meese, D.A., Shuman, C.A., Gow, A.J., Taylor, K.C., Grootes, P.M., White, J.W.C., Ram, M., Waddington, E.D., Mayewski, P.A., Zielinski, G.A., 1993. Abrupt increase in Greenland snow accumulation at the end of the Younger Dryas event. Nature 362, 527–529

Almquist, H., Dieffenbacher-Krall, A.C., Brown, R., Sanger, D., 2001. An 8000-yr holocene record of lake-levels at Mansell Pond, Central Maine, USA. The Holocene 11, 189–201.

Barber, D.C., Dyke, A., Hillaire-Marcel, C., Jennings, A.E. Andrews, J.T., Kerwin, M.W., Bilodeau, G., McNeely, R., Southon, J., Morehead, M.D., Gagnon, J.-M., 1999. Forcing of the cold event 8,200 years ago by catastrophic drainage of Laurentide lakes. Nature 400, 344–348.

Björck, S., Walker, M.J.C., Cwynar, L.C., Johnsen, S., Knudsen, K.- L., Lowe, J.J., Wohlfarth, B., INTIMATE members, 1998. An event stratigraphy for the Last Termination in the North Atlantic region based on the Greenland ice-core record: a proposal by the INTIMATE group. Journal of Quaternary Science 13, 283–292.

Bond, G., Kromer, B., Beer, J., Muscheler, R., Evans, M.N., Showers, W., Hoffmann, S., Lotti-Bond, R., Hadjas, I., Bonani, G., 2001. Persistent Solar Influence on North Atlantic Climate During the Holocene. Science 294, 2130–2136.

.

Bradley, R.S., England, J.H., 2008. The Younger Dryas and the Sea of Ancient Ice. Quaternary Research 70, 1–10.

Broecker, W.S., 2006. Was the Younger Dryas Triggered by a Flood? Science 312, 1146–1148.

Broecker, W.S., Peteet, D.M., Rind, D., 1985. Does the ocean-atmosphere system have more than one stable mode of operation? Nature 315, 21–26.

Broecker, W.S., Kennett, J.P., Flower, B.P., Teller, J.T., Trumbore, S., Bonani, G., Wolfli, W., 1989. Routing of meltwater from the Laurentide Ice sheet during the Younger Dryas cold episode. Nature 341, 318–321.

Came, R.E., Oppo, D.W., McManus, J.F., 2007. Amplitude and timing of temperature and salinity variability in the subpolar North Atlantic over the past 10 k.y.Geology 35, 4, 315–318.

Clark, P.U., Marshall, S.J., Clarke, G.K.C., Hostetler, S.W., Licciardi, J.M., Teller, J.T., 2001. Freshwater Forcing of Abrupt Climate Change during the Last Glaciation. Science 293, 283–287.

Clark, P.U., Pisias, N.G., Stocker, T.F., Weaver, A.J., 2002. The role of the thermohaline circulation in abrupt climate change. Nature 415, 863–869.

COHMAP Members, 1988. Climatic changes of the last 18,000 years, observations and model simulations. Science 241, 1043–1052.

Dean Jr.,W.E., 1974. Determination of carbonate and organic matter in calcareous sediments and sedimentary rocks by loss on ignition: comparison with other methods. Journal of Sedimentary Petrology 44, 242–248.

Diefendorf, A.F., Patterson, W.P., Mullins, H. T., Tibert, N., Martini, A., 2006. Evidence for high-frequency late Glacial to mid-Holocene (16,800 to 5500 cal yr B.P.) climate variability from oxygen isotope values of Lough Inchiquin, Ireland
Quaternary Research 65, 78–86.

Dieffenbacher-Krall, A.C., Nurse, A.M., 2005. Late-glacial and Holocene record of lake levels of Mathews Pond and Whitehead Lake, northern Maine. Journal of Paleolimnology 34, 283–310.

Digerfeldt, G., 1986. Studies on past lake-level fluctuations. In: Berglund, B.E., (Ed.), Handbook of Holocene palaeoecology and palaeohydrology. John Wiley and Sons, Chichester, UK, pp. 127–142.

Donnelly, J.D., Bertness, M.D., 2001. Rapid shoreward encroachment of salt marsh cordgrass in response to accelerated sea-level rise. Proceedings of the National Academy Sciences 98, 4218–4223.

Donnelly, J.D., Bryant, S. S., Butler, J., Dowling, J., Fan, L., Hausmann, N., Newby, P., Shuman, B., Stern, J., Westover, K., Webb III, T., 2001. 700 yr sedimentary record of intense hurricane landfalls in southern New England. Geological Society of America Bulletin 113, 6, 714–727.

Donnelly, J.D., Driscoll, N.W., Uchupi, E., Keigwin, L.D., Schwab, W.C., Thieler, E.R., Stephen A. Swift, S.A., 2005. Catastrophic meltwater discharge down the Hudson Valley: A potential trigger for the Intra-Allerød cold period. Geology 33, 2, 89–92.

Ellis, C.R.W., Chapman, M.R., Hall, I.R., 2006. Surface and Deep Ocean Interactions During the Cold Climate Event 8200 Years Ago. Science 312, 1929–1932.

Firestone, R.B., West, A., Kennett, J.P., Becker, L., Bunch T.E., Revay, Z.S., Schultz, P.H., Belgya, T., Kennett, D.J., Elandson, D.J., Dickerson, O.J., Goodyear, A.C., Harris, R.S., Howard, G.A., Kloosterman, J.B., Lechler, P., Mayewski, P.A., Montgomery, J., Poreda, R., Darrah, T., Que Hee, S.S., Smith, A.R., Stich, A., Topping, W., Wittke, J.H., Wolbach, W.S., 2007. Evidence for an extraterrestrial impact 12,900 years ago that contributed to the megafaunal extinctions and the Younger Dryas cooling. Proceedings of the National Academy of Science 104, 41, 16016–16021.

Fisher, T.G., Smith, D.G., Andrews, J.T., 2002. Preboreal oscillation caused by a glacial Lake Agassiz flood. Quaternary Science Reviews 21, 873–878.

Fleitmann, D., Mudelsee, M., Burns, S.J., Bradley, R.S., Kramers, J., Matter, A., 2008. Evidence for a widespread climatic anomaly at around 9.2 ka before present. Paleoceanography 23, 1–6.

Guiles-Ellis, K., Mullins, H.T., Patterson, W.P., 2004. Deglacial to middle Holocene (16,600 to 6000 calendar years BP) climate change in the northeastern United States inferred from multi-proxy stable isotope data, Seneca Lake, New York. Journal of Paleolimnology 31, 343–361.

Hald, M., Hagen, S., 1998. Early Preboreal cooling in the Nordic Seas region triggered by meltwater. Geology 26, 7, 615–618.

Hansen, B.P., Lapham, W.W., 1992. Geohydrology and Simulated Groundwater Flow, Plymouth–Carver aquifer, Southeastern Massachusetts. United States Geological Survey Water Resources Investigation Report 90– 4204, Marlborough, Massachusetts.

Harrison, S.H., 1989. Lake-level and climate changes in eastern North America. Climate Dynamics 3, 157–167.

Hou, J., Huang, Y., Wang, Y., Shuman, B., Oswald, W.W., Faison, E., Foster, D.R., 2006. Postglacial climate reconstruction based on compound-specific D/H ratios of fatty acids from Blood Pond, New England. Geochemistry Geophysics Geosystems 7, 1–7.

Hua, Q., Barbetti, M., 2004. Review of Tropospheric Bomb ^{14}C Data for Carbon Cycle Modeling and Age Calibration Purposes. Radiocarbon 46, 1273–1298.

Huang, Y., Shuman, B.N., Wang, Y., Webb III, T., 2002. Hydrogen isotope ratios of palmitic acid in lacustrine sediments record late-Quaternary climate variations. Geology 30, 1103–1106.

IPCC, 2007. Climate Change 2007: Synthesis Report. Contribution of Working Groups I, II and III to the Fourth Assessment Report of the Intergovernmental Panel on Climate Change, Core Writing Team, Pachauri, R.K and Reisinger, A., (Eds.), IPCC, Geneva, Switzerland.

Johnsen, S., Clausen, H., Dansgaard, W., Fuhrer, K., Gundestrup, N., Hammer, C., Iversen, P., Jouzel, J., Stauffer, B., Steffensen, J., 1992. Irregular glacial interstadials recorded in a new Greenland ice core. Nature 359, 311–313.

Karl, T.R., Williams Jr., C.N., Quinlan, F.T., 1990. NDP-019/R. United States Historical Climatology Network (HCN) Serial Temperature and Precipitation Data. National Oceanic and Atmospheric Administration, National Climatic Data Center, Asheville, North Carolina.

Keigwin, L.D., Sachs, J.P., Rosenthal, Y., Boyle, E.A., 2005. The 8200 year B.P. event in the slope water system, western subpolar North Atlantic. Paleoceanography 20, 1–14.

Kennett, D.J., Kennett, J.P., West, A., Mercer, C., Que Hee, S.S., Bement, L., Bunch, T.E., Sellers, M. Wolbach, W.W., 2009. Nanodiamonds in the Younger Dryas Boundary Sediment Layer. Science 323, 94.

Kirby, M.E., Mullins, H.T., Patterson, W.P., Burnett, A.W., 2002. Late glacial–Holocene atmospheric circulation and precipitation in the northeast United States inferred from modern calibrated stable oxygen and carbon isotopes. Geological Society of America Bulletin 114, 10, 1327–1340.

Kleiven, H.F., Kissel, C., Laj, C., Ninnemann, U.S., Richter, T.O., Cortijo, E., 2008. Reduced North Atlantic Deep Water Coeval with the Glacial Lake Agassiz Freshwater Outburst. Science 319, 60–64.

Larson, G.J., 1982. Nonsynchronous Retreat of Ice Lobes from Southeastern Massachusetts. In: Late Wisconsin Glaciation of New England, Larson, G.J., Stone, B.D., (Eds.), Kendall Hunt Publishing Co., Dubuque, Iowa, pp. 101–114.

Lavoie, M., Richard, P.J.H., 2000. Postglacial water-level changes of a small lake in southern Quebec, Canada. The Holocene 10, 621– 634.

LeGrande, A.N., Schmidt, G.A., Shindell, D.T., Field, C.V., Miller, R.L., Koch, D.M., Faluvegi, G., Hoffmann, G., 2006. Consistent simulations of multiple proxy response to an abrupt climate change event. Proceedings of the National Academy of Scientists 103, 4, 837–842.

Levesque, A.J., Cwynar, L.C., Walker, I.R., 1997. Exceptionally steep north-south gradients in lake temperatures during the last deglaciation. Nature 385, 423–426.

Levesque, A.J., Mayle, F., Walker, I.R., Cwynar, L.C., 1993. A previously unrecognized late glacial cold event in eastern North America. Nature 361, 623–626.

Li, Y-X., Yu, Z., Kodama, K., 2006. Sensitive moisture response to Holocene millennial-scale climate variations in the Mid-Atlantic region, USA. The Holocene 16, 8, 1043–1048.

Licciardi, J.M., Teller, J.T., Clark, P.U., 1999. Freshwater routing of the Laurentide Ice-Sheet during the last deglaciation. In: Clark, P.U., Webb, R.S., Keigwin, L.D. (Eds.) Mechanisms of Global climate change at millennial time scales. American Geophysical Union, Washington, DC. Geophysical Monographs 112, pp.177–201.

Lowell, T.V., Fisher, T.G., Comer, G.C., Hajdas, I., Waterson, N., Glover, K., Loope, H. M., Schaefer, J.M., Rinterknecht, V., Broecker, W., Denton, G., Teller, J.T., 2005. Testing the Lake Agassiz Meltwater Trigger for the Younger Dryas. EOS, Transactions American Geophysical Union 86, 40, 365–373.

Magny, M., Begeot, C., 2004. Hydrological changes in the European midlatitudes associated with freshwater outbursts from Lake Agassiz during the Younger Dryas event and the early Holocene. Quaternary Research 61, 181–192.

Marshall, J.D., Lang, B., Crowley, S.F., Weedon, G.P., van Calsetren, P., Fisher, E.H., Holme, R., Holmes, J.A., Jones, R.T., Bedfore, A., Brooks, S.J., Bloemendal, J., Kiriakoulakis, K., Ball, J.D., 2007. Terrestrial impact of abrupt changes in the North Atlantic thermohaline circulation: Early Holocene, UK. Geology 35, 7, 639–642.

McManus, J.F., Francois, R., Gherardi, J.-M., Keigwin, L.D., 2004. Collapse and rapid resumption of Atlantic Meriodional circulation linked to deglacial climate changes. Nature 428, 834–837.

Meissner, K.J., Clark, P.U., 2006. Impact of floods versus routing events on the thermohaline circulation. Geophysical Research Letters 33, 1–4.

Mott, R.J., Matthews Jr., J.V., Grant, D.R., Beke, G.J., 1986. A late glacial buried organic profile near Brookside, Nova Scotia. Geological Survey of Canada Paper 86–1B, 289–294.

Muller, S.D., Richard, P.J.H., Guiot, J., de Beaulieu, J.-L., Fortin, D., 2003. Post-glacial climate in the Saint Laurence lowlands, southern Quebec: pollen and lake-level evidence. Palaeogeography, Palaeoclimatology, Palaeoecology 193, 51–72.

Namias, J., 1966. Nature and Possible Causes of the Northeastern United Sates Drought During 1962-65. Monthly Weather Review 94, 9, 543–554.

Newby, P., Killoran, P., Waldorf, M., Shuman, B., Webb III, T., Webb, R., 2000. 14,000 years of sediment, vegetation and water level changes at the Makepeace Cedar Swamp, southeastern Massachusetts. Quaternary Research 53, 352–368.

Peteet, D.M., Vogel, J.S., Nelson, D.E., Southon, J.R., Nickmann, R.J., Heusser, L.E., 1990. Younger Dryas climatic reversal in northeastern USA? AMS ages for an old problem. Quaternary Research 33, 219–230.

Rahmstorf, S., 1995, Bifurcations of the Atlantic thermohaline circulation in response to changes in the hydrological cycle: Nature 378, 145–149.

Rasmussen, S.O., Andersen, K.K., Svensson, A.M., Steffensen, J.P., Vinther, B.M., Clausen, H.B., Siggaard-Andersen, M-L., Johnsen, S.J., Larsen, L.B., Dahl-Jensen, D., Bigler, M., Rotheetberger, R., Fischer, H., Goto-Azuma, K., Hansson, M.E., Ruth, U., 2006. A new Greenland ice core chronology for the last glacial termination. Journal of Geophysical Research 111, 1–16.

Rasmussen, S.O., Vinther, B.M., Clausen, H.B., Andersen, K.K., 2007. Early Holocene climate oscillations recorded in three Greenland ice cores. Quaternary Science Reviews 26, 1907–1194.

Rayner, N.A., Parker, D.E., Horton, E.B., Folland, C.K., Alexander, L.V., Rowell, D.P., Kent, E.C., Kaplan, A., 2003. Global analyses of sea surface temperature, sea ice and night marine air temperature since the late nineteenth century. Journal of Geophysical Research 108, D14, 1–37.

Reimer, P.J., Baillie, M.G.L., Bard, E., Baylis, A., Beck, J.W., Bertrand, C.J.H., Blackwell, P.G., Buck, C.E., Burr, G.S., Cutler, K.B., Damon, P.E., Edwards, R.L., Fairbanks, R.G., Friedrich, M., Guilderson, T.P., Hogg, A.G., Hughen, K.A., Kromer, B., 2004a. IntCal04 terrestrial radiocarbon age calibration, 0–26 cal kyr BP. Radiocarbon 46, 1029–1058.

Reimer, P.J., Brown, X., Reimer, R., 2004b. Discussion: Reporting and Calibration of Post-Bomb14C Data. Radiocarbon 46, 1299–1304.

Richard, P.J.H., Occhieti, S., 2005. ^{14}C chronology for ice retreat and inception of Champlain Sea in the St. Lawrence Lowlands, Canada. Quaternary Research 63, 353–358.

Ridge, J.C., 2003. The last deglaciation of the northeastern United States: A combined varve, paleomagnetic, and calibrated 14C chronology. New York State Museum Bulletin 497, 15–45.

Rind, D., Peteet, D., Broecker, W., McIntyre, A., Ruddiman, W., 1986. The impact of cold North Atlantic sea-surface temperatures on climate: implications for the Younger Dryas cooling (11-10k). Climate Dynamics 1, 3–33.

Robinson Jr.,G.R., Kapo, K.E., 2003. Generalized lithology and lithogeochemical character of near-surface bedrock in the New England region. U.S. Dept. of the Interior, U.S. Geological Survey. Reston, VA. http://pubs.usgs.gov/of/2003/of03-225/.

Rohling, E., Pälike, J., 2005. Centennial-scale climate cooling with a sudden cold event around 8200 years ago. Nature 434, 975–979.

Ruddiman, W.F., McIntyre, A., 1981. The North Atlantic Ocean during the last deglaciation. Paleogeography Paleoclimatology Paleoecology 35, 145–214.

Shemesh, A., Peteet, D., 1998. Oxygen isotopes in fresh water biogenic opal-Northeastern US Alleröd-Younger Dryas temperature shift. Geophysical Research Letters 25, 11, 1935–1938.

Shuman, B., Bartlein, P., Logar, N., Newby, P., Webb III, T., 2002. Parallel Climate and Vegetation Responses to the Early-Holocene Collapse of the Laurentide Ice-Sheet. Quaternary Science Reviews 21, 1793–1805.

Shuman, B., Bravo, J., Kaye, J., Lynch, J.A., Newby, P., Webb III, T., 2001. Late-Quaternary Water-Level Variations and Vegetation History at Crooked Pond, Southeastern Massachusetts. Quaternary Research 56, 401–410.

Shuman, B., Donnelly, J.D., 2006. The influence of seasonal precipitation and temperature regimes on lake levels in the northeastern United States during the Holocene. Quaternary Research 65, 44–56.

Shuman, B., Donnelly, J.D., Newby, P., 2009. Abrupt Climate Change as a Catalyst of Ecological Change in the Northeast U.S. over the Past 15,000 Years. Quaternary Science Reviews 28, 1167-1296.

Shuman, B., Newby, P., Donnelly, J., Tarbox, A., Webb III, T., 2005. A record of late-Quaternary moisture-balance change and vegetation response in the White Mountains, New Hampshire. Annals of the American Association of Geographers 95, 237– 248.

Stanford, J.D., Rohling, E.J., Hunter, S.E., Roberts, A.P., Rasmussen, S.O., Bard, E., McManus, J., Fairbanks, R.G., (2006). Timing of meltwater pulse 1a and climate responses to meltwater injections. Paleoceanography 21, 1–9.

Stuiver, M., Grootes, P., 2000. GISP2 oxygen isotope ratios. Quaternary Research 53, 277–284.

Swain, P.C., Kearsley, J.B., 2001. Classification of the Natural Communities of Massachusetts, 1.3. Natural Heritage & Endangered Species Program, Massachusetts Division of Fisheries & Wildlife. Westborough, MA.

Teller, J., Leverington, D., 2004. Glacial Lake Agassiz: A 5000 yr history of change and its relationship to the $\delta^{18}O$ record of Greenland. Geological Society of America Bulletin 116, 5/6, 729–742.

Teller, J., Leverington, D., Mann, J., 2002. Freshwater outbursts to the oceans from glacial Lake Agassiz and their role in climate change during the last deglaciation. Quaternary Science Reviews 21, 879–887.

Teller, J., Boyd, M., Yange, A., Kor, P.S.G., Fard, A.M., 2005. Alternative routing of Lake Agassiz overflow during the Younger Dryas: new dates, paleotopography, and a re-evaluation. Quaternary Science Reviews 24, 1890–1905.

van Geel, B., Raspopov, O.M., Renssen, H., van der Plicht, J., Dergachev, V.A., Meijer, H.A.J., 1999. The role of solar forcing upon climate change. Quaternary Science Reviews 18, 331–338.

Veski, S., Heikki, S., Ojala, A., 2004. Cold event at 8200 yr B.P. recorded in annually laminated lake sediments in eastern Europe. Geology 32, 681–684.

Wandle Jr., W.S., 1991. Massachusetts Floods and Droughts. In: Paulson, R.W., Chase, E.B., Roberts, R.S., Moody, D.W. National Water Summary 1988-1989: hydrologic events and floods and droughts. U.S. Geological Survey Water-Supply Paper 2375, pp. 327–334.

Webb, R. S., 1990. Late-Quaternary Lake-Level Changes in the Northeastern United States. Ph.D. Thesis, Brown University, Providence, RI.

Webb, R.S., Anderson, K.H., Webb III, T., 1993. Pollen response-surface estimates of late-Quaternary changes in the moisture balance of the northeastern United States. Quaternary Research 40, 213–227.

Webb, R.S., Webb III, T., 1988. Rates of sediment accumulation in pollen cores from small lakes and mires of eastern North America. Quaternary Research 30, 284–297.

Webb, T. III, Bartlein, P.J., Harrison, S., Anderson, K.H., 1993. Vegetation, lake level, and climate change in eastern North America. In: Wright Jr., H.E., Kutzbach, J.E., Webb III, T., Ruddiman, W.F. Street-Perrott, A., Bartlein, P.J. (Eds.), Global Climates Since the Last Glacial Maximum. University of Minnesota Press, Minneapolis, MN, pp. 415–467.

Wiersma, A.P., Renssen, H., 2006. Model-data comparison for the 8.2 ka BP event: confirmation of a forcing mechanism by catastrophic drainage of Laurentide Lake. Quaternary Science Reviews 25, 63–88.

Wiersma, A.P., Renssen, H., Goosse, E.T., Fichefet, T., 2006. Evaluation of different freshwater forcing scenarios for the 8.2 ka BP event in a coupled climate model. Climate Dynamics 27, 831–849.

Winkler, M.G., 1985. A 12,000-year history of vegetation and climate for Cape Cod, Massachusetts. Quaternary Research 23, 235–250.

Yu, Z., Eicher, U., 1998. Abrupt Climate Oscillations During the Last Deglaciation in Central North America. Science 282, 2235–2238.

Yu, Z., Eicher, U., 2001. Three amphi-Atlantic century-scale cold events during the Bølling-Alleröd warm period. Géographie physique et Quaternaire 55, 2, 171–179.

Yu, Z., Wright, H.E., 2001. Response of interior North America to abrupt climate oscillations in the North Atlantic region during the last deglaciation. Earth Science Reviews 52, 4, 333–369.

Table 2-1. Radiocarbon Dates from New Long Pond and Rocky Pond

OSAMS Lab No. Lab No.	Depth Below Sediment Water Interface (cm)	Type of Date and Material	14C Age	Age Error	Cal yr B.P. Median	2-sigma range	Prob.
New Long Pond 161							
OS-69031	205.5	1-2 mm plant fragments	10750	70	12797	12668-12875	1
OS-68919	274	1-2 mm plant fragments	11900	80	13764	13572-13964	1
New Long Pond 65							
OS-46414	81.5	rootlets	4450	30	5103	4892-4898	0.004
						4912-4927	0.011
						4960-5087	0.472
						5100-5141	0.081
						5159-5284	0.433
OS-44431[a]	119.5	wood	4890	200	5626	5049-5194	0.044
						5212-6023	0.939
						6049-6063	0.003
						6078-6114	0.009
						6153-6175	0.005
OS-46829	131.5	rootlets	6050	45	6902	6755-6763	0.006
						6779-7011	0.98
						7129-7145	0.015
OS-46415	151.5	rootlets	6690	45	7560	7476-7624	0.973
						7636-7654	0.027
OS-50149	170.5	> 500 µm stems	7720	60	8501	8405-8597	1
OS-44427[a]	199.5	organic matter	8140	200	9064	8585-9504	0.996
						9506-9518	0.004
OS-42079[a]	211.5	bulk sediment	8390	45	9426	9294-9498	1

OSAMS Lab No.	Depth Below	Type of Date	14C Age	Age	Cal yr B.P.	2-sigma range	Prob.
	Sediment Water	**and Material**		**Error**			
Lab No.	**Interface (cm)**				**Median**		
OS-42283[a]	224.5	> 500 µm organics	9180	170	10369	9781-9850	0.012
						9861-9878	0.003
						9884-10791	0.971
						10967-11002	0.007
						11028-11064	0.007
OS-44313[a]	241.5	*Tsuga* cone	9450	45	10686	10566-10791	0.946
						10969-11002	0.026
						11029-11063	0.028
OS-42080[a]	364.5	> 500 µm organics	11700	70	13553	13390-13727	1
OS-42081[a]	426.5	180-500 µm organics	11150	55	13051	12932-13170	1
New Long Pond 53							
OS-69071	434.5	macrofossils >63 µm	11800	80	13657	13443-13812	1
OS-68998	460	macrofossils >63 µm	12400	55	14412	14129-14809	1
New Long Pond 43							
OS-63087 [a]	6	rootlets	>Mod.				
OS-63138	15	rootlets	705	30	666	564-588	0.152
						643-691	0.848
OS-65925	36.5	rootlets	1300	35	1240	1174-1294	1
OS-63108	45	rootlets	1860	35	1796	1714-1875	1
OS-63102	48	> 500 µm organics	1800	25	1736	1628-1655	0.089
						1691-1819	0.911
OS-65937	52.25	rootlets	2040	40	1999	1899-1913	0.033
						1920-2116	0.967
OS-63137	61	rootlets	2340	30	2350	2320-2377	0.822
						2383-2459	0.178
OS-65936	67.5	rootlets	2630	40	2756	2624-2627	0.006

OSAMS Lab No.	Depth Below	Type of Date	14C Age	Age	Cal yr B.P.	2-sigma range	Prob.
	Sediment Water	**and Material**		**Error**			
Lab No.	**Interface (cm)**				**Median**		
						2714-2813	0.937
						2816-2844	0.057
OS-63104	73	rootlets	2760	35	2852	2778-2946	1
OS-66077	83.75	rootlets	3320	30	3542	3472-3632	1
OS-65926	91.25	rootlets	3460	30	3733	3641-3668	0.116
						3679-3830	0.884
OS-63105	98	rootlets	3860	35	4290	4156-4205	0.144
						4222-4412	0.856
OS-63040	102	rootlets	3850	35	4273	4154-4209	0.211
						4216-4408	0.789
OS-66078	104.5	rootlets	4090	35	4600	4444-4481	0.058
						4514-4658	0.651
						4666-4708	0.089
						4755-4812	0.202
OS-63546	113	rootlets	4080	40	4583	4438-4488	0.12
						4496-4655	0.631
						4667-4707	0.076
						4656-4811	0.174
OS-63109	118	rootlets	4690	40	5406	5317-5481	0.846
						5530-5579	0.154
OS-65932	124.25	rootlets	4490	60	5145	4891-4899	0.005
						4909-4928	0.013
						4959-5313	0.982
OS-63103	132	rootlets	4920	35	5642	5594-5719	1
OS-63039	135.5	rootlets	5010	40	5746	5653-5797	0.715
						5802-5893	0.372
OS-63142	210	rootlets	7650	45	8444	8358-8540	1

OSAMS Lab No.	Depth Below	Type of Date	14C Age	Age	Cal yr B.P.	2-sigma range	Prob.
	Sediment Water	**and Material**		**Error**			
Lab No.	**Interface (cm)**				**Median**		
OS-63101	241.5	rootlets	7980	50	8850	8648-8675	0.042
						8683-9000	0.958
OS-63141 [2]	247	> 500 µm organics	9250	45	10423	10273-10557	1
OS-65933	282	> 500 µm organics	9140	40	10288	10226-10412	1
OS-65930 [3]	299	180-500 µm organics	8720	70	9705	9538-9921	0.979
						10075-10115	0.021
OS-63140	299	> 500 µm organics	9050	45	10219	10160-10273	1
OS-63136	321.5	> 500 µm organics	10850	60	12851	12793-12915	1
OS-63084	332.5	> 500 µm organics	10900	65	12874	12808-12952	1
OS-63080	355.5	> 500 µm organics	12450	75	14512	14161-14916	1
New Long Pond 31							
OS-63139	22	rootlets	1300	35	1240	1174-1294	1
OS-65912	33.5	rootlets	2220	35	2232	2151-2331	1
OS-65931	59.5	leaf fragments	4580	35	5298	5057-5114	0.161
						5117-5186	0.196
						5216-5222	0.005
						5238-5241	0.002
						5266-5327	0.45
						5386-5447	0.185
OS-63143	74.5	> 500 µm organics	5430	35	6239	6184-6296	1
OS-63144	90.5	rootlets	6290	40	7218	7034-7036	0.002
						7157-7316	0.998
OS-63145	97.5	rootlets	6580	45	7482	7426-7524	0.815
						7530-7566	0.185
OS-63111	108	180-500 µm organics	7380	60	8208	8042-8340	1
OS-68703	151.5	bract from unidentifed cone	8800	45	9831	9633-9643	0.006
						9659-9956	0.845

OSAMS Lab No.	Depth Below	Type of Date	14C Age	Age	Cal yr B.P.	2-sigma range	Prob.
	Sediment Water	**and Material**		**Error**			
Lab No.	**Interface (cm)**				**Median**		
						9988-10014	0.021
						10021-10042	0.016
						10059-10149	0.111
OS-65935	210.0	macro charcoal	10250	85	12000	11622-11677	0.022
						11691-12385	0.978
Rocky Pond 96							
OS-60097	74.5	bulk sediment	5320	35	6191	5992-6208	1
OS-49302	110.5	> 500 µm organics	6160	60	7063	6895-7178	0.955
						7198-7242	0.045
OS-58247	138.5	bulk sediment	7260	30	8091	8009-8164	1
OS-58496	184.5	bulk sediment	9120	35	10259	10218-10302	0.809
						10313-10392	0.191
OS-49321	210.5	> 500 µm organics	9400	60	10631	10430-10462	0.018
						10484-10784	0.977
						11040-11055	0.005
OS-58551	247.5	bulk sediment	10650	95	12690	12393-12843	1
OS-63136	290.5	> 500 µm organics	10850	55	12851	12799-12908	1
Rocky Pond 110							
OS-69598	88.5	bulk sediment	6260	30	7208	7029-7041	0.011
						7070-7077	0.006
						7087-7094	0.005
						7101-7110	0.007
						7156-7266	0.971
OS-69589	128.5	bulk sediment	7220	45	8032	7961-8077	0.693
						8081-8161	0.307
OS-69527	155.5	bulk sediment	7960	40	8838	8648-8675	0.053

OSAMS Lab No.	Depth Below	Type of Date	14C Age	Age	Cal yr B.P.	2-sigma range	Prob.
	Sediment Water	**and Material**		**Error**			
Lab No.	**Interface (cm)**				**Median**		
						8683-8991	0.947
OS-63099	185.5	macrofossil	8770	40	9800	9563-9571	0.004
						9595-9918	0.986
						10097-10112	0.01
OS-63300	207.5	> 500 µm organics	8900	200	9973	9530-10439	0.988
						10455-10491	0.012
OS-63286	247.5	> 500 µm organics	9300	160	10519	10187-10898	0.931
						10918-11088	0.079
OS-63010	347.5	1-2 mm plant fragments	10400	65	12292	12052-12412	0.789
						12445-12621	0.211
OS-63086	432.5	bulk sediment	11300	70	13200	13064-13308	1
OS-62980	519.5	bulk sediment	12300	65	14200	13991-14633	1
OS-62982	548.5	bulk sediment	12750	55	15057	14794-15304	1

[a] Dates previously published in Shuman and Donnelly (2006).

[b] Modern date calibrated using CALIbomb.

[c] Excluded as too old in age model.

[d] Excluded as too young in age model.

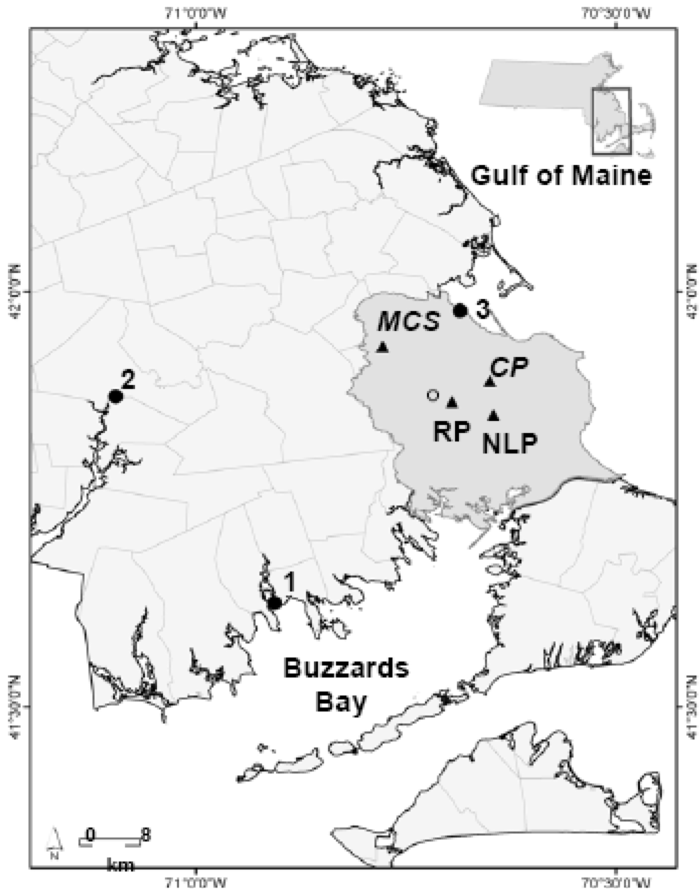

Figure 2-1. Location of study sites, Rocky Pond (RP) and New Long Pond (NLP), and two sites from previous studies mentioned in text, Crooked Pond (*CP*) and Makepeace Cedar Swamp (*MCS*), within the Plymouth-Carver aquifer (shaded in darker grey). Open circle is location of ground water monitoring well PW-22 and filled circles (1–3) are precipitation stations (1-New Bedford, 2-Taunton, 3-Plymouth). Inset shows the location of the study area within Massachusetts.

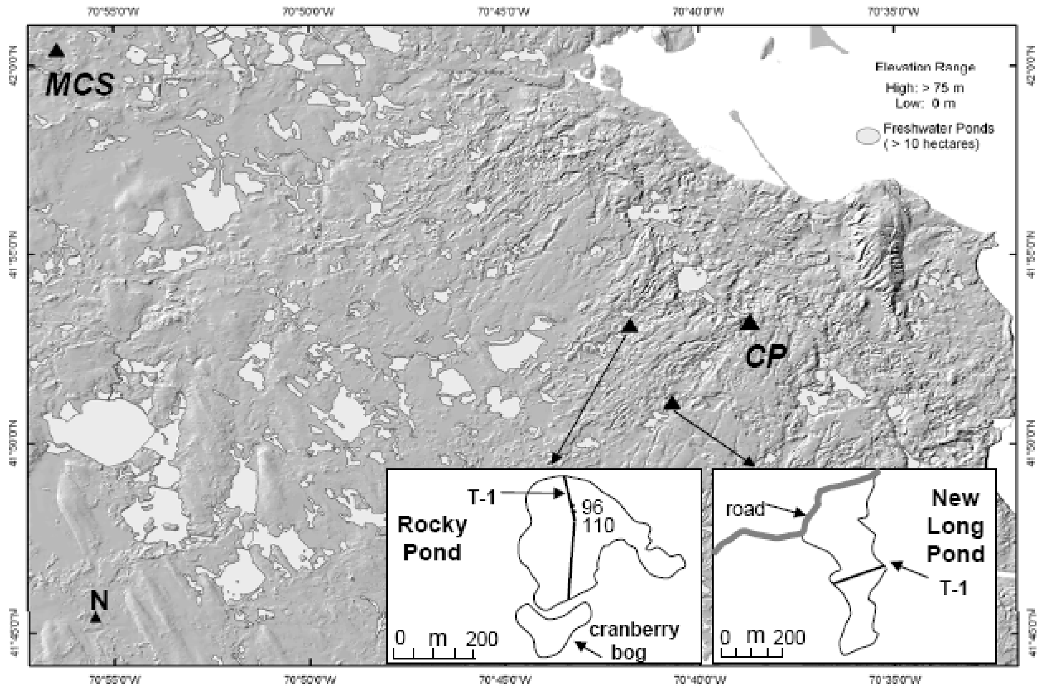

Figure 2-2. Location of study sites New Long Pond and Rocky Pond within the low relief topography characteristic of the Plymouth-Carver aquifer; labeled black triangles for Makepeace Cedar Swamp (*MCS*) and Crooked Pond (*CP*) show proximity of these previously studied sites. Insets show aerial views of Rocky Pond and New Long Pond and locations of transects from which cores were collected. The two cores used in this study from Rocky Pond are shown on the transect. The 13 cores from New Long Pond cluster too closely to show at this scale (see Fig. 4).

Figure 2-3. A portion of the southern shoreline at New Long Pond, showing broad, sandy shoreline seasonal pondshore vegetation and pondweed, aquatic plants, shrub border and typical pitch pine/scrub oak vegetation. Detailed vegetation is described in the text. A strandline is visible along the shore; photograph taken in October, 2005.

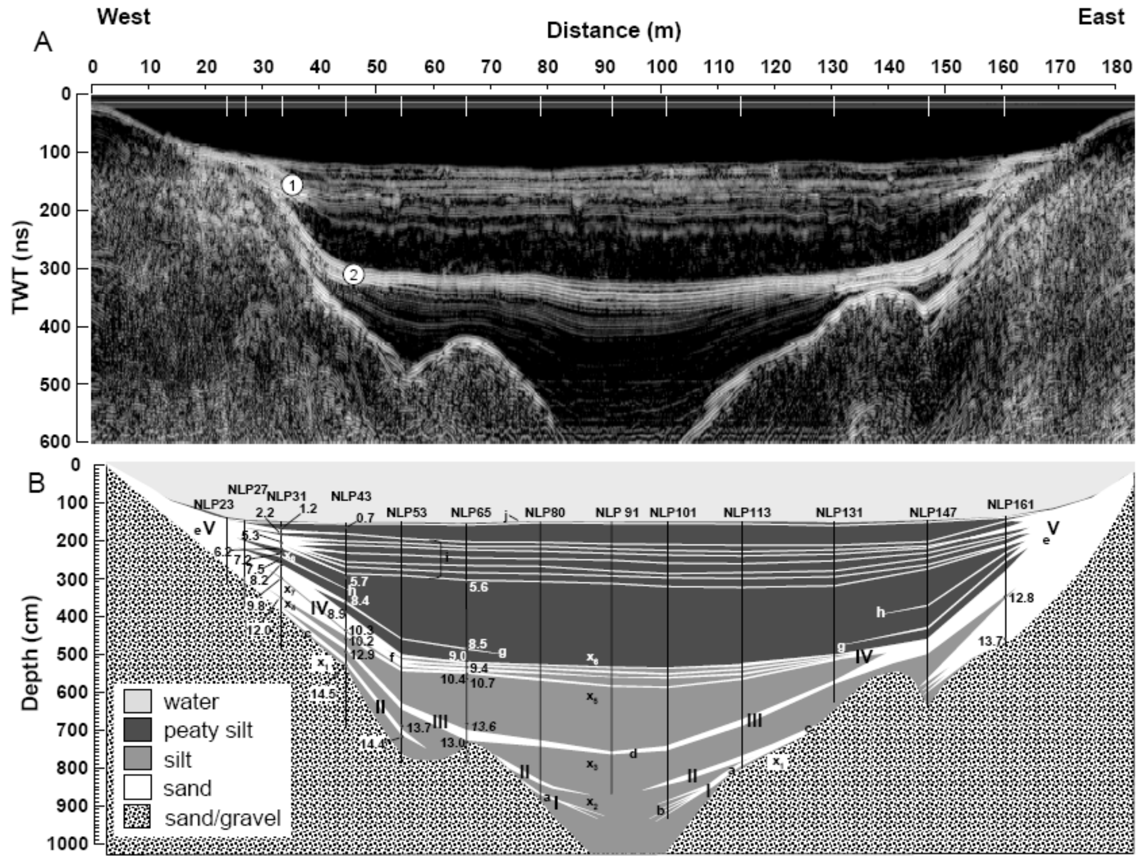

Figure 2-4. A. West-to-east ground penetrating radar profile from New Long Pond with mid-Holocene (1) and early Holocene (2) sedimentary unconformities identified in Shuman and Donnelly (2006). White ticks marks along distance axis mark locations of 13 cores. B. Reconstructed basin profile from ground penetrating radar data and 13 cores (dark vertical lines) collected along the transect. Units I-V refer to packets of sand layers described in the text; radiocarbon ages are medians of 2σ calibrated ranges and show temporal correlations among sedimentary changes across the basin. The full range for all ages is in Table 1. The radiocarbon date in italics (NLP 65) shows an out-of-sequence age; 12.9 ka in NLP43 represents two closely-spaced radiocarbon dates (see Table 1). Letters a-j refer to sand layers and x_1-x_8 to silt deposition described in the text.

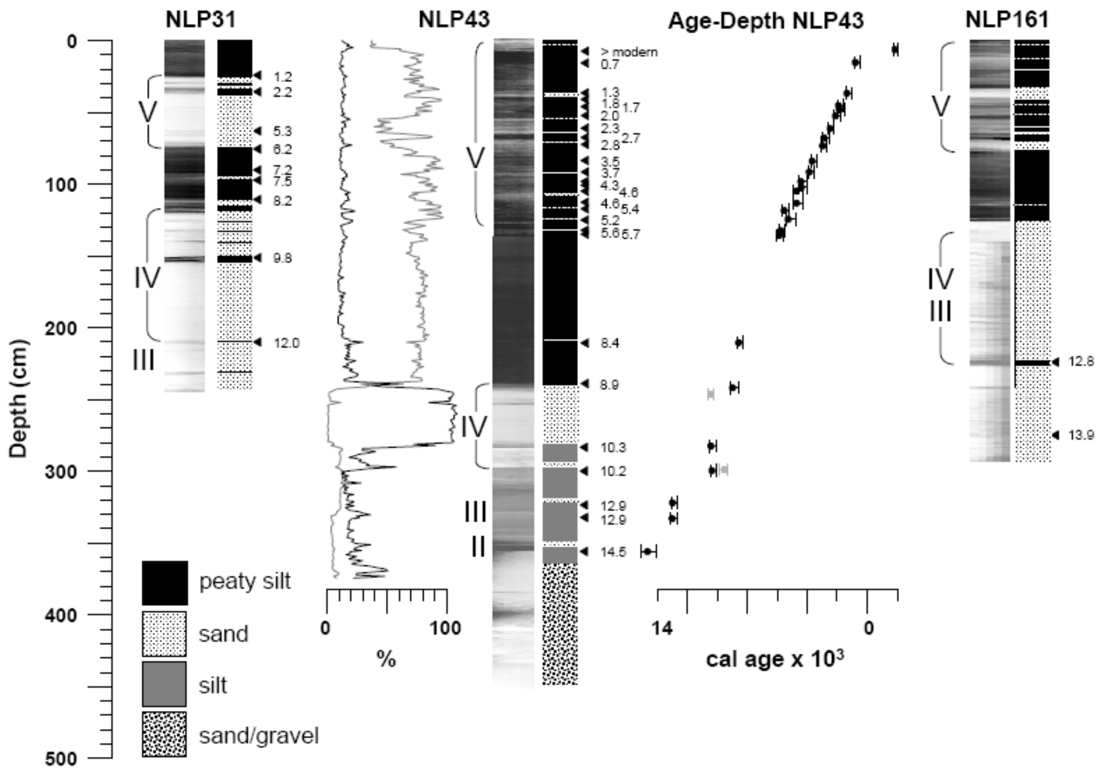

Figure 2-5. Radiographs with calibrated median radiocarbon ages for NLP31, NLP43 and NLP161, respectively. NLP43 data include percent organic matter (gray), percent coarse fraction (black) and age/depth plot for radiocarbon dates (see Table 1). The fall and abrupt rise in percent organic matter ca. 10.4 to 9.0 ka shows the opposite trend to values for percent coarse fraction for the same interval. Gray points on the age/depth plot show AMS dates excluded from the age model; seven of these dates were previously published in Shuman and Donnelly (2006; see Table 1). Correlative packets of sand layers (Units I-V) are shown among the cores.

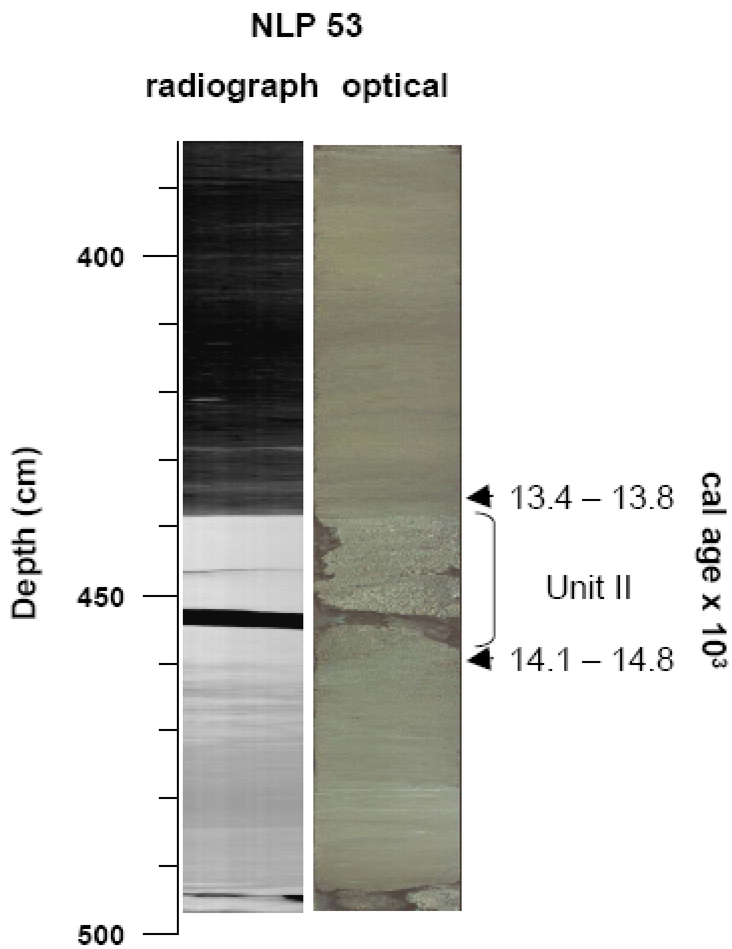

Figure 2-6. Radiograph and optical of NLP53, showing correspondence between changes in density and sediments. Median ages (14.4 and 13.7 ka) bracketing this sand layer in NLP53 define the Unit II low stand.

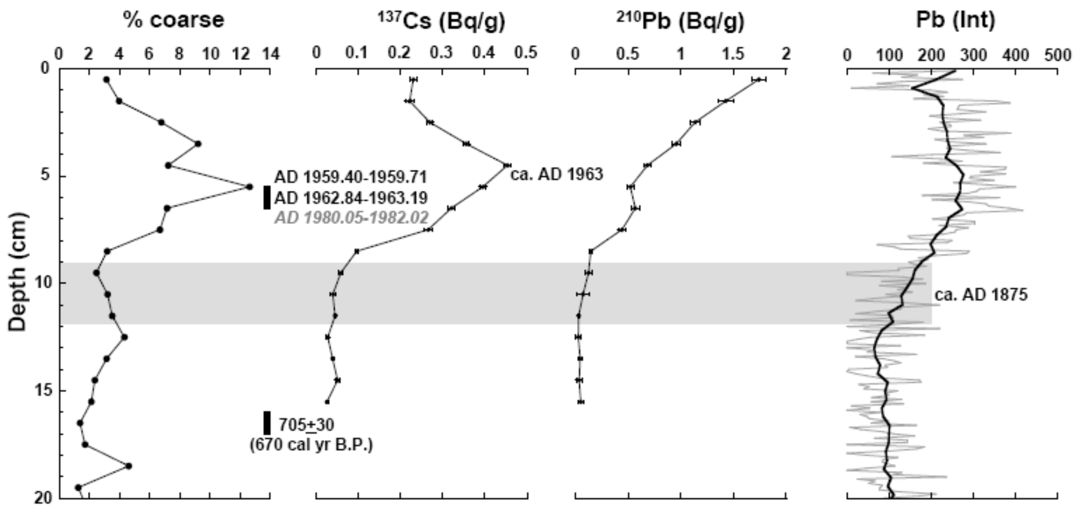

Figure 2-7. Changes in percent coarse fraction with radiometric dating results, using ^{14}C, ^{137}Cs, ^{210}Pb and Pb (Int), from the uppermost 20 cm of NLP43. The grey bar highlights the interval, between ca. 12.0 and 9.0 cm, which shows the rise in Pb (Int) associated with increased industrialization ca. AD 1875. CALIbomb (Reimer et al., 2004b) data ranges for greater than AD 1950 age are shown. Given the correspondence between the ^{137}Cs peak and the older two CALIbomb age ranges, the youngest range can be eliminated (gray).

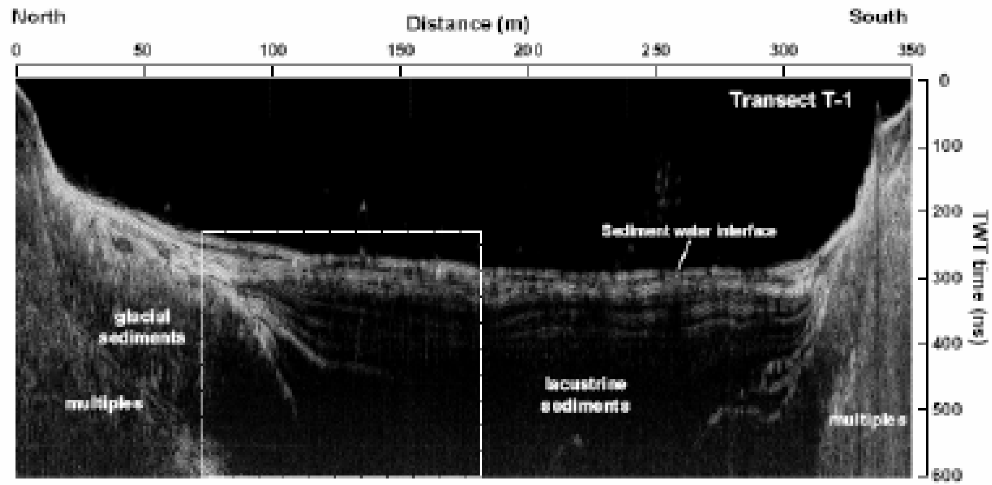

Figure 2-8. North-to-south (T-1) ground penetrating radar profiles from Rocky Pond (for location in basin see Fig. 1). The ground penetrating radar signal attenuated at >12.0 m below modern water. Box indicates enlargement in figure 9.

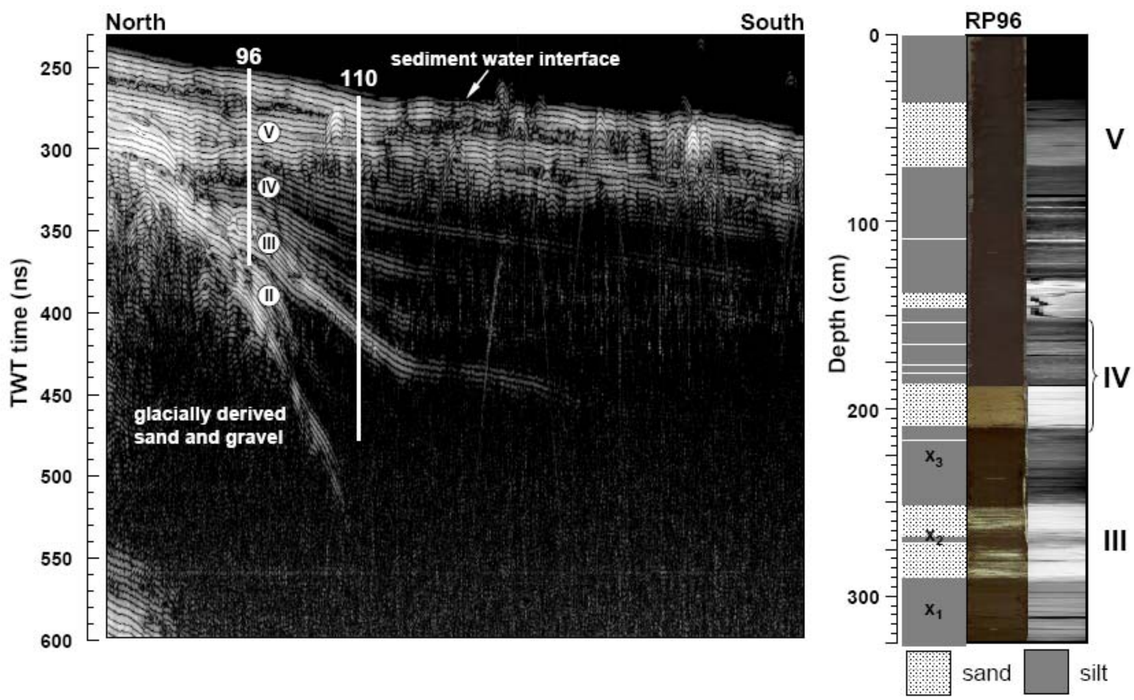

Figure 2-9. Segment of Rocky Pond T-1 ground penetrating radar profile, showing locations of RP96 and RP110 and associated Units II – V. Stratigraphic column, optical image, and radiographic image of RP96 (right). The optical for RP96 shows the distinct changes between silt and sand sediments that are also reflected in changes in density in the adjacent radiograph.

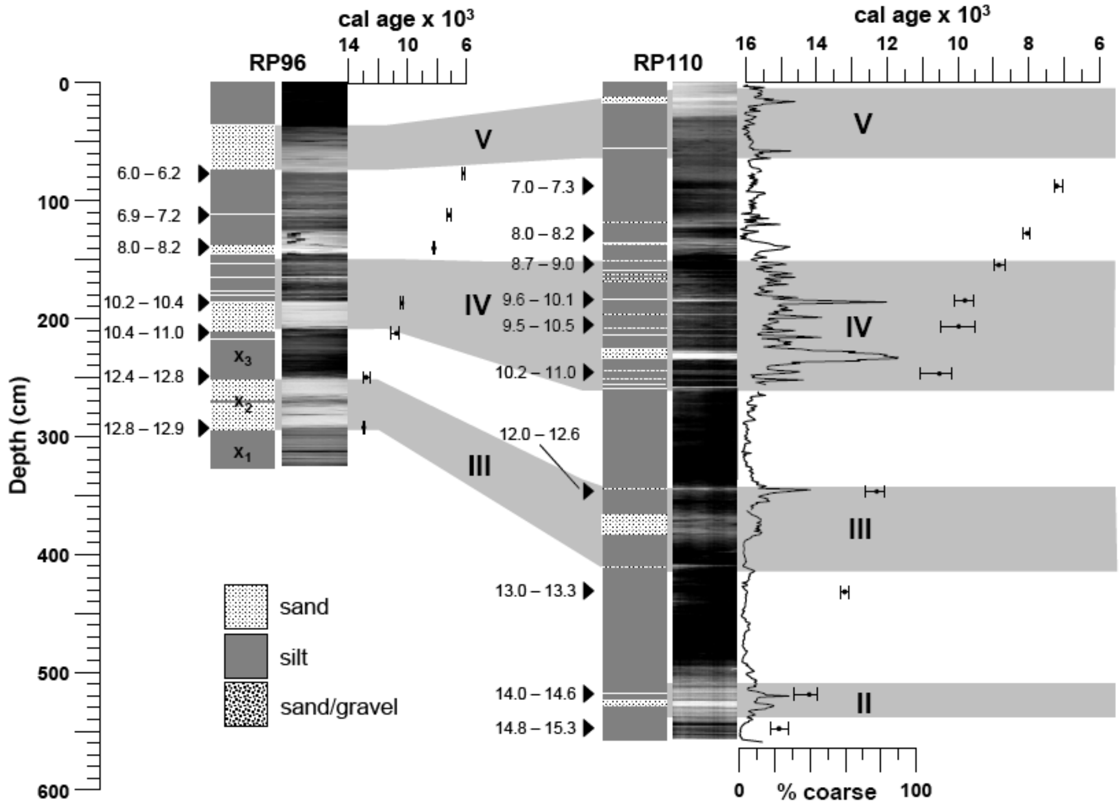

Figure 2-10. Calibrated 2σ age ranges with changes in sediments and radiographs in RP96 and RP110, with age/depth plots. Percent coarse fraction for RP110 is also displayed. Grey bands delineate correlations among packets of sand layers (Units II-V); X_1-X_3 refer to silt deposition described in the text.

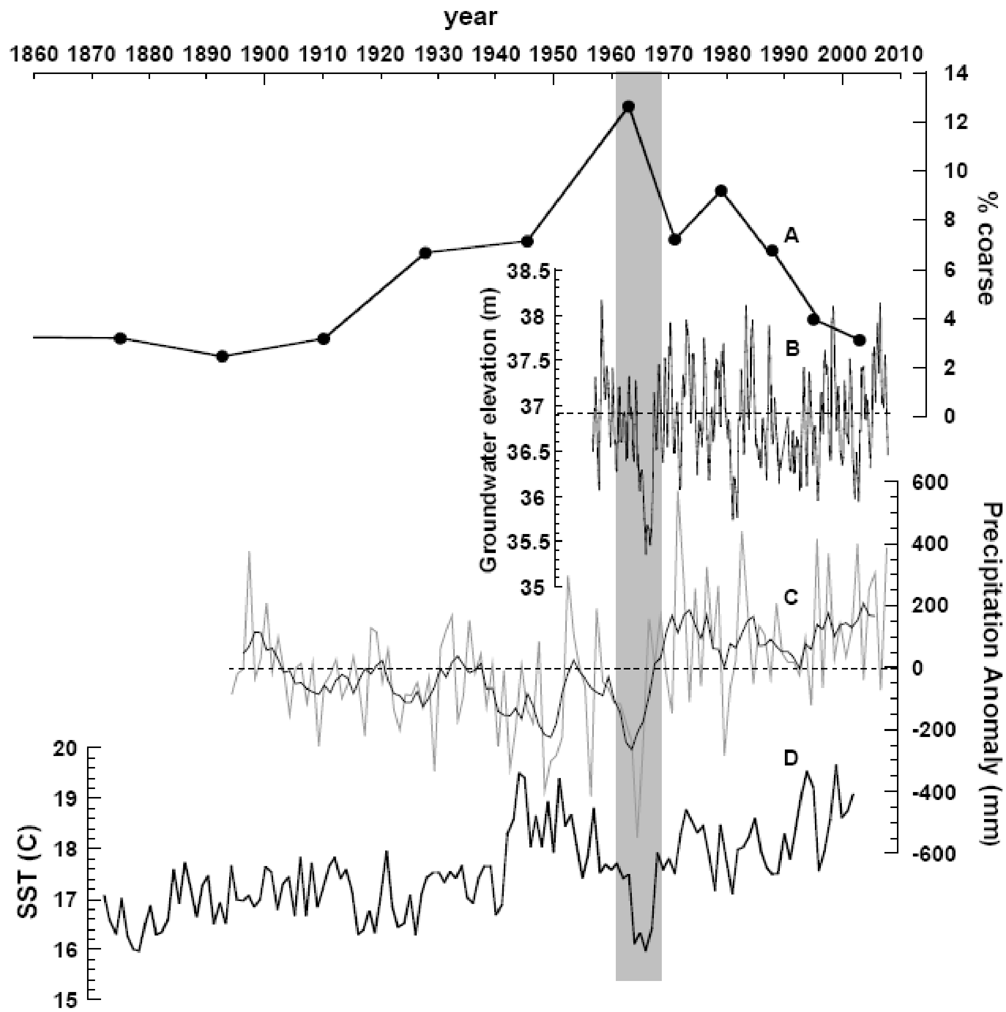

Figure 2-11. Comparison among recent data from the (A) uppermost sediments of New Long Pond (NLP43 coarse fraction) with (B) ground water elevation; dashed line is the mean (monitoring well PWW22 in Fig. 1), (C) precipitation anomaly between AD 1890 and 2007; dark line is the running average, and (D) sea-surface temperatures from 1875 to 2007. Vertical gray bar highlights conditions corresponding to the AD 1960s drought. Historic droughts are defined in Wandle's (1991) analysis as the annual and cumulative departures from long-term average stream-flow; drought is also more simply defined as an interval of drier-than-normal conditions.

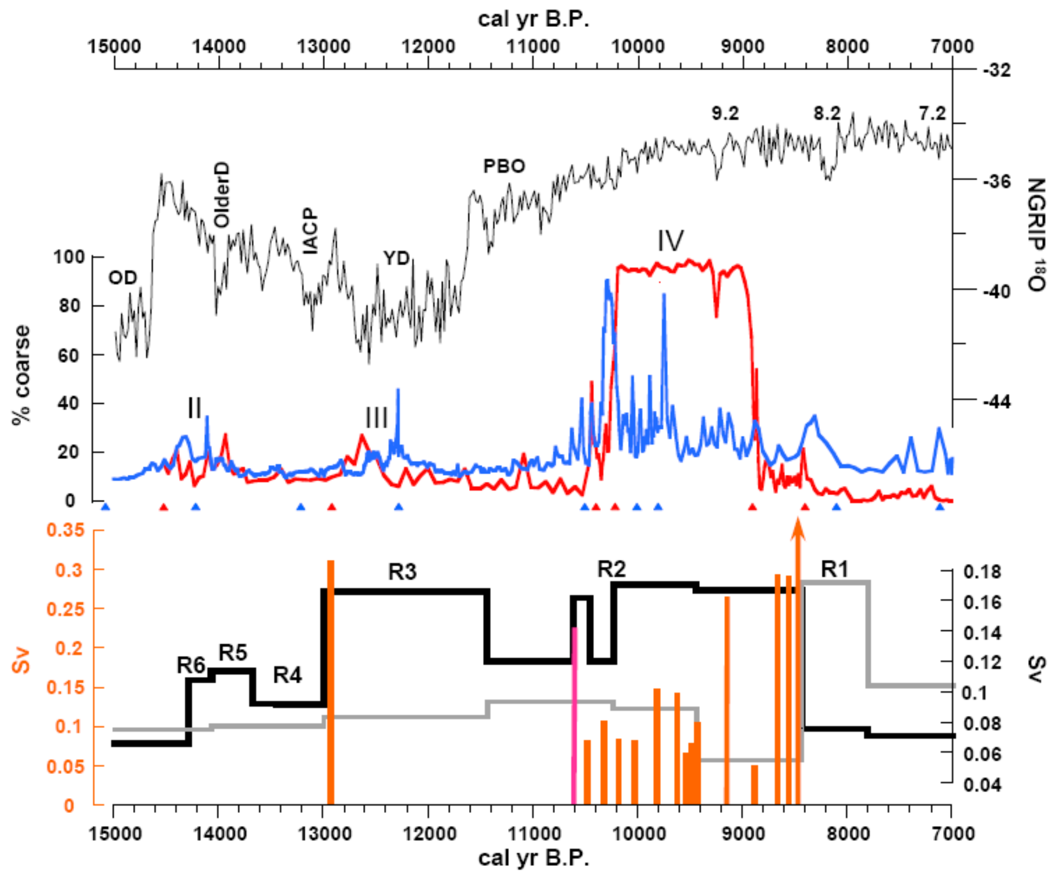

Figure 2-12. The NGRIP ^{18}O from Greenland (GICC05; Rasmussen et al., 2006, in ka) compared with (1) changes in values for percent coarse fraction from NLP43 (red) and RP110 (blue). ▲are median ages used in the age models for NLP43 and RP110 and (2) the timing, duration and magnitude of freshwater routings. R1 – R6 are from Clark et al.'s (2001) time series showing the combined flux of freshwater from the Hudson and St. Lawrence Rivers (black lines) and Hudson Strait (gray lines) to Atlantic Ocean. The discharge events from Lake Agassiz are from Teller and Leverington (2004) and show the flux of freshwater (Teller et al., 2002) to the Atlantic Ocean and Hudson Bay (orange vertical lines) and to the Gulf of Mexico/Atlantic Ocean (pink line). Sv = sverdrup.

CHAPTER THREE

REPEATED CENTURY-SCALE DROUGHTS OVER THE PAST 13,000 YEARS NEAR THE HUDSON RIVER WATERSHED, U.S.A.

PAIGE E. NEWBY[a]

BRYAN N. SHUMAN[b]

JEFFREY P. DONNELLY[c]

DANA MACDONALD[a]

BROWN UNIVERSITY, Department of Geological Sciences

[b] **UNIVERSITY OF WYOMING**, Department of Geology and Geophysics

[c] **WOODS HOLE OCEANOGRAPHIC INSTITUTE,**

Department of Geology and Geophysics

Submitted to:

Quaternary Research, February, 2010

Abstract

Long-term sediment and ground-penetrating radar data from Davis Pond, a small lake near the Hudson River valley, reveal past droughts in a historically humid region that presently supplies water to millions of people in and around New York City. A minimum of eleven sandy paleoshoreline deposits in the lake date from 13.4-0.6 cal yr BP. The deposits span 1500 to 200 years between bracketing radiocarbon dates, and intrude into lacustrine silts up to 9.0 m below the modern lake surface in a transect of six sediment cores. Three lowstands, ca. 13.4-10.9, 9.2 and 8.2 cal yr BP indicate low regional moisture balance when low temperatures affected the North Atlantic region. Consistent with insolation trends, water levels rose from ca. 8.0 cal yr BP to present, but five low stands interrupted the rise and are likely associated with ocean-atmosphere interactions. Similar to evidence from other studies, the data from Davis Pond indicate repeated multi-century periods of prolonged or frequent droughts super-imposed on long-term regional trends toward high water levels. The patterns indicate that water supplies in this heavily populated region have continuously varied at multiple time scales, and confirm that humid regions such as the northeastern United States are more prone to severe drought than historically expected.

Introduction

Water is a vital resource for sustaining life, and an abundant water supply within many temperate humid regions, such as the northeastern United States ("New England"), is typically provided by precipitation throughout the year, principally from frontal systems and tropical storms. Future trends in precipitation for New England, relative to the observed record from AD1961-1990, also project an increase in annual precipitation (Hayhoe et al., 2007). Despite such historic and predicted abundance, however, societal usage can exceed the normal water supply (Degaetano, 1999; Hill and Polsky, 2007), posing a continuing challenge for maintaining regional water availability. Furthermore, currently rising temperatures and changes in hydroclimate, such as less winter moisture in the form of snow and decreased snowpack, raise the possibility of an increase in drought frequency (Hayhoe et al., 2007).

Like other humid regions, the instrumental record for New England (Griffith, 1994; Hayhoe et al., 2007; Kinnison, 1931; Leathers et al., 2000; Namias, 1966) shows droughts of varying magnitude and longevity, which variously strained regional water resources and availability. Most prominent is the severest drought on record in AD 1962-1965, when, for example, New York City reservoirs were depleted to dangerously low levels (Andrews in Cook, 1982). Four of six subsequent droughts (post-AD 1965) also curtailed water supply, and initiated involuntary water restrictions in the New York City metropolitan area (http://www.nyc.gov/html/dep/html/drinking_water/index.shtml). Thus, despite the modern imprint of moist conditions, understanding the frequency and magnitude of paleo-droughts appears critical in light of potential changing water supply and rising populations.

Studies of late-Quaternary lake levels reveal that water supplies in regions like New England may indeed be prone to even larger magnitude variation than experienced historically. Records from the region show multi-millennial trends in water levels with lower-than-modern levels from 11.0-8.0 cal yr BP, intermediate levels from 8.0-5.5 cal yr BP, low levels from 5.5-3.0 cal yr BP and high levels from 3.0 cal yr BP to present (Almquist et al., 2001; Dieffenbacher-Krall and Nurse, 2005; Newby et al., 2000; Shuman et al., 2001, 2005; Webb et al., 1993). More recent work has emphasized the potential for sub-millennial scale hydroclimate variation within this regional framework. The closest study to the Hudson River watershed indicates four (ca. 1.3, 3.0, 4.4, 6.1 cal yr BP) centennial-scale droughts in New Jersey (Li et al., 2007), and two lakes in Massachusetts contain evidence of repeated century to multi-century droughts throughout the past 14.0 cal yr BP (Newby et al., 2009).

Here, we examine paleo-drought frequency by developing a centennial-resolution, lake-level history from Davis Pond (42°8.13'N, 73°24.46'W, 213 m elevation), a small (4 ha, 2 m maximum depth) surficially-closed basin 40 km east of the Hudson River and 60 km east of New York City's 122.9 billion gallon (0.465 km^3) Ashokan Reservoir in the Catskill Mountains (http://www.nyc.gov/html/dep/html/watershed_protection/ashokan.shtml). Davis Pond is also located 175 and 230 km respectively from the detailed study locations at White

Lake, New Jersey (Li et al., 2007) and on the Plymouth-Carver Sand Plain of Massachusetts (Newby et al., 2009; Shuman et al., 2009). Despite numerous local paleoevironmental studies in the region (Kirby et al., 2002; Maenza-Gmelch, 1997; Peteet et al., 1990), no other paleohydrologic studies have been conducted at century-scale resolution within 350 km. Dendroclimatic data, however, indicate a series of multi-year droughts dating back 1500 years in the Hudson Valley (Cook et al., 1999). We aim to provide a long-term water-level history for this highly-populated region by extending the longevity of the drought record, and by linking our results with those from the emerging array of other long-term high-resolution records.

Site Description and Methods

Davis Pond lies within the broad, slightly-sloping lowlands of the Housatonic River valley at the eastern margin of the Taconic Mountains, which forms the eastern edge of the Hudson River watershed in southwestern Massachusetts (Fig. 1). Surficial sediments are glacially-derived sand and gravel deposits (Norvitch, 1968), and overlie Cambrian–Ordivician-age Berkshire schist (Dale, 1923). A transitional hardwood conifer forest containing predominantly sugar maple (*Acer saccahrum*) and red oak (*Quercus rubra*), with stands of hemlock (*Tsuga canadensis*) and white pine (*Pinus strobus*), surrounds the basin. Sweet peppercorn (*Clethra alterniflora*), holly (*Ilex opaca*), tamarack (*Larix laricina*) and herbaceous flora, including leatherleaf (*Chamaedaphne calyculata*), fringe the basin. Waterlilies (*Nuphar* and *Nymphea* spp.) cover the pond in summer.

In the Northeast, the average January temperature (AD 2008) was -2.8^{o}C, and 21.3^{o}C in July (AD 1895-2008 January range -10.4 to 1.6 ^{o}C; July range 19.2 to 23.3 ^{o}C). Regional average annual precipitation (AD 2008) was 1262 mm, about 58% higher than the annual average (729.9 mm) recorded during the final year of the AD 1962-65 drought in Massachusetts (www.nrcc.cornell.edu/page_summaries.html). Amidst the AD 1929-32 drought in

southern New England, Kinnison (1931) noted lower-than-normal precipitation and depleted water supplies in numerous municipalities. Near Davis Pond, estimated departures from Hudson Valley precipitation data between AD 1895 and 2005 show 28 (>6 month duration) droughts (Lyon et al., 2005).

Our approach to lake-level reconstruction (Newby et al., 2000; Newby et al., 2009; Shuman et al., 2001, 2005) is based on facies changes identified within a transect of sediment cores (Digerfeldt, 1986) and in ground-penetrating radar (GPR) profiles. Using a hand-driven piston corer, we obtained six sediment cores (Fig. 1) in AD 1999 at Davis Pond along a transect where GPR data were also collected using a GSSI SIR-2000 system with a 200-mhz antenna floated in a small raft (Fig. 2). The GPR profiles track changes in subsurface facies based on different dielectric constants within the sediments, but the signal at Davis Pond attenuates below about 5.0 m water depth and reveals only the upper portion of the stratigraphy.

We assume that fine-grained lacustrine silts captured in the cores and GPR profiles accumulated in deeper water than sand-rich sediments, which accumulate near the shore and extend into the basin during low water periods. Low sedimentation rates associated with sand-rich sediments provide further evidence of near-shore winnowing and erosion as expected if the deposition took place above wave base. Other factors could potentially transport sand into the pond, such as wind and surface run-off, but would be associated with high sedimentation rates. Additional transects of GPR data (not shown) indicate that the major sedimentary units identified in our cores also extend around the periphery of the basin, and thus confirm that these units are not the products of local slumps or surface water-flow. At present, the local topography has little to no gradient near the margin of the lake, and the lake is primarily fed by groundwater.

Laboratory analyses on the cores included loss-on-ignition (LOI) at contiguous 1-cm intervals to measure relative changes in sediment organic content (Dean, 1974). Based on the LOI of the core tops, we used 60% LOI (40% mineral content) as the boundary between the zones of lacustrine silt deposition offshore and sandy deposition in the near-shore littoral zone. To reconstruct the shoreline position through time, we track the position of sediments with >40% mineral content. Such sediments are commonly found in near-shore cores, such as B1.7, and rarely in off-shore cores, such as A100. Ten pollen samples from C-5 were processed using standard laboratory techniques (Faegri and Iversen, 1989), and a minimum of 200 grains were counted per sample at 400X. High-resolution (200 μm) x-radiographs of cores E40 and A100 were obtained using an ITRAX X-Ray Fluorescence (XRF) Core Scanner at Woods Hole Oceanographic Institution, and were examined to confirm that low LOI (<40%) intervals represented sand-rich sediments (Fig. 3). Visible sand layers in other cores were also documented with digital photography (Fig. 3).

Thirty-one samples of sediment or macrofossil material from the cores were submitted to the National Ocean Sciences Accelerator Mass Spectrometry (NOSAMS) facility to obtain radiocarbon dates (Table 1). We calibrated the dates for atmospheric radiocarbon variations using CALIB 5.0.2 (Reimer et al., 2004), and use the median calibrated ages throughout the text. The maximum and minimum of the 2σ calibrated age ranges represent the age span for each date in Table 1. We calculated sediment accumulation rates using the median ages.

Results

The radiocarbon-dated (Table 1) sediment cores span from ca.13.4 cal yr BP to present, and contain organic-rich (>60% LOI) sediments off-shore and sandy sediments near-shore (Figs. 3, 4). The boundaries between organic-rich and sandy deposition, however, fluctuated through time, thereby providing evidence for water-level changes. At least eleven sandy sediment units (I-XI; Fig. 4) in the different cores represent expansions of littoral sediment facies into the pond at times when lake levels declined (Fig. 5). Visible sand and gravel layers with low sedimentation rates define these units near shore, with synchronous declines in LOI and increases in the sand content representing the units in the most off-shore cores. Most of the units typically have several LOI minima, and likely represent multiple short-lived events.

Only a few intervals of organic sediment older than ca. 10.0 cal yr BP were recovered in the cores. In D20, however, a short sedimentary sequence of lacustrine silt interspersed with two distinct sand layers comprises the first two low water-level units (Fig. 3, 4). Unit I in D20 (Fig. 4) is located 627-623 cm below the modern lake surface (bmls), and is bracketed by two radiocarbon dates of 13.4 and 10.9 cal yr BP, which indicate a slow sediment accumulation rate of < 2 cm/kyr. A radiocarbon age above the Unit II sand layer (618-615 cm bmls) in D20 indicates that this low stand ended before ca. 10.4 cal yr BP, with sediment accumulating from the top of Unit I to the top of Unit II at 15.3 cm/kyr (Fig. 3). These accumulation rates, in Unit I and II, are lower than for any other portion of D20 (Table 1). Core A100 records Unit II as a steady decline in LOI after 10.6 cal yr BP, and E40 appears to contain Units I and II within sands below a radiocarbon age of 10.0 cal yr BP (Fig. 4).

The onset of lacustrine silt in E40 above the date of 10.0 cal yr BP (Fig. 5), and in D20 after 10.4 cal yr BP signals a brief rise in water levels (R1, Fig. 4) also recorded in A100 by a rise in LOI at 925 cm bmls. Both E40 and D20 then contain a series of low LOI intervals (Units III-VI) associated with sand deposition (Fig. 3), which we infer to represent low water levels that shifted sand to positions as deep as 819 cm bmls in E40 (Fig. 4). Two radiocarbon ages from E40 of 9.1 and 9.0 cal yr BP bracket two sandy layers (Fig. 3) within an interval of overall low LOI in Unit IV, and a radiocarbon age of 7.7 cal yr BP in D20 provides an age limit on the youngest portion of Unit V (Fig. 4). The sharp decline in LOI just above 7.7 cal yr BP in D20 represents the Unit VI lowstand (Fig. 4). After Unit VI, high LOI intervals in D20, E40 and A100 indicate a lack of sand transport into the basin at this time, while the onset of lacustrine silt deposition at the base of F10 around 6.6 cal yr BP shows that water levels rose during this 1100 yr interval (R2, Fig. 4).

After 6.6 cal yr BP, water levels dropped and sand accumulated as far into the basin as A100 (Unit VII, Fig. 3), as indicated by declines in LOI to 40-60% (Unit VII) in F10, D20, E40 and A100 above radiocarbon ages of 6.6-6.4 cal yr BP (Fig. 4). After the deposition of Unit VII, water levels rose (R3, Fig. 4) but then fell by ca. 5.6 cal yr BP, as indicated by sand layers and low LOI (Unit VIII) in C5, F10, D20, E40 and A100 (Fig. 4). The GPR data also show a bright reflector that truncates older sediments, and is consistent with the Unit VIII sand layer at the locations of C5 and F10 (Fig. 2). Radiocarbon ages of 5.6 and 4.9 cal yr BP in F10 best constrain the age of Unit VIII, and bracket the larger and upper of two sand layers within the unit (Fig. 4). These ages also confirm a slow sediment accumulation rate across Unit VIII (30.0 cm/kyr) compared to most of F10 (Table 1). A radiocarbon age of 4.7 cal yr BP at the upper boundary of Unit VIII in D20 is consistent with the F10 dates (Fig. 4).

The data from F10 and the GPR profile indicate that the Unit VIII sands, deposited from 5.6-4.9 cal yr BP, may represent the driest interval in the past 6.6 cal yr BP (Fig. 5). A sand layer in C5 at 190-180 cm bmls, below the radiocarbon age of 5.7 cal yr BP, may also record the Unit VIII low stand (Fig. 4). We surmise that this radiocarbon age should be ca. 4.9 cal yr BP, based on stratigraphic correlations with sand layers in F10 (4.9 cal yr BP) and D20 (4.7 cal yr BP). The 5.7 cal yr BP age from the radiocarbon-dated sample from C5 probably contained older reworked material. Two pollen samples (Fig. 6) from above the 5.6 cal yr BP radiocarbon date in C5 both contain high (38%) oak (*Quercus*) and low (1.5%) hemlock (*Tsuga*) pollen, and support our inference because regional pollen data only contain such low hemlock pollen percentages after 5.4 cal yr BP (Oswald et al., 2007).

After ca. 4.9 cal yr BP, the onset of lacustrine silt deposition above the Unit VIII sand layers in C5 and in F10 marks the next rise in water levels (R4, Fig. 4) at Davis Pond (Fig. 5). Radiocarbon dates of 4.9 and 3.4 cal yr BP indicate an increase in sediment accumulation rates to >60 cm/kyr in F10 at this time (Fig. 4), which further supports the inferred rise. During this rise, a series of drops in LOI (Unit IX) after 4.9 cal yr BP in F10 (at 247 and 235 cm bmls), D20 (at 352 cm bmls), E40 (at 414 cm bmls) and A100 (at 476 cm bmls; Fig. 3) indicate brief low stands, but these intervals are not well constrained by radiocarbon dates (Fig. 4).

By ca. 3.5 cal yr BP, water levels fell substantially based on sand and gravel layers (Unit X; Fig. 3-5), which are bounded by radiocarbon ages of 3.5 cal yr BP in C5 (145 cm bmls) and 3.4 cal yr BP in F10 (190 cm bmls)(Fig. 4). In C5, Unit X contains two coarse gravel layers below a date of 2.3 cal yr BP, and a radiocarbon age of 3.0 cal yr BP obtained from the high-LOI silts between the layers may indicate a brief high stand (Fig. 5). Sediment accumulation rates in F10 drop to their lowest value (22.7 cm/kyr) in association with Unit X, e.g. compare with 30.0 cm/kyr in Unit VIII from 5.6-4.9 cal yr BP and ca. 40-70 cm/kyr for most other portions of the core (Table 1). Unit X also appears in the GPR data as a bright reflector at the approximate depth of the sand and gravel layers in C5 and F10 (Fig. 2). Based on these results, Unit X appears to represent the most substantial or frequent drought of the past 4.9 cal yr BP (Fig. 5).

After 2.3 cal yr BP, rising water levels are recorded by intervals with high LOI in all the cores, including B1.7 (R5, Figs. 4, 5). The timing of this rise in LOI is best constrained by a radiocarbon date in C5 of 2.3 cal yr BP (118 cm bmls). A terrace surrounding the pond at ~0.5 m above the modern lake surface attests to at least one former period when the pond reached higher than modern levels, but the C5 and B1.7 cores indicate that near-modern levels have only persistently existed since ca. 2.3 cal yr BP . The low-stand deposits associated with Unit XI interrupt this “high-stand” evidence (Fig. 5), and are defined by low-LOI sediments from 94-51 and 148-76 cm bmls in C5 and F10 respectively (Fig. 4). GPR data show a significant reflector near the position of B1.7, which may represent Unit XI (Fig. 2). Radiocarbon ages from F10 and A100 indicate that this low stand (Unit XI) began at ca. 1.6 cal yr BP, and a radiocarbon age in F10 constrains the end of the event to be after 0.6 cal yr BP.

Discussion

Two features of the Davis Pond record provide insight into the regional hydroclimate over the past 13,000 years: evidence of a long-term rise and repeated short-term low-stands. The low stands are superimposed on the overall trend toward higher water levels after ca. 10.4 cal yr BP (Unit II), which is evident from the progressively younger basal ages of F10 and C5 (Figs. 4, 5). From ca.10.4 to 6.6 cal yr BP (Units II-VI), the paleoshoreline fluctuated between 20 and 40 m from the modern shore with sediments only accumulating in cores D20, E40 and A100. After 6.6 cal yr BP (Unit VII), F10 began to accumulate sediment as Davis Pond expanded to within 10 m of the modern shoreline. By ca. 4.9 cal yr BP, silts began to accumulate in C5 and the shoreline fluctuated among locations within 5-10 m of the modern shore (during the deposition of Units VII-XI). We infer the modern shoreline was likely reached by ca. 2.3 cal yr BP when silt began to accumulate in B1.7 (Fig. 4).

The long-term tendency toward high water levels in the Davis Pond (Fig. 5) may be explained by seasonal insolation trends during the Holocene, which drove atmospheric circulation changes that likely contributed to an increase in effective moisture in the region throughout the Holocene (Diffenbaugh et al., 2006). The direct effects of the insolation trends would have also caused a progressive decline in evaporation rates since before 10.4 cal yr BP (Webb et al., 1998). Furthermore, an increase in water levels after ca. 8.0 cal yr BP (Unit V) conforms with the inference (Shuman et al., 2002) that lake levels rose in New England after the collapse of the Hudson Bay ice dome ca. 8.2 cal yr BP . Regional conditions then moistened as subtropical moisture was readily advected northward.

In addition to the long-term trend, the eleven low stand units (many containing multiple individual event layers) indicate the regional importance of multi-century hydroclimatic variability consistent with that inferred from an emerging group of recent studies (Li et al., 2007; Newby et al., 2009). In southeastern Massachusetts, multiple sand layers in the sediment stratigraphies of Rocky and New Long Ponds record repeated Pleistocene and Holocene low stands (Newby et al., 2009; Shuman et al., 2009). The ages of these low stands overlap with those identified here: Unit I (13.4-10.9 ka) at Davis Pond overlaps in time with early low stands at Rocky and New Long Ponds during the Younger Dryas; Unit II (10.9-10.4 ka) at Davis Pond correlates in time with low-stand sand layers at Rocky and New Long Ponds dating to 11.0-10.2 cal yr BP and before 10.3 cal yr BP respectively; Units IV and V at Davis Pond coincide in time with sand layers at Rocky and New Long Ponds that indicate low-water levels during the 9.2 cal yr BP (Fleitmann et al., 2008) and the 8.2 cal yr BP (Alley et al., 1997) events. After ca. 6.0 cal yr BP, the record at Rocky Pond is poorly resolved but the ages of Davis Pond low-stand continue to overlap with those at New Long Pond from 5.7-1.2 cal yr BP: Davis Pond Unit VIII (5.6-4.9 cal yr BP) coincides with a New Long Pond low stand at 5.7-4.9 cal yr BP, Davis Pond Unit IX (before 3.5 cal yr BP) corresponds to a New Long Pond low stand at 4.1-3.6 cal yr BP, Davis Pond Unit X (3.0-2.3 cal yr BP; likely two events before and after 2.7 cal yr BP) overlaps to two New Long Pond low stands at 3.6-2.7 and 2.5-1.9 cal yr BP, and Davis Pond Unit XI (1.6-0.6 cal yr BP) correlates with one at New Long Pond at 1.9-1.2 cal yr BP . Further afield, the four low-stand intervals at White Lake in New Jersey (Li et al., 2007) also correspond in time with Units VIII-XI at Davis Pond. Taken together, the regional network of datasets appears to coherently indicate numerous century-scale and longer droughts in New England during the Holocene.

In addition, the similar timing of low stands during the late-Pleistocene and early-Holocene at multiple lakes in New England indicates a possible link between drought and abrupt temperature changes in the North Atlantic region, such as during the Younger Dryas, 9.2 cal yr BP, and 8.2 cal yr BP events (Newby et al., 2009). As noted by Li et al.

(Li et al., 2007), the influence of the North Atlantic Ocean may have continued to play an important role in forcing prolonged regional droughts during the remainder of the Holocene, just as it did in the most severe historic drought in AD 1962-1966 (Namias, 1966). For example, the coincident low stands at Davis Pond (esp. Units V, VIII, and IX) and New Long Pond are also synchronous with cold episodes in Greenland (Shuman et al., 2009). The Davis Pond data, thus, appear consistent with Newby et al.'s (Newby et al., 2009) suggestion that changes in Atlantic Meridional Overturning Circulation and sea-surface temperatures off the coast of New England may be an important mechanism for initiating long-term drought periods in the region.

Conclusion

Our detailed multi-core record from Davis Pond includes well resolved evidence of hydrological changes that show high-frequency changes superimposed on previously-documented, multi-millennial changes in moisture conditions during the late-Quaternary in New England. The recent AD 1960s drought showed how such events impact natural systems (streamflow, lake levels and groundwater) and human needs (agriculture, water supply). Our data confirm the potential for regional changes with similar consequences in the future, if regional drought frequency increases as climate models project for the end of this century, driven by increased evaporation across the northeastern United States (Hayhoe et al., 2007). Enhanced evaporation compared to today during the early-Holocene may similarly explain the particularly low water levels at Davis Pond before 6.6 cal yr BP, and thus sets a precedent for the predicted future changes. Our results also confirm that the regional hydroclimate may be more variable than experienced historically, and that multiple droughts of different magnitude and longevity have accompanied past climatic changes and could do so in the future. In particular, the apparent sensitivity of regional water supplies to conditions in the North Atlantic raises concerns about the hydrologic impacts of potential future changes in oceanic circulation (Alley et al., 2003). Thus, our data underscore the potential for future climate change to impact the water resources of this highly populated region.

Acknowledgements

We thank The Ocean and Climate Change Institute at Woods Hole Oceanographic Institution and NSF Earth System History program grants (EAR-0602380 to J. Donnelly and EAR-0602408 to B. Shuman) for supporting this research. P. Leduc, J. Tierney, M. Gomes, J. Williams and B. Zipser skillfully assisted in the field and laboratory. We thank L. Carlson for Geographic Information Systems work and G. Smith for his enthusiasm and for granting access to the pond.

References

Alley, R. B., Marotzke, J., Nordhaus, W. D., Overpeck, J. T., Peteet, D. M., Pielke, R. A., Jr., Pierrehumbert, R. T., Rhines, P. B., Stocker, T. F., Talley, L. D., and Wallace, J. M. (2003). Abrupt Climate Change. *Science* **299,** 2005-2010.

Alley, R. B., Mayewski, P. A., Sowers, T., Stuiver, M., Taylor, K. C., and Clark, P. U. (1997). Holocene climatic instability: A prominent, widespread event 8200 yr ago. *Geology* **25,** 483-486.

Almquist, H., Dieffenbacher-Krall, A. C., Flanagan-Brown, R., and Sanger, D. (2001). The Holocene record of lake levels of Mansell Pond, central Maine, USA. *The Holocene* **11,** 189-201.

Andrews, J. F. (1965). The weather and circulation of July 1965. *Monthly Weather Review* **93** (10), 647-654.

Cook, E. R., Meko, D. M., Stahle, D. W., and Cleaveland, M. K. (1999). Drought reconstructions for the continental United States. *Journal of Climate* **12,** 1145-1162.

Dale, T. N. (1923). The Lime Belt of Massachusetts and Parts of Eastern New York and Western Connecticut. United States Geological Survey, Bulletin **744**, Washington DC, 71 pp.

Dean, W. E. (1974). Determination of carbonate and organic matter in calcareous sediments and sedimentary rocks by loss on ignition: comparison with other methods. *Journal of Sedimentary Petrology* **44,** 242-248.

Degaetano, A. T. (1999). A Temporal Comparison of Drought Impacts and Responses in the New York City Metropolitan Area. *Climatic Change* **42,** 539-560.

Dieffenbacher-Krall, A. C., and Nurse, A. M. (2005). Late-Glacial and Holocene Record of Lake Levels of Mathews Pond and Whitehead Lake, Northern Maine, USA. *Journal of Paleolimnology* **34,** 283-309.

Diffenbaugh, N. S., Ashfaq, M., Shuman, B., Williams, J. W., and Bartlein, P. J. (2006). Summer aridity in the United States: Response to mid-Holocene changes in insolation and sea surface temperature. *Geophysical Research Letters* **33,** L22712.

Digerfeldt, G. 1986. Studies on past lake-level fluctuations, *in* Berglund, B.E., ed., Handbook of Holocene palaeoecology and palaeohydrology: John Wiley and Sons, Chichester, United Kingdom, p. 127–142.

Faegri, K. and Iversen J. (1989). Textbook of Pollen Analysis. (4th edn). John Wiley and Sons, Chichester, 328 pp.

Fleitmann, D., Mudelsee, M., Burns, S. J., Bradley, R. S., Kramers, J., and Matter, A. (2008). Evidence for a widespread climatic anomaly at around 9.2 ka before present. *Paleoceanography* **23,** PA1102.

Griffith, G. E., Omernik, J. M. Pierson, S. M. and Kiilsgaard, C. W. (1994). The Massachusetts ecological regions project. United States Environmental Protection Agency, Publication No. 17587-74-6/94-DEP, Washington D.C.

Hayhoe, K., Wake, C., Huntington, T., Luo, L., Schwartz, M., Sheffield, J., Wood, E., Anderson, B., Bradbury, J., DeGaetano, A., Troy, T., and Wolfe, D. (2007). Past and future changes in climate and hydrological indicators in the US Northeast. *Climate Dynamics* **28,** 381-407.

Hill, T. D., and Polsky, C. (2007). Suburbanization and drought: A mixed methods vulnerability assessment in rainy Massachusetts. *Environmental Hazards* **7,** 291-301.

Kinnison, H. B. (1931). The 1929-1930 Drought in New England. . *Journal of New England Water Works Association* **45,** 145-163.

Kirby, M., Patterson, Patterson, W., Mullins, Mullins, H., Burnett, and Burnett, A. (2002). Post-Younger Dryas climate interval linked to circumpolar vortex variability: isotopic evidence from Fayetteville Green Lake, New York. *Climate Dynamics* **19,** 321-330.

Leathers, D. J., Grundstein, A. J., and Ellis, A. W. (2000). Growing season moisture deficits across the northeastern United States. Climate Dynamics **14**, 43-55.

Li, Y.-X., Yu, Z., and Kodama, K. P. (2007). Sensitive moisture response to Holocene millennial-scale climate variations in the Mid-Atlantic region, USA. *The Holocene* **17,** 3-8.

Lyon, B., Christie-Blick, N. and Gluzberg, Y. (2005). Water shortages, development, and drought in Rockland County, New York. *Journal of the American Water Resources Association (JA)* **41** (6), 1457-1469.

Maenza-Gmelch, T. E. (1997). Holocene vegetation, climate, and fire history of the Hudson Highlands, southeastern New York, USA. *The Holocene* **7,** 25-37.

Namias, J. (1966). Nature and possible causes of the northeastern United States drought during 1962-65 *Monthly Weather Review* **94,** 543-554.

Newby, P. C., Killoran, P., Waldorf, M., Shuman, B. N., Webb, T., III, and Webb, R. S. (2000). 14,000 years of sediment, vegetation, and water level changes at the Makepeace Cedar Swamp, southeastern Massachusetts. *Quaternary Research* **53,** 352-368.

Newby, P. E., Donnelly, J. P., Shuman, B. N., and MacDonald, D. (2009). Evidence of centennial-scale drought from southeastern Massachusetts during the Pleistocene/Holocene transition. *Quaternary Science Reviews* **28,** 1675-1692.

Norvitch, R. F., and Lamb, M. E. S. (1966). Housatonic River Basin, United States Geological Survey Massachusetts Basic-Data Report **9**, Ground-Water Series, Washington D. C., 40 pp.

Oswald, W. W., Faison, E. K., Foster, D. R., Doughty, E. D., Hall, B. R., and Hansen, B. C. S. (2007). Post-glacial changes in spatial patterns of vegetation across southern New England. *Journal of Biogeography* **34,** 900-913.

Peteet, D. M., Vogel, J. S., Nelson, D. E., Southron, J. R., Nickmann, R. J., and Heusser, L. E. (1990). Younger Dryas climatic reversal in northeastern USA? AMS ages for an older problem. *Quaternary Research* **33,** 219.

Reimer, P. J., Baillie, M. G. L., Bard, E., Bayliss, A., Beck, J. W., Bertrand, C. J. H., Blackwell, P. G., Buck, C. E., Burr, G. S., Cutler, K. B., Damon, P. E., Edwards, R. L., Fairbanks, R. G., Friedrich, M., Guilderson, T. P., Hogg, A. G., Hughen, K. A., Kromer, B., McCormac, F. G., Manning, S. W., Ramsey, C. B., Reimer, R. W., Remmele, S., Southon, J. R., Stuiver, M., Talamo, S., Taylor, F. W., van der Plicht, J., and Weyhenmeyer, C. E. (2004). IntCal04 Terrestrial radiocarbon age calibration, 26 - 0 ka BP. *Radiocarbon* **46,** 1029.

Shuman, B., Bravo, J., Kaye, J., Lynch, J. A., Newby, P., and Webb, T., III. (2001). Late-Quaternary water-level variations and vegetation history at Crooked Pond, southeastern Massachusetts. *Quaternary Research* **56,** 401-410.

Shuman, B., Newby, P., Donnelly, J. P., Tarbox, A., and Webb, T., III. (2005). A Record of Late-Quaternary Moisture-Balance Change and Vegetation Response from the White Mountains, New Hampshire. *Annals of the Association of American Geographers* **95,** 237-248.

Shuman, B. N., Bartlein, P. J., Logar, N., Newby, P., and Webb, T., III. (2002). Parallel climate and vegetation responses to the early Holocene collapse of the Laurentide Ice Sheet. *Quaternary Science Reviews* **21,** 1793-1805.

Shuman, B. N., Newby, P., and Donnelly, J. P. (2009). Abrupt climate change as an important agent of ecological change in the Northeast U.S. throughout the past 15,000 years. *Quaternary Science Reviews* **28,** 1693-1709.

Webb, R. S., Anderson, K. H., and Webb, T. (1993). Pollen Response-Surface Estimates of Late-Quaternary Changes in the Moisture Balance of the Northeastern United States. *Quaternary Research* **40,** 213-227.

Webb, T., III, Anderson, K. H., Webb, R. S., and Bartlein, P. J. (1998). Late Quaternary climate changes in eastern North America: a comparison of pollen-derived estimates with climate model results. *Quaternary Science Reviews* **17,** 333-357.

Table 3-1. Radiocarbon Dates and Sedimentation Rates from Davis Pond

No.	Core	Depth (cm) bmls*	NOSAMS Lab No.	^{14}C yr BP	Age error	Calib Median cal yr BP	Calib Low cal yr BP	Calib High cal yr BP	Material Dated**	Sedimentation Rates cm/kyr
1	A	276.5	OS-58072	1720	30	1629	1554	1704	1	69.7
2	A	414.5	OS-58073	3020	35	3234	3080	3341	2	86.0
3	A	519.5	OS-57913	4400	30	4962	4866	5211	3	60.8
4	A	647.5	OS-58068	5820	45	6626	6502	6731	1	76.9
5	A	748.5	OS-59706	7030	40	7872	7763	7953	2	81.1
6	A	838.5	OS-58065	8150	40	9086	9007	9252	1	74.1
7	A	949.5	OS-58066	9390	55	10621	10439	10754	1	72.3
8	A	1006.5	OS-59530	9630	45	10953	10778	11179	4	171.7
9	A	1034.5	OS-55125	12500	50	14624	14245	14952	1	7.6
10	C	118.5	OS-38532	2310	30	2338	2183	2358	5	28.7
11	C	129.5	OS-38533	2860	30	2978	2878	3073	5	17.2
12	C	144.5	OS-58074	3290	40	3519	3412	3630	1	27.7
13	C	180.5	OS-58027	4930	45	5656	5589	5745	1	16.8

14	D	232.5	OS-54852	1590	40	1471	1389	1557	6	89.4
15	D	391	OS-54983	4140	35	4684	4537	4824	1	49.3
16	D	455	OS-54984	5620	40	6397	6310	6479	1	37.4
17	D	532.5	OS-60578	6920	40	7748	7674	7839	1	57.4
18	D	615	OS-38531	9240	40	10409	10262	10543	1	31.0
19	D	623	OS-55126	9570	40	10933	10736	11100	7	15.3
20	D	627	OS-38790	11600	60	13440	13302	13618	1	1.6
21	E	578.5	OS-60128	5730	40	6527	6414	6637	1	65.3
22	E	623.5	OS-59968	5860	40	6683	6562	6779	8	288.5
23	E	726.5	OS-58071	8100	50	9041	8780	9253	1	43.7
24	E	744.5	OS-55124	8180	45	9125	9016	9268	1	214.3
25	E	856.5	OS-60577	8940	60	10050	9828	10233	1	121.1
26	F	86.5	OS-57908	735	30	679	657	726	9	46.0
27	F	149.5	OS-57909	1700	25	1603	1540	1693	9	68.2
28	F	189.5	OS-57910	3130	25	3363	3267	3439	9	22.7

29	F	289.5	OS-54867	4300	50	4871	4829	4959	5	66.3
30	F	312.5	OS-54985	4920	30	5638	5595	5715	10	30.1
31	F	348.5	OS-55039	5700	290	6524	5908	7243	11	40.6

Table Legends
*bmls: below modern lake surface.

**Material Dated: 1-Bulk Sediment, 2-Bulk Sediment with Fibrous Material, 3-Macrofossils, 4-Seed, 5-Fine Rootlets, 6- Rootlets and Algae, 7-Sedge (*Carex* sp. Fragments), 8-Sediment with Organics, 9-Plant/Wood, 10-Wood, 11-Cone Scales.

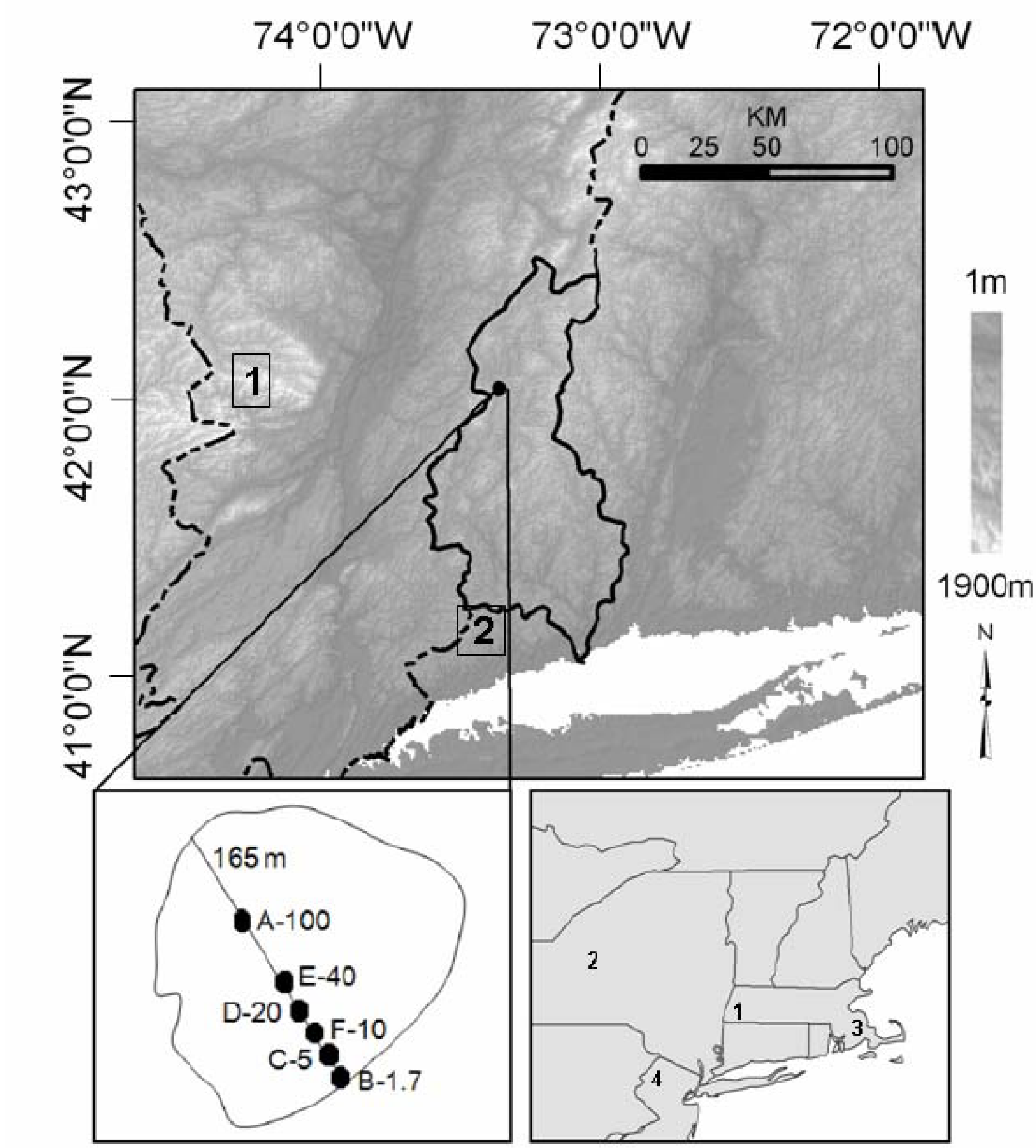

Figure 3-1. Location of Davis Pond (circle) in southwestern Massachusetts within Housatonic River watershed (dark line). Nearby are the Hudson River watershed (dotted line) and New York City's water reservoirs (boxed labels 1-Catskills/Delaware Watersheds and 2-Groton Watershed). Lower left: location of GPR transect with six cores in this study. Lower right: location of sites in text: 1-Davis Pond, 2-Fayetteville Green Lake (Kirby et al., 2002), 3-Rocky and New Long Ponds (Newby et al., 2009; Shuman et al., 2009) and 4-White Pond (Li et al., 2007).

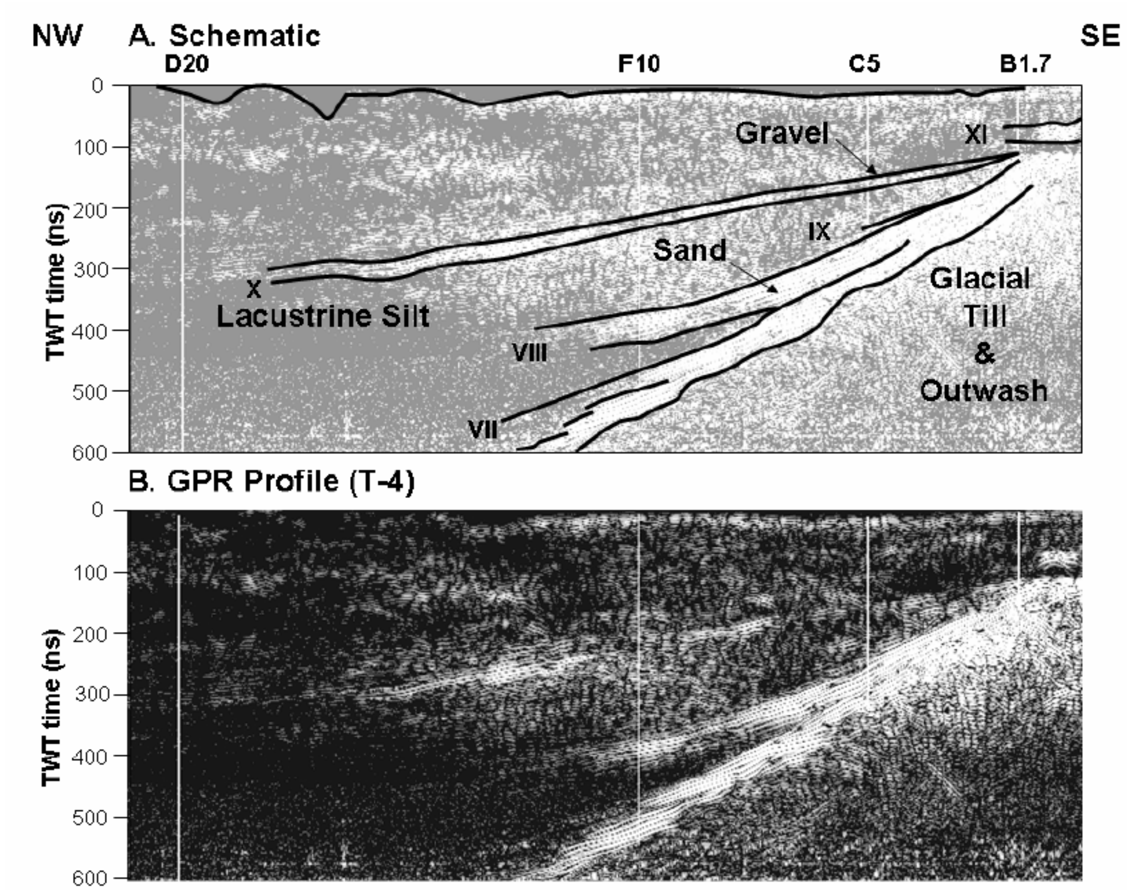

Figure 3-2. Davis Pond GPR schematic and profile. Vertical white lines show locations of D20, F10, C5 and B1.7. Dark horizontally-oriented lines outline GPR reflectors; low stand Units VII-XI are described in the text.

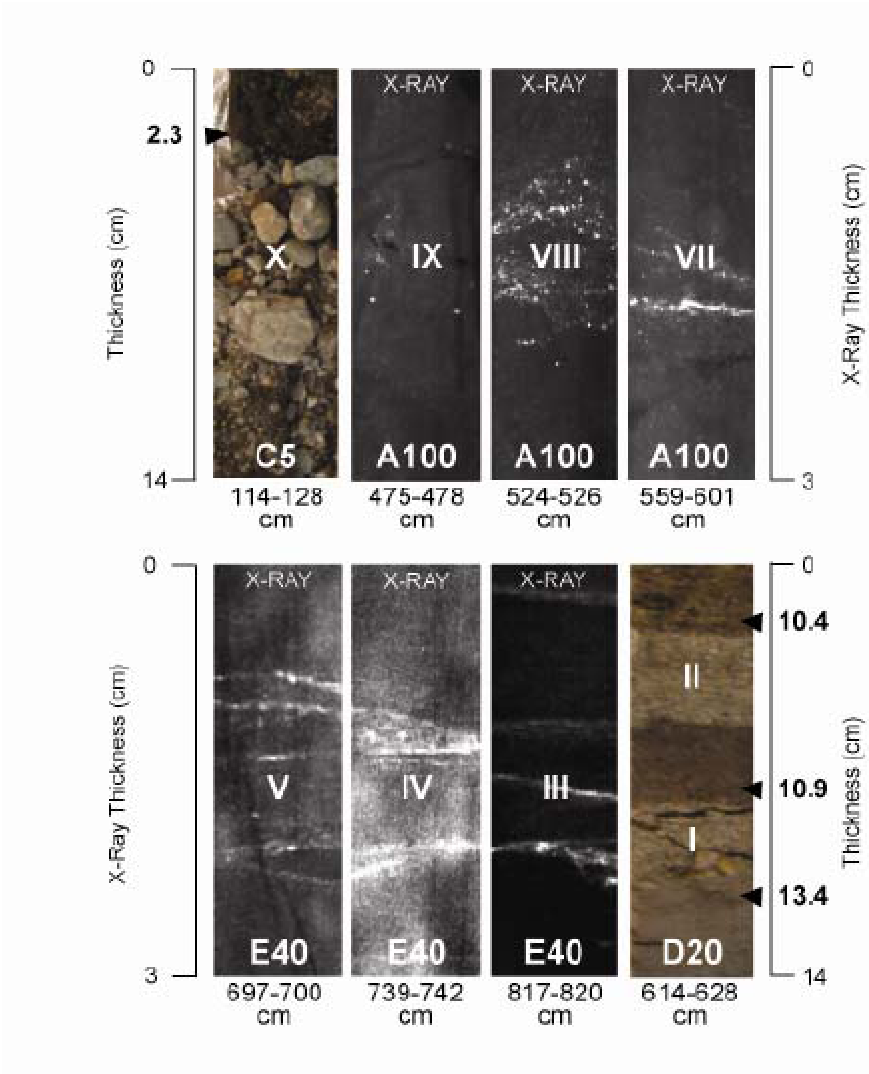

Figure 3-4. Digital and radiographic images from Davis Pond. Digital images from D20 (Units I and II) and C5 (Unit X) show sand and gravel (respectively) deposits. Light (dense) portions of x-radiographic (200 μm resolution) images from A100 and E40 reveal sand fractions within lacustrine sediments. Further details on radiocarbon ages (►; cal ka BP) are in Table 1. In Fig. 4, Unit III (E40) is displayed as two sand layers and Unit V as one sand layer.

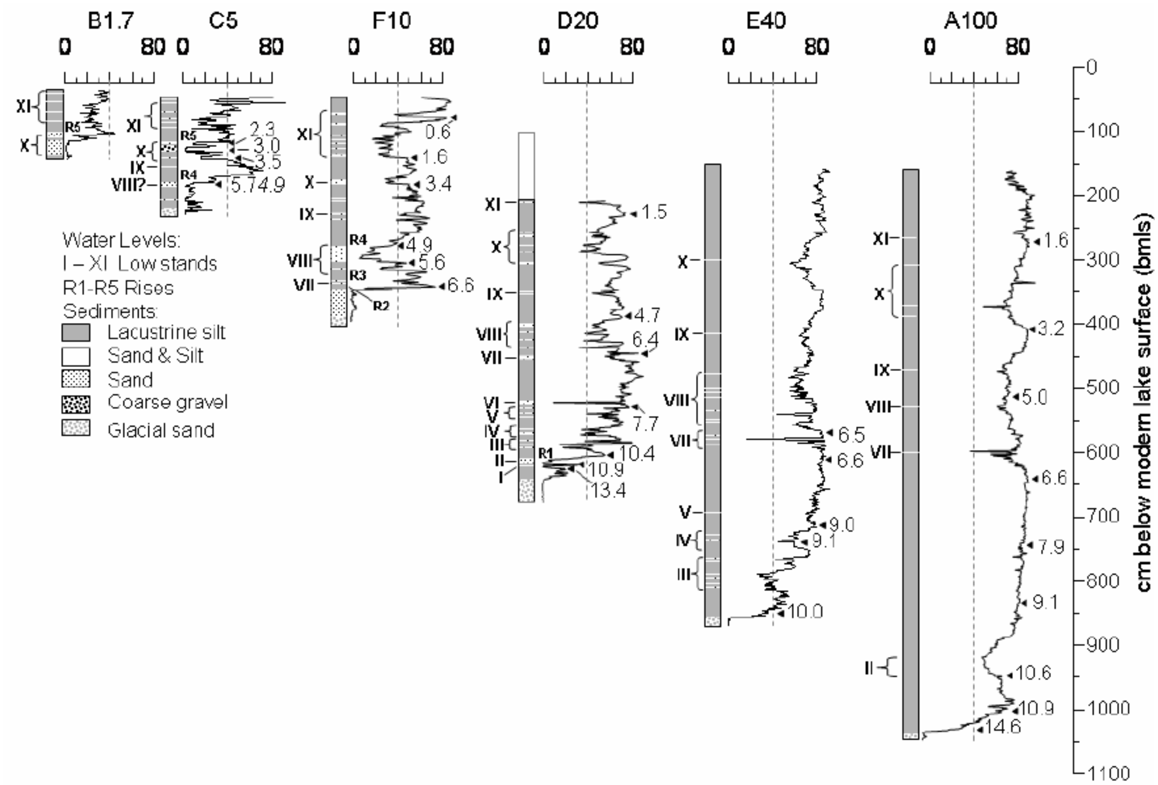

Figure 3-4. Correlation among low stand Units I-XI and LOI by depth in Davis Pond, with radiocarbon dates (◄, cal ka BP; cm bmls). Left of vertical dashed lines show sandy (<40% organic) mineral-rich sediments, which as expected, become increasingly inorganic closer to the shore. The upper meter (dashed box) of D20 was not collected.

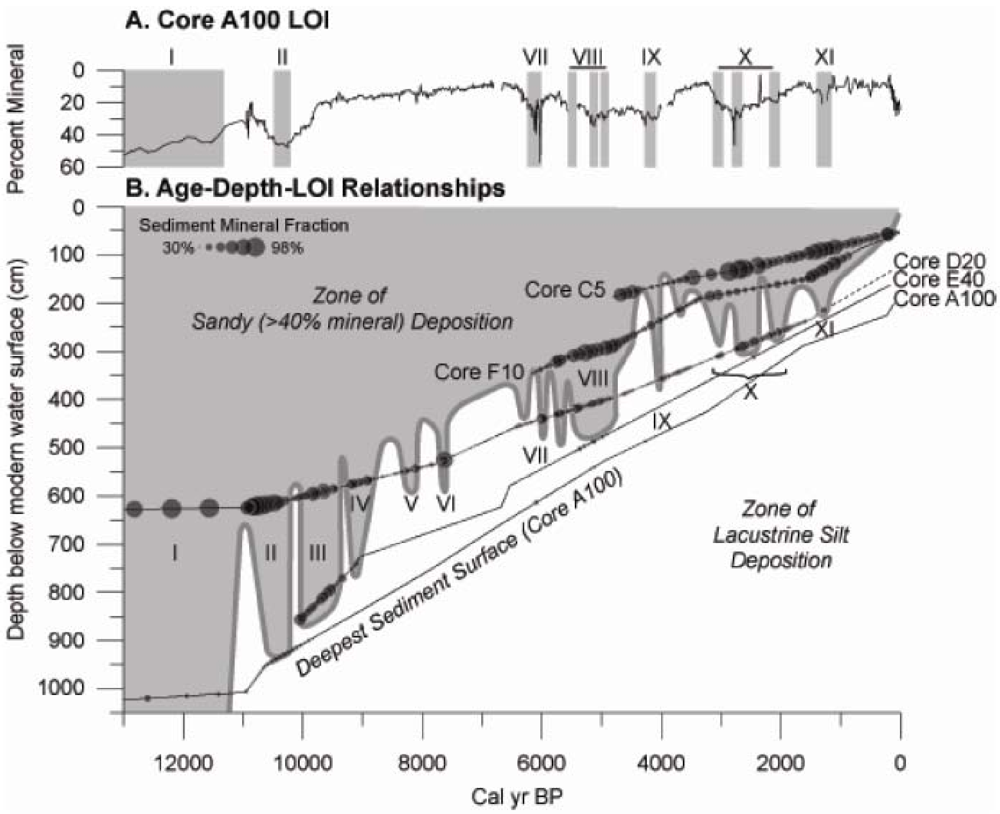

Figure 3-5. Changes in water level at Davis Pond by age (cal yr BP). A. Gray bands show low-stand Units I-XI on percent mineral fraction in A100; note that the youngest event in Unit VIII overlaps a core break. B. Changes in water level displayed by extensions of sand (gray) from modern shore into the basin for each Unit. R1-R5 indicate rises in water level as per text.

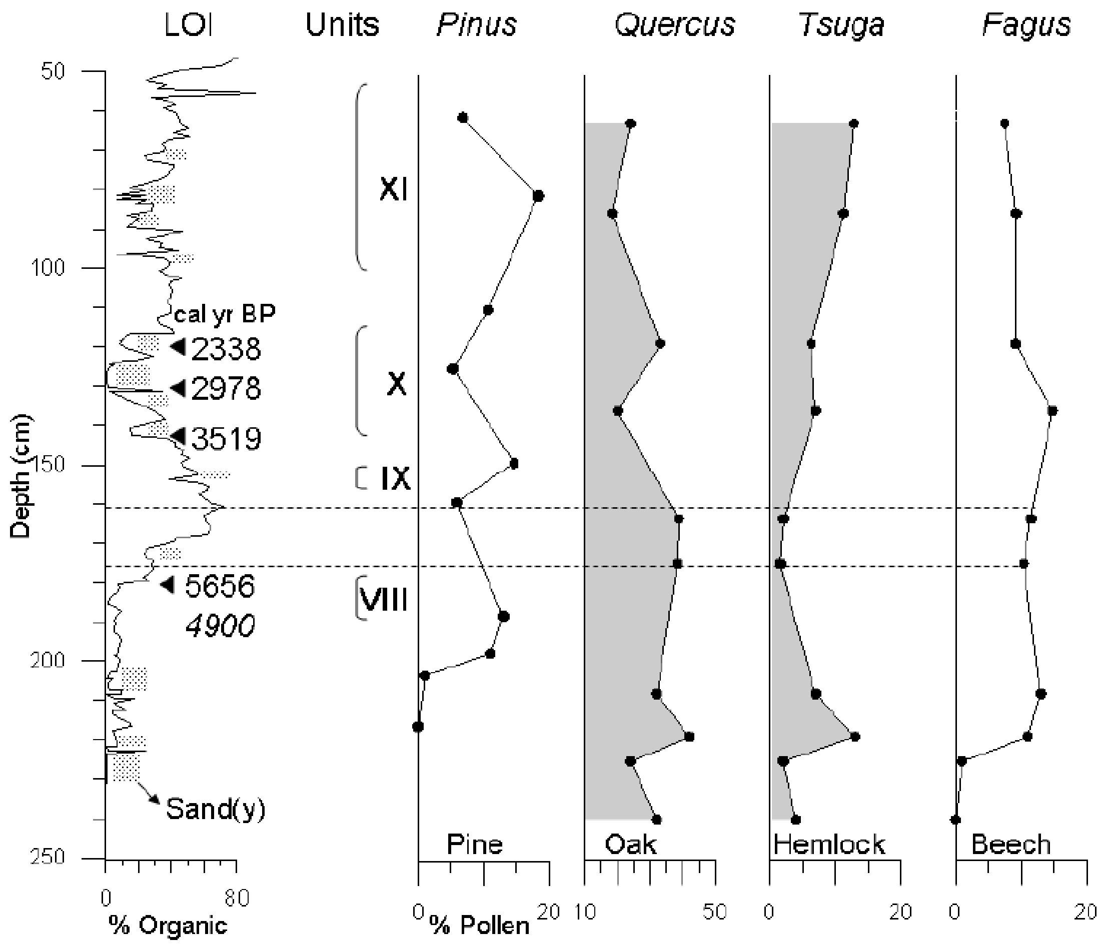

Figure 3-6. Select regional pollen taxa from Core C5, showing high and then low abundance in oak and hemlock pollen associated with the timing of the regional decline in hemlock pollen at ca.5.7 ka. Sedimentary units VIII-XI are described in text.

CHAPTER FOUR

REGIONALLY SYNCHRONOUS HOLOCENE-AGE DROUGHTS IN THE NORTHEASTERN USA

PAIGE E. NEWBY[a]

JEFFREY P. DONNELLY[b]

BRYAN N. SHUMAN[c]

KRIS KARNAUSKAS[b]

[a] BROWN UNIVERSITY, Department of Geological Sciences

[b] WOODS HOLE OCEANOGRAPHIC INSTITUTE, Department of Geology and Geophysics

[c] UNIVERSITY OF WYOMING, Department of Geology and Geophysics

Abstract

The natural variability and mechanisms underlying the post-Laurentide Ice Sheet (8.0 ka) to pre-Industrial age hydroclimate can provide valuable information about the potential impact of future droughts under global-warming scenarios for the Northeastern USA. Here we present ground-penetrating radar data in conjunction with reconstructed lake-level data from southeastern New England that show repeated sub-millennial scale, spatially coherent, lake level changes from 8.0 ka to present, with an increase in drought frequency after ca. 6.0 ka. Sedimentary evidence from New Long Pond in southeastern Massachusetts indicates a prolonged low water stand/drought (AD 800-1300) during the Medieval Climate Anomaly that parallels the American southwest "megadroughts", and overlaps a 100-yr interval of warm tropical Atlantic sea surface temperatures and cool La Niña-like Pacific conditions. In contrast, evidence for high water levels is recorded during the Little Ice Age. Although greater-than-modern summer insolation after 7.0 ka may be instrumental in an early sequence of droughts from 6.2-4.8 ka, the ca. 6.0 ka droughts and a drought from 3.1-2.7 ka also coincide with reduced meridional overturning circulation and cool conditions in the North Atlantic region. Through the Holocene, droughts appear to become increasingly linked to more proximal forcing as well as other atmospheric and ocean mechanisms, and by ca. 6.0 ka, correspondence of drought with Atlantic and Pacific Ocean and atmosphere variability underscores the potential for both far-field and near-field to initiate, amplify and/or sustain low moisture conditions.

Introduction

Drought is seldom associated with the northeastern United States ("New England"). Indeed, observational data show an increase in annual precipitation over the last century, and a slight seasonal shift to more winter precipitation since AD 1970 (Hayhoe et al., 2007). None the less, during the last century, multiple droughts, including the historically unprecedented AD 1962-65 event, punctuate the observational record (Kinnison, 1931; Wandle, 1991; Leathers et al., 2000). Moreover, anthropogenic-induced climate change scenarios predict that alterations in seasonal precipitation (increase in winter, less to no change in summer precipitation) could give rise to more frequent future droughts (Hayhoe et al., 2007). Paleo-lake-level reconstructions provide important information about past fluctuations between high and low water levels and are a principal source of information about past changes in hydroclimate. When past variations in lake levels are regionally synchronous, climatic changes, rather than localized events, are implicated as the underlying mechanism. Understanding the magnitude, duration, spatial extent and underlying forcing mechanisms that accompany such variations in water resources is particularly important for New England. Even multiple short-term droughts within the region may pose significant difficulties for growing urban areas, and may curtail water availability when seasonally sensitive local economies need it the most (Hayhoe et al., 2007).

Little is known about the natural variability and mechanisms underlying the post-Laurentide Ice Sheet (LIS, 8.0 ka) to pre-Industrial age (AD 1850) (henceforth the

Holocene) hydroclimate within the region. Instrumental data are available for the short historic record back to the early 19th century (Kinnison, 1931; Wandle, 1991; www.bluehills.org/climate.html). Lengthier, high-resolution tree-ring data in the region extend back 1500 years, but are significantly limited by extensive forest clearance associated with European settlement (Cook, 1982). The development of new long-term reconstructions of hydroclimate from the region is essential in order to understand the full range of drought variability and potential forcing mechanisms.

The role of moisture in Holocene-age climate variability is poorly understood. At the millennial-scale, the waning LIS and long-term changes in insolation influenced regional patterns for lake levels (Webb et al., 1993). Decreasing insolation progressively shifted to warmer winters and cooler summers after ca. 9.0 ka, and pollen data indicate that annual mean temperatures in New England were warmer during the mid-Holocene than today by 3-5^{o} C, and then cooled after 3.0 ka (Webb et al., 1993; Shuman et al., 2004). Using heuristic modeling, Shuman and Donnelly (2006) suggest that seasonal shifts in precipitation during the Holocene could account for sub-millennial hydroclimatic variations. Short-term climate events in the North Atlantic may have prompted abrupt changes in vegetation during some low water-level intervals (Newby et al., 2009; Shuman et al., 2009), and likewise, cool periods documented in Greenland (Alley, 2000) fit well with records showing global “rapid climate changes” (Mayewski et al., 2004) during the Holocene.

Our aim is to elucidate the hydroclimatic changes in southern New England during this 8000-yr interval, in two parts. First, we couple ground-penetrating radar (GPR) data with stratigraphic reconstructions of lake levels to test the hypothesis that similarities in the sedimentary records from multiple lakes in New England represent regionally coherent changes in hydroclimate during the Holocene. Previous lake-level studies within the region reveal basin-specific consistencies between frequent changes in core stratigraphies and nearshore GPR reflectors (Shuman et al., 2001; Newby et al., 2000; Shuman and Donnelly, 2006; Newby et al., 2009; Newby et al., in review). We also aim to determine if these stratigraphic consistencies, inferred as multiple and pervasive droughts during the Holocene, are caused by local factors or representative of a regional response to climate changes. We accomplish this determination by examining GPR data from a geographically diverse selection of sites that includes previously published profiles from New Long Pond (Newby et al., 2009; Shuman et al., 2009) and Davis Pond (Newby et al., in review) in southeastern and western Massachusetts, respectively, and two new GPR profiles from Flax Pond and Round Pond in southeastern Massachusetts. To further examine regional synchroneity, we compare the Holocene interval lake-level reconstructions (inferred using facies shifts) from cores New Long Pond 43 (Newby et al., 2009; Shuman et al., 2009) and Davis Pond D20 (Newby et al., in review).

In part two, we draw on our hypothesis that similarities in the sedimentary records from multiple lakes in New England represent regionally coherent changes in hydroclimate during the Holocene, and previous work, which shows super-imposed short-term variations on millennial-scale trends in lake levels, to explore mechanisms which may account for the observed hydroclimatic variability during the Holocene. Studies of drought from North America utilizing the short historic record indicate decadal-scale drought related to the Atlantic (Atlantic Multidecadal Oscillation, AMO) and the Pacific (Pacific Decadal Oscillation, PDO) Ocean climate indices (McCabe et al., 2004), and anomalously cool La Niña conditions (Barlow et al., 2001; Seager et al., 2005; Herweijer et al., 2006; McCabe et al., 2008) that are largely associated with the central and western United States. Correlations with New England are less evident, probably in part because recent drought is less severe within the region than in other parts of the United States, e.g. the mid-western Dustbowl in the AD 1930s. For New England, Bradley et al. (2002) propose that repositioning the polar jet stream can favor less inland precipitation, as was documented during the AD 1960s drought, when Pacific-area circulation anomalies and anomalously cool, local Atlantic Ocean SST edged storm tracks eastward over the ocean (Namias, 1966, 1967; Karoly et al., 1989; Nigram et al., 1999, Barlow et al., 2001). Likewise, changes in moisture may result from zonal orientation of storm tracks across the Atlantic Ocean, which can amplify cooling in the North Atlantic region and western Europe by reducing heat from southern source waters (Seager et al., 2003).

We place our hypothesized regional drought record within the broader context of natural climate variability over the last 2500 years in order to examine potential hydroclimatic responses to the Roman Warm Period (RWP), Medieval Climate Anomaly (MCA) and Little Ice Age (LIA). Pollen-based analysis from 2000-yr records of laminated-lake sediments from Maine to Minnesota reveal parallel, century-scale changes in vegetation with different compositions across the region (Gajewski, 1998). Results from regional studies for this interval are mixed: warm/dry conditions during the MCA, and cool/wet conditions during the LIA from Piermont Marsh, near New York City and further south along the eastern seaboard (Pederson et al., 2005) contrast with less-pronounced changes in vegetation in the Cape Cod region (Parshall et al., 2003) and central New England (Russell et al., 1993; Fuller et al., 1998). In the western United States, protracted droughts during the MCA appear to be linked with La Niña-like conditions, similar to those associated with historic droughts in the same region (Herweijer et al., 2007). A broader view for the Northern Hemisphere shows the highest reconstructed temperature anomalies from ca. AD 1000-1200 and the lowest from ca. AD 1400-1600 (Moberg et al., 2005).

We also aim to test the hypothesis that proposed changes in meridional ocean circulation (MOC) may be linked with Holocene-age droughts in New England, and if so, possibly to changes in NAO phases (Hurrell and Deser, 2009). We have already shown that punctuated intervals with low lake-levels between 15.0 and 7.0 ka in southeastern New England coincide with proposed meltwater release events or abrupt climate oscillations in the North Atlantic region and inferred changes in MOC (Newby et al., 2009). North Atlantic proxies record sub-millennial scale changes in MOC during the mid- to late-Holocene (Oppo et al., 2003; Hall et al., 2004; Keigwin et al., 2005; Came, 2007), even though (unlike the late Pleistocene/Early Holocene), drainage ceased from the Laurentide Ice Sheet by 6.4 ka (Jansson and Kleman, 2004). Here, we compare key paleoclimatic proxy records from the North Atlantic region between 8.5 and 1.0 ka (AD 1850) with the coarse fraction data from New Long Pond 43 to determine if hydroclimate in southern New England is connected with MOC.

Sites and Study Area

The region we describe as southern New England ranges from approximately 41-43^{o}N and 74-70^{o}W (Fig. 1). The study sites are in Massachusetts, and include Davis Pond (Newby et al., in review) and New Long Pond (Newby et al., 2009; Shuman et al., 2009) and two new sites, Flax Pond (41^{o}41'21.26"N, 70^{o}35'43.02"W) and Round Pond (41^{o}51'26.79"N, 70^{o}36'15.14"W) (Fig. 1).

We selected our sites from the northwestern highlands and the southeastern coast to sample different hydrologic settings. Most westerly, Davis Pond (213 m above sea level; asl) is situated near the Ordovician-age, high uplands of the Taconic and Berkshire Ranges and flanks the Housatonic River Valley (Dale, 1923). Deep surficial sediments in the river valley are glacially-derived sand and gravel deposits (Norvitch and Lamb, 1968). Near the Atlantic Coasts, New Long, Round and Flax Ponds are located in the coastal plain and Cape Cod regions, which are covered by sandy outwash and moraine deposits left by the retreating LIS (Fig. 1). (Hansen and Lapham,1992). Depth to Paleozoic crystalline bedrock increases from east to west (30.5->305 m asl) (Larson, 1982).

Round Pond (42 m asl; 4.05 hectare) is a kettle basin six km east of New Long Pond (30.2 m asl), and both are within the well-sorted sand and gravel deposits that characterize the Plymouth-Carver aquifer in southeastern Massachusetts (Hansen and Lapham, 1992). Both ponds intersect the water table with no interference from stream or rivers.

In contrast, nearby (20 km southeast of New Long Pond) Flax Pond (4 m asl; 10.93 hectare) lies within the Cape Cod aquifer, at the indistinct western margin of the Buzzards Bay moraine (till and boulder veneer on top of stratified drift; sand and gravel, abundant very fine sand and clay) and the Buzzards Bay outwash (sand and gravel) (Larson, 1982; Oldale and Barlow, 1986). In both aquifers, ground water flows radially outward to the coast from a series of mounds formed by the water table; elevation grades from 36.5-6.0 m asl in the Plymouth-Carver aquifer and from 21.3-3.0 m asl in the western portion of the Cape Cod aquifer underlying Flax Pond (AD 2000-2005 conditions from Masterson and Walter, 2009). Newby et al. (2009, in review) provide detailed site information about Davis Pond, as do Newby et al. (2009), Shuman et al. (2009), and Shuman and Donnelly (2006) for New Long Pond and the Plymouth-Carver aquifer.

Local, instrumental climate records from the Blue Hills Observatory in Massachusetts (AD 1891-2000) show an annual mean temperature of 9 ^{o}C, with warm summers (mean July temperature 21 ^{o}C) and cold winters (mean January temperature -4 ^{o}C;

(www.bluehills.org/climate.html). For the entire Northeast, the regional average annual temperature from AD 1961-1990 was 7.8^{o}C (-4.8^{o}C winter, 20.0^{o}C summer) (Hayhoe et al., 2007). Annual precipitation averages ca. 1280 mm, with a seasonal average of 520 mm from March to August and 640 mm from September to February (http://cdiac.ornl.gov/r3d/ushcn/ushcn.html#TOP). Year-round storms, principally from the Atlantic Ocean, provide a significant source of precipitation.

Methods and Data

Previous studies of Davis Pond (Newby et al., in review) and New Long Pond (Newby et al., 2009; Shuman et al., 2009) reconstructed detailed changes in water levels for the past 15,000 years from transects of sediment cores collected using piston- or vibra-core equipment. These moisture histories were inferred using the principles of lake level analysis as described in Digerfeldt (1986), coupled with mineral content (Davis Pond) and siliciclastic coarse fraction analyses from New Long Pond, and GPR data, which provided continuous images of sub-surface lithological boundaries. In these studies, the percent coarse fraction materials increased within sediments when water levels were lower than today.

The lake level record from New Long Pond contains multiple lowstand units from 9.0 ka to present (Divisions B-E in Shuman et al., 2009). At Davis Pond, Newby et al. (in review) identified eleven lowstand units (I-XI) from 15.0 ka to present, of which seven units (V-IX) are of Holocene age (e.g. 8.0 ka to present). As part of our test of the regional coherence of Holocene drought in New England, we compare the contiguous (1-cm^3 interval sampling) records of the percent >63µm (sand) sediment fraction from New Long Pond 43 (43 m from shore) from 8.0 ka to present, and the percent mineral content from Davis Pond D20 (20 m from shore). Both of these cores are relatively complete archives of the Holocene-age changes in water level inferred from the multi-core analyses for each site. In addition, both cores are from strategic positions relative to their modern shorelines (*sensu* Digerfeldt, 1986). We normalized these data by subtracting the median for each series of data from every value within that series, and then dividing each resulting value by the median.

The GPR profiles were collected using a GSSI SIR-2000 system with a 200-mhz antenna floated in a small raft. The X-ray Fluorescence (XRF) scanner at Woods Hole Oceanographic Institution, Massachusetts was used for radiographic imaging (200 µm resolution; lighter is denser) and high-resolution elemental analysis (1000 µm resolution).

A total of 52 accelerator mass spectrometry (AMS) radiocarbon dates were obtained from multiple cores collected at New Long Pond, of which 28 are from New Long Pond 43, and seven of a total of 31 radiocarbon dates from Davis Pond are from Davis Pond D20 (see Tables in Chapters 2 and 3). The radiocarbon dates were calibrated using CALIB v5.02, and we used the median age and the maximum and the minimum ages of the 2σ range to represent the age span for each date (Reimer et al., 2004a).

Results

The full sedimentary record for New Long Pond (NLP) is a lacustrine sequence, which begins with low-organic silt (<20%) deposited over glacially derived sand and gravel that transitions at 9.0 ka to a peaty silt (predominantly in situ rootlets and plant detritus from shallow aquatic vegetation and algal remains; >60% organic; Fig. 2). Beginning at ca. 6.0 ka, the peaty silt associated with Unit V is interrupted by multiple sand lenses, events 1-10, in which values for coarse fraction (CF) range between 10 and 30% (Fig. 2).

The first lowstand in the Holocene sequence is associated with an age that is best constrained by two radiocarbon dates of ca. 7.5-7.2 ka in NLP31, which we relate to cool conditions in the North Atlantic (Fig. 2, see Newby et al., 2009). About 15 cm above the radiocarbon age of 7.2 ka in NLP31, the peaty silt changes to a ca. 45 cm interval of visible sand, bracketed by radiocarbon ages of 6.2 ka and 1.2 ka. After 1.2 ka, a thin ca. 5 cm interval of peaty silt is followed by a 12 cm interval in which the peaty silt becomes mixed with sand, which we associate with the MCA. Peaty silt then accumulates to the top of the core.

The massive sand-rich interval in NLP31 is recorded as multiple, closely spaced sand layers (events 1-8) within the peaty silt in NLP43 (Fig. 2). The first of these sandy layers in NLP43 is associated with event 1 (6% CF), and a radiocarbon age from below the massive sands in NLP31 indicates this event began after 6.2 ka. Next, two radiocarbon ages above a sandy deposits in NLP 43 indicate event 1 ended by ca. 5.7 ka.

Events 2 (12% CF) and 3 (16% CF) are associated with two separate sand layers in NLP43 with a radiocarbon age from below the lower sand layer (event 2) of 5.2 ka and a radiocarbon age of 4.6 ka from above the upper sand layer (event 3). An additional radiocarbon age of 5.4 ka is older than the radiocarbon age of 5.2 ka below it, but fits within the overall timing for the sequence (Fig. 2). A radiocarbon age of 5.3 ka obtained from leaf fragments embedded in the massive sand in NLP31 likely correlates with the silty peat deposition between these two events (2 and 3). Above event 3, a thin interval of peaty silt is interrupted by the sandy deposits associated with event 4 (10% CF).

Two radiocarbon ages of 4.6 bracket about 10 cm of sandy peat associated with event 4. The upper radiocarbon age of 4.6 also constrains the lower age boundary of a second increase in CF associated with event 4, above which, two radiocarbon ages indicate the end of this event by 4.3 ka (Fig. 2).

These two radiocarbon ages (4.3 ka) from the peaty silt above event 4 also provide the maximum age for the sandy layer associated with event 5 (8% CF), and a radiocarbon age from the sediments immediately above a visible sand layer indicate that the peak event ended at ca. 3.7 ka. After ca. 3.7 ka, the peaty silt becomes more organic until 3.5 ka, then progressively less organic, and culminates with the sand layer associated with event 6 (12% CF) and a radiocarbon age of 2.8 ka. Just above the event 6 sand layer, a radiocarbon age of 2.7 ka indicates the timing of a pronounced rise in the organic content of the peaty silt, followed by another sandy interval with radiocarbon dates of 2.3 and 2.0 ka associated with event 7 (10% CF).

Event 7 contains at least two intervening lowstands, and a radiocarbon age of 2.0 ka constrains the end of the event. A brief interval of predominantly high organic peaty silts (2.0-1.8 ka) is interrupted by the sand-rich sediments associated with event 8 (5% CF), which is bracketed by radiocarbon dates of 1.8 and 1.3 ka. In NLP31, a radiocarbon age of 2.2 ka from peaty silt just below a sand layer and a radiocarbon age of 1.2 ka from peaty silt just above a sand layer correspond with events 7 and 8 in NLP43. A thin interval of peaty silt deposition above event 8 becomes increasingly less organic, and marks the onset of event 9 (6-8% CF) at ca. 1.2 ka. A radiocarbon age constrains the end of event 9 to before 0.6 ka, after which a rise and then pronounced decline in organic content is associated with the final event 10 (16% CF), which dates to the AD 20th century (see Newby et al., 2009).

Lake-level records and ground penetrating radar

The full GPR profile from New Long Pond provides an expansive sub-surface view, and shows multiple reflectors beneath the modern surface of the pond that extend laterally across the basin (Fig. 3a). This sub-surface profile also reveals an interval of closely spaced reflectors that is bracketed by intervals showing minimal reflectors. The section of GPR data from the shore also shows this sequence (Fig. 3b), and x-radiographs from four (of thirteen) cores highlight the correspondence among the multiple GPR reflectors and sandy deposits ("light"), associated with events 1-9 discussed earlier.

New Long Pond and Round Pond (Figs. 3b,c) are located close to one another in the same aquifer. Placed side by side, the sequence of reflectors from New Long Pond (Fig. 3b) corresponds in detail with those from Round Pond (Fig. 3c). Similarly, Flax Pond also shows the same sequence of closely-spaced reflectors above a uniformly opaque interval (Fig. 3d), even though this pond is located in a different aquifer and within morainal sediments. An additional GPR profile from Davis Pond (Fig. 3e) in western Massachusetts also shows similar reflectors above an opaque interval. The similar, finer scale variability among the reflectors at these ponds, associated with lake-level droughts events 1-9, shows a spatially coherent, replicable signal among basins, which record the same low-stand episodes despite differences in basin morphology and locations.

As a further test for this regional synchroniety, we compared the timing of the seven previously identified Holocene-age lowstand units (Units V-XI) as recorded in Davis Pond 20 with the grain-size data from New Long Pond 43 (Fig. 4). We find evidence for consistent timing among the fluctuations in water between these two cores.

From ca. 8.0-6.0 ka (Fig. 4; Event 5), the data from each pond show a prevailing high-stand interval containing some evidence of lower water levels (modest peaks in coarse fraction) between 7.6 and 7.2 ka. From 6.2-0.6 ka (events 1-9), we find similar evidence from Davis Pond 20 as that described from New Long Pond 43, in which multiple lowstands inferred from inorganic material interrupt organic-rich lacustrine silt. Unit VII at Davis Pond fits well with event 1, Unit VIII with events 2-4, Unit IX with event 5, Unit X with events 6 and 7, and Unit XI with events 8. The uppermost sediments associated with events 9 and 10 were not collected in Davis Pond 20.

Considering the different locations and sedimentary components analyzed at each site (coarse fraction vs. mineral), and the differences in the number, accuracy and precision of radiocarbon ages, the similar timing in these water level histories also affirms the broader-scale GPR-based evidence for regionally synchronous multiple droughts during the Holocene. We use the coarse grain fraction data from New Long Pond 43 as our regional proxy for drought in further comparisons because this record has many more radiocarbon dates than Davis Pond. The New Long Pond 43 data also has more radiocarbon dates than other cores from New Long Pond, and a full basin GPR profiles (the GPR signal was significantly attenuated at Davis Pond).

Deciphering the nature of drought

In Newby et al. (2009), we identified a relationship in New Long Pond 43 (Fig. 5; event 10) between the steady rise to peak values in percent coarse fraction and the

AD mid-20th century precipitation anomaly and the most severe drought on record in the AD 1960's (Newby et al., 2009). Here, we re-emphasize this relationship using three different series of Palmer Drought Severity Index (PDSI) data. PDSI is a measure derived using long-term differences between moisture supply (positive values) and demand (negative values) (originally by Palmer, 1965). From the same PDSI location in western Massachusetts, we use a tree-ring derived (summer; AD 481-2003) and an instrumental (summer; AD 1900-2003) PDSI series from Cook et al. (2004), and the closet (annual) PDSI data point in southern New England from the global compilation by Dai et al. (2004) (Fig. 5).

Each PDSI series contains values <0, indicating low moisture periods. Four intervals surpass -3 (severe drought) in the annual PDSI (Dai et al., 2004) at ca. AD 1930, 1950, 1965 and 1980, whereas the summer PDSI instrumental series (Cook et al., 2004) only exceeds -3 in conjunction with the AD 1960 drought. The annual PDSI series may capture seasonal variations in temperature and moisture compared to primarily evaporation and temperature trends during summer months.

The precipitation anomaly record from Amherst, Massachusetts shows the same negative AD 20th century anomaly (AD 1910-1950) as the precipitation data in Newby et al. (2009), here with departures consistently around -200 mm (Fig. 5). During the AD 1960's drought, the negative anomaly doubles to -400 mm, becomes positive until ca. AD 1980, and then returns to departures as low as -200 mm. The short record of river discharge from a branch of the Housatonic River, north of Davis

Pond in western Massachusetts (Fig. 1), reflects similar intervals with discharge below the mean as in the precipitation record. In particular, the lowest rates of discharge (1.5 m^3/sec) for this series also are during the AD 1960's drought.

The local, instrumental SST record (AD 1860 to 2007, off New England; 39-40ºN; 65-66ºW; HadSSTs) (Rayner et al., 2003) shows cool SST associated with the AD 1960's drought. Overall, the SST record shows a distinctive shift from cooler than average SST from AD 1870-1935 to warmer than average SST after ca. AD 1935. The SST during the mid AD 1960s are the coolest average SST in the historic record.

Changes in grain-size data from New Long Pond 43 also track these hydrologic variations (Fig. 5), and show a consistent trend among observational data and PDSI, which incorporates previous and current measures of moisture balance. A logical question arises: can iterative estimates from observational data, such as PDSI, simulate the climatic impact on lake processes we infer from sedimentary records? We applied a (non-centered) 20-yr window to the Dai et al. (2004) PDSI, assuming conditions are more influenced by the past than by the future. We then used a 20-yr window to determine the percent of months with PDSI >-3, e.g. what percent of the time within those 20 years was this area experiencing severe drought?
The results show a trend that closely mimics the changes in grain-size data: both rise during the AD 1910-1950 negative precipitation anomaly, and show two subsequent peaks in AD 1965 and 1980 (Fig. 5). This close correspondence suggests New Long Pond recorded the impact from multi-decadal climatic variability. Furthermore, it

supports our findings that the systematic accumulations of different fractions of sediment within lakes during the Holocene, as shown in the GPR and grain size data, indicate drought.

Discussion

We have shown evidence for regional coherency in hydroclimate across southern New England during the Holocene, using a combination of past lake-level reconstructions and GPR data. Our results indicate that during the Holocene, multiple and pervasive droughts, from 7.5-7.1 (in Newby et al., 2009), 6.2-5.5 ka (Event 1), 5.4-5.1 ka (Event 2), 5.0-4.9 ka (Event 3), 4.8-4.3 ka (Event 4), 4.1-3.6 ka (Event 5), 3.1-2.7 ka (Event 6), 2.5-1.8 ka (Event 7), 1.6-1.3 ka (Event 8), 1.2-0.6 ka (Event 9) and a 20th century event (10) took place across southern New England. In addition, these records reveal an increase in the drought frequency after 6.0 ka, from which we infer that paleohydrological conditions during this time were episodically drier than during the preceding 2000-yr interval.

The similarity among regional GPR profiles emphasizes robust, climate-driven responses, even though the lakes have differences in substrate, morphology and hydrology. Similar timing for four centennial-scale droughts (6.1, 4.2, 3.0 and 1.3 ka) from White Lake in New Jersey (Li et al., 2007) and hiatuses (6.1-4.4 ka) in Lake Albion in southern Quebec (Lavoie and Richard, 2000) and (6.0-ca. 4.0-3.0 ka) in

Rice Lake in Ontario (Yu and McAndrews, 1994) indicate that some of the droughts recorded in New England lakes may be more widespread.

We also find the agreement between the individual cores (New Long Pond 43 and Davis Pond D20) is striking, given differences in radiocarbon age control. Furthermore, individual cores cannot capture the full time range of any time-transgressive aspects of the changes in the lake level (i.e., a core nearer to shore might have a longer period of sand deposition than one that is off shore).

The sediment archive at New Long Pond appears to be sensitive to multi-decadal changes in moisture balance. The correspondence among the PDSI series, modern %CF, and local instrumental records reinforces our inference that New Long Pond was progressively preconditioned (anomalously low precipitation ca. AD 1910-1950 and the AD 1960 drought) by low water conditions, which increased the coarse fraction material in the sediments. Although the data from New Long Pond are relatively low resolution and represent a single modern analog, they provide some insights into the nature of past events. In particular, the %CF departures associated with all of the Holocene-age droughts occur over longer intervals (ca. 700-100 years) than the 20th century event (ca. 55 years; event 10), which may suggest the Holocene-age events had long-standing, severe episodes. Obviously there is still much to understand about deconstructing the sedimentary evidence for droughts into their constituent parts (e.g., how many consecutive years of severely limited moisture conditions, if any, are present in the events we have shown for the Holocene? Were any of these intervals persistently dry enough to be consequential for humans and biota?). We postulate that the cumulative impact from decades-long low precipitation lowers water levels and progrades shorelines, much like the modern analog we have described. Likewise, multiple years of interannual extremes in moisture balance, in which evaporation exceeded precipitation, could also produce a similar result. Furthermore, particular areas, years and seasons can be more appreciably or variously impacted from a range of moisture conditions, as was the case with the magnitude and timing of maximum low water conditions during the AD 1960's drought: from AD 1964-1966, the Plymouth-Carver aquifer received little to no recharge and this lowered groundwater 1.5-3.0 m and stream discharge by 50% (Hansen and Lapham, 1992), whereas, the Hudson River valley was already in extreme drought by AD 1964 (Andrews, 1965). As we have shown, however, such local differences during the Holocene were apparently not large enough to significantly blur the region-wide coherency archived in these GPR profiles and sedimentary records.

Drought forcing

Our goal is to relate broad-scale changes in the North Atlantic region with the timing for individual and collective trends among droughts during the Holocene. We recognize the limitations of such time-sensitive inferences due to the inherent variability associated with different proxies, age control, sampling resolution and locations. None the less, high resolution proxy data series and detailed, regional hydroclimatic records that span the Holocene, which show some potentially consistent timing at multiple time-scales, encourage this comparison (Bianchi and McCave, 1999; O'Brien et al., 1995; Alley, 2000; Oppo et al., 2003; Hall et al., 2004; Meeker and Mayewski, 2002; Keigwin et al., 2005; among others).

We infer that reduced MOC, and an expanded Polar vortex with high atmospheric transport (slow ice accumulation rates, high aerosol concentrations) characterize a cool, "active" North Atlantic region. In contrast, intervals when changes in MOC accompany mild North Atlantic conditions are characterized by fast ice accumulation rates and low aerosol concentrations.

We associate a cool North Atlantic region with:

Reduced MOC inferred from low values in $\delta^{13}C$ of the epifaunal benthic foram *Cibicidoides wuellerstorfi*; ODP core 980 (Oppo et al., 2003).

Positive ^{14}C anomalies in the residual ^{14}C, where anomalies indicate limited sequestration of ^{14}C in the deep ocean ((>MOC) (Reimer et al., 2004b).

GISP2 data which provide synchronous information about:

1. Regional climate: High concentrations of terrestrial-source potassium (K) and sea-salt (Na) aerosols indicate winter-like conditions, associated with an expanded polar vortex or enhanced MOC during the Holocene (O'Brien et al., 1995; Alley, 2000).

2. Local climate in Greenland: Cool temperatures are associated with slow ice accumulation rates (O'Brien et al., 1995; Alley, 2000).

The post-8.0 ka proxy climate data lack the coherent patterns evident in the high amplitudes of the data we associate with remnant glacial-like conditions from ca. 8.5-8.0 ka (Fig. 6). During the 500 years preceding 8.0 ka, the proxies align and collectively indicate cool North Atlantic conditions, consistent with the "8.2" event (Alley et al., 1997), in association with drought in southeastern New England (Newby et al., 2009) (Fig. 6).

Compared to this pre- 8.0 ka proxy convergence, the Holocene record is dominated by lower amplitude changes, associated with an increase in the frequency of drought after ca. 6.0 ka (Fig. 6). Based on the criteria described above, we find evidence for cool conditions during events 1-4 (6.2-4.3 ka) and event 6 (3.1-2.7 ka). Events 2-4 and 6 are also associated with reduced MOC. The LIA overlaps an interval (0.55 – 0.1 ka) with cool and wet conditions.

Event 1 is associated with a slow-down from modern rates in ice accumulation and the onset of an expanded polar vortex that continues through event 3 (Fig. 6). The associations among proxies during events 2-3 offer the most compelling evidence for reduced MOC and drought in the record. Events 2 and 8 may show linked, century-scale variability with progressively higher %CF, with concomitant fluctuations among sustained increases in K and Na concentrations and depleted $\delta^{13}C$. Oppo et al. (2003) suggest the minimum in $\delta^{13}C$ at ca. 5.0 ka (event 3) represents the most severe event in their record. Keigwin et al. (2005) find similar timing for declines in $\delta^{13}C$ in the Laurentian Fan. The overall low %CF during event 4 (4.8-4.3 ka) contrasts with the high values in events 2 and 3, and only the onset of event 4 is associated with depleted $\delta^{13}C$, and an increase in only marine-source aerosols (Na). The end of event 4 shows a slight depletion in $\delta^{13}C$ with minor increases in K and Na concentrations.

Event 6 (ca. 3.1-2.7 ka) also corresponds with an interval associated with an expanded polar vortex and reduced MOC that is also recorded in the Laurentian Fan region (Keigwin et al., 2005) and is especially evident in the $\delta^{13}C$ data from marine core NEAP4 (northwest of Oppo et al.'s ODP 980 core in the Feni Drift; Hall et al., 2004) (Fig. 6). Hence, this event may correspond with similar, widespread conditions across the North Atlantic region around the timing of event 6.

The LIA is associated with strengthening in the Iceland Low and Siberian High at ca. 550 cal yr B.P.(Meeker and Mayewski, 2002) (Figs. 6 and 7). The low %CF during the LIA (550-150 cal yr B.P.) indicates primarily high water levels during this time, while the slight increase in the variance of summer PDSI values (Cook et al., 2004) shows more negative than positive values. Our data agree with historical accounts, which indicate frequent extreme winters and cool summers accompanied the LIA (Baron, 1992 among others); such a climate regime is consistent with our finding high water levels if snowy, rather than dry winters were common (Shuman and Donnelly, 2006).

A range of varied responses is inferred for LIA conditions. Our data fit well with findings from Piermont Marsh, near New York City for moist (and cool) conditions, associated with a decrease in the abundance of charcoal, and slight increases in beech (*Fagus*), hemlock (*Tsuga*) and spruce (*Picea*) pollen abudance during the LIA (Pederson et al., 2005). In northward, westward, and upland areas of New England, pollen data are inferred to indicate variations in cool and/or dry conditions. Russell et al.'s (1993) regional analysis of pollen data indicates cooler conditions in northern versus southern New England during the LIA, but equivocal results for changes in moisture. Pollen-based summer temperature and annual precipitation reconstructions from laminated lake sediments in Maine and New York show a decrease in temperature and annual precipitation beginning at ca. 500-600 cal yr B.P. (Gajewski, 1998). Fuller et al. (1998) suggest that upland sites in northern central Massachusetts may show a shift to dry conditions from gradual declines in moisture-sensitive beech, hemlock and sugar maple (*Acer sacharum*) pollen abundance. These pollen data do not show increases in the abundance of taxa associated with cool conditions, such as spruce (*Picea*) pollen. Further south in the Chesapeake Bay estuary, wet conditions (associated with high precipitation) are inferred from 800-400 cal yr B.P.

The remaining events, 5 (4.1-3.6 ka) and 7-9, are associated with mild North Atlantic conditions, e.g. with little change in MOC or changes to consistently high K and Na concentrations (Fig. 6). Like preceding events 1-4, event 5 is also associated with slower-than-modern rates of ice accumulation; however, when compared to the mean rate for ice accumulation, events 2-7 and 9 each show good correspondence between drought and a rise in the rate for ice accumulation.

The later portion of Event 7 (2.5-1.8 ka) overlaps the initial timing of the RWP (ca. BC 200 – AD 400), between 2.1 and 1.8 ka. The 700-yr span of event 7 (2.5-1.8 ka) clearly overlaps a sustained rise above the mean for ice accumulation rates (Figs. 6 and 7). Two of three interim droughts during the event show little correspondence with episodes of strengthened Icelandic Low, but the third short-term event (2.0-1.8 ka) ends with an interval of heightened Icelandic Low and Siberian High.

Event 9 (1.2-0.6 ka) is associated with the MCA (Figs. 6 and 7). Ice accumulation rates rise during event 8, but peak afterwards, during event 9. None of the PDSI values associated with event 9 exceed –2 or +2, but shift mid-way from predominantly negative to positive values. In the western United States, PDSI values during the MCA range between -2 and 2, and are centered around a lower ("drier") mean (Herweijer et al., 2007).

Pollen-based climate reconstructions for the MCA show warmer (July) temperatures (1^{o} C) than modern, with little change in (annual) precipitation from lakes in Maine and New York (Gajewski, 1998). Multi-proxy evidence for drought is inferred from Piermont Marsh, near New York City, by an increase in erosion, more abundant charcoal and shifts to more warm-tolerant taxa (e.g. hickory (*Carya*) pollen) from moisture-sensitive taxa (e.g. like hemlock pollen) (Pederson et al., 2005). The MCA-age pollen data from both upland and lowland sites in north central Massachusetts do not indicate any shifts in forest composition, and more abundant charcoal at the lowland sites may be related to warm conditions or to human-related activities within the area (Fuller et al., 1998). Further south, studies in the Chesapeake Bay estuary indicate warm and dry conditions during the MCA (Brush, 2001; Cronin et al., 2003).

Midway through event 9, an interval with increased tropical Atlantic cyclones is inferred from the most positive tropical Atlantic SST anomaly (except for present), concurrent with the most negative NINO3 anomaly (Mann et al., 2009), and a strengthened Icelandic Low (Fig. 7). Modern and MCA droughts in the western United States are predominantly forced by similar climate conditions (La Niña-like conditions, warm subtropical North Atlantic SST, and a positive North Atlantic Oscillation (Mann et al., 2009; Herweijer et al., 2007, Seager et al., 2007)), raising the possibility for an Atlantic/Pacific SST role during the MCA in southeastern New England. An earlier connection between the Pacific region and southern New England drought is also possible, given the similar timing in Chazen et al.'s (2009) inferred upswing in ENSO-like atmosphere-ocean activity at ca. 6.0 ka from their high resolution record off the Peruvian coast and the onset of droughts in our record. However, a number of studies show no clear link between modern ENSO and New England climate (see review in Bradley et al., 2002).

The frequent droughts during the Holocene indicate more variability in regional climate than would be expected from the transition between the HTM and modern conditions, associated with the progressive decline in seasonal insolation contrast (Webb et al., 1993). What mechanisms, then, might account for their occurrence, particularly when we see evidence for concomitant cool conditions in the North

Atlantic region with some of the droughts (events 1-4, and 6) and with wet conditions (e.g. LIA) throughout the Holocene?

We speculate that maximum effect of insolation (after 9.0 ka in the Northeast) may have contributed to the early Holocene droughts (events 1-4) perhaps by more seasonal winters and summers before ca. 6.0 ka. It is tempting to infer that an overall decline in %CF after 7.0 ka leading to drought (event 1) may relate to enhanced warming, after which the cool North Atlantic conditions may have played a role, especially with events 2-3. Maximum insolation was not at 6.0 ka, but with the LIS gone, the onset of drought may have been the result of proximal forcing from insolation alone.

Land-ocean interactions with insolation may have also contributed to drought in southern New England during the mid-Holocene. Paleodata and coupled model simulations for 6.0 ka show far-reaching impacts from the monsoon system in the southwestern United States (Harrison et al., 2003). Enhanced monsoon conditions at 6.0 ka (compared to today) produced wet conditions in the southwestern United States and Mexico, and dry conditions in the Pacific Northwest and Great Plains (Harrison et al., 2003; Diffenbaugh et al., 2006).

Droughts re-initiate in the later part of the Holocene around 3.1 ka (event 6, 3.1-2.7 ka) after ca. 400 years of high water levels, and are likely associated with different forcing conditions. Although event 6 is strongly associated with cool conditions and intensified atmospheric circulation in the North Atlantic region, far less seasonal insolation is present compared to the early Holocene. Additionally, after 3.1 ka, droughts most clearly become associated with rises in ice accumulation rates that exceed both the mean and modern rate.

After 2.5 ka, the mean state for atmospheric circulation is less active, and there is little change in MOC until 0.55 ka (Meeker and Mayewski, 2002) (Fig. 6 and 7). The shifts in the GISP2 ice accumulation and aerosol data between the early and the later Holocene may indicate different source regions and increasingly regional environmental change (O'Brien et al., 1995). More proximal forcings may have produced droughts, e.g. cooler than average Atlantic Ocean SST, and enhanced equatorward transport of cold water in the Labrador Current in the shelf waters off the northeastern coast of the USA may have caused a rapid and large fishkill in AD 1882 (Marsh et al., 1999), concomitant with a drought in AD1879-83 (Kinnison, 1931). Forcings from further afield, however, are also indicated by the coincident timing for a prolonged drought during the MCA and cool La Niña conditions in the Pacific Ocean and increased storminess in the Atlantic Ocean.

Conclusion

We conclude with a synopsis of our key findings.

1. Coherent sub-millennial-to-centennial scale hydrologic variations are present in the Holocene-age sedimentary records of lakes and ponds in southern New England.

2. At least ten multi-centennial-to-centennial scale droughts are recorded between 8.0 to 0.5 ka, with an increase in frequency after 6.0 ka.
3. Humid regions, like southern New England, are more prone to drought than expected, based on the historic record.
4. While multiple mechanisms appear to force droughts, hydroclimate in southern New England appears sensitive to or to co-vary with changes in the North Atlantic region.
5. Droughts during the mid-Holocene (after 6.0 ka) appear to be proximally forced by prolonged cool conditions in the North Atlantic region, but seasonal insolation and ENSO-like activity in the Pacific region cannot be discounted. Pronounced aridity during the mid-Holocene from the west may also have generated a more continental climate (dry air) versus maritime climate (moist air) in southern New England.
6. Droughts during the later Holocene (after 2.5 ka) may have been caused by more proximal forcings, and by interactions among the atmosphere, the Atlantic Ocean and the Pacific Ocean.
8. Droughts during the last 2500 years may be related to warmth, e.g. a 300-year drought associated with the Roman Warm Period, and a 500-year drought associated with the Medieval Climate Anomaly. Furthermore, warming since ca. AD 1910 indicates drought is possible with an increase in temperature. The Medieval Climate Anomaly drought overlaps a brief 100-yr interval of cool La Niña-like conditions in the Pacific Ocean and warm SST in the Atlantic Ocean; conversely, the LIA is associated with slightly cooler tropical Atlantic SST, less La Niña-like Pacific conditions and wet conditions in southern New England.

Acknowledgments

The National Science Foundation (NSF-ESH 0602408 to Shuman and Donnelly) and the Woods Hole Oceanographic Institution, Ocean and Climate Change Institute (to Donnelly) funded this research. Many people contributed to the laboratory and field work of this project: K. Boldt, Z. Fjeldheim, M. Gomes, Z. Klaus, D. MacDonald, R. Sorell. I thank L. Carlson at Brown University for GIS work.

References

Alley, R.B., Mayewski, P.A., Sowers, T., Stuiver, M., Taylor, K.C., and Clark, P.U. (1997). Holocene climatic instability: A prominent, widespread event 8200 yr ago. Geology 25, 483-486.

Alley, R.B., 2000. The Younger Dryas cold interval as viewed from central Greenland. Quaternary Science Reviews 19, 213-226.

Barlow, M., Nigam, S., Berbery, E.H., 2001. ENSO, Pacific Decadal Variability, and U.S. Summertime Precipitation, Drought, and Stream. Journal of Climate 14, 2105-2128.

Bianchi, G. G., McCave, N., 1999. Holocene periodicity in North Atlantic climate and deep-ocean flow south of Iceland. Nature 397, 515-517.

Bradbury , J.A., Keim, B.D., Wake, C.P., 2002. U.S. East Coast Trough Indices at 500 hPa and New England Winter Climate Variability. Journal of Climate 15(23), 3509-3517.

Chazen, C.R., Altabet, M.A., Herbert, T.D., 2009. Abrupt mid-Holocene onset of centennial-scale climate variability. Geophysical Research Letters 36, 1-5.

Cook, E.R., Woodhouse, C.A., Eakin, C.M., Meko, D.M., Stahle, D.W., 2004a. Long-Term Aridity Changes in the Western United States. Science 306(5698), 1015-1018.

Cook, E.R., Woodhouse, C.A., Easkin, C.M., Meko, D.M., Stahle, D.W., 2004b. IGBP PAGES/World Data Center for Paleoclimatology, Data Contribution Series #2004-045. NOAA/NGDC Paleoclimatology Program, Boulder, CO.

Dai, A., Trenberth, K.E., Qian, T., 2004a. A global data set of Palmer Drought Severity Index for 1870-2002: Relationship with soil moisture and effects of surface warming. Journal of Hydrometeorology 5, 1117-1130.

Dai, A., 2004b. Palmer Drought Severity Index data provided by the NOAA/ OAR/ESRL PSD, Boulder, Colorado, USA, from their Web site at http://www.esrl.noaa.gov/psd/

Dale, T.N., 1923. The Lime Belt of Massachusetts and Parts of Eastern New York and Western Connecticut. United States Geological Survey, Bulletin 744, Washington DC, 71 pp.

Dawson, A., Elliot, L., Noone, S., Hickey, K., Holt, T., Wadhams, P., Foster, I., 2004. Historical storminess and climate 'see-saws' in the North Atlantic region. Marine Geology 210, 247-259.

Diffenbaugh, N.S., Ashfaq, M., Shuman, B., Williams, J.W., and Bartlein, P.J., 2006. Summer aridity in the United States: Response to mid-Holocene changes in insolation and sea surface temperature. Geophysical Research Letters 33**,** L22712.

Digerfeldt, G., 1986. Studies on past lake-level fluctuations. In: Berglund, B.E. (Ed.), Handbook of Holocene Palaeoecology and Palaeohydrology. John Wiley and Sons, Chichester, UK, pp. 127–142.

Easterling, D.R., Karl, T.R., Lawrimore, J.H., Del Greco, S.A., 1999. United States Historical Climatology Network Daily Temperature, Precipitation, and Snow Data for 1871-1997. ORNL/CDIAC-118, NDP-070. Carbon Dioxide Information Analysis Center, Oak Ridge National Laboratory, U.S. Department of Energy, Oak Ridge, Tennessee.

Hansen, B.P., Lapham, W.W., 1992. Geohydrology and Simulated Groundwater Flow, Plymouth–Carver aquifer, Southeastern Massachusetts. United States Geological Survey Water Resources Investigation Report 90-4204, Marlborough, MA.

Harrison, S.P., Kutzbach, J.E., Liu, Z., Bartlein,P.J., Otto-Bleisner, B., Muhs, D., Prentice, I.C., Thompson, R.S., 2003. Mid-Holocene climates of the Americas: A dynamical response to changed seasonality. Climate Dynamics 20, 663-688.

Hayhoe, K., Wake, C.P., Huntington, T.G., Luo, L., Schwartz, M.D., Sheffield, J., Wood, E., Anderson, B., Bradbury, J., DeGaetano, A., Troy, T.J., Wolfe, D., 2007. Past and future changes in climate and hydrological indicators in the US Northeast. Climate Dynamics 28, 381-407.

Herweijer, C., Seager, R., Cook, E.R., 2006. North American droughts of the mid to late nineteenth century: a history, simulation and implication for Mediaeval drought. The Holocene 16(2), 159-171.

Herweijer, C., Seager, R., Cook, E.R., Emile-Geay, J., 2007. North American Droughts of the Last Millennium from a Gridded Network of Tree-Ring Data. Journal of Climate 20, 1353-1376.

Hurrell, J.W., Deser, C., 2009. North Atlantic climate variability: The role of the North Atlantic Oscillation. Journal of Marine Systems 78, 28-41.

Jansson, K.N., Kleman, J., 2004. Early Holocene glacial lake meltwater injections into the Labrador Sea and Ungava Bay. Paleoceanography 19, 1-12.

Keigwin, L.D., Sachs, J.P., Rosenthal, Y., Boyle, E.A., 2005. The 8200 year B.P. event in the slope water system, western subpolar North Atlantic. Paleoceanography 20, 1–14.

Kinnison, H.B.,1931. The 1929-1930 Drought in New England. Journal of New England Water Works Association 45**,** 145-163.

Larson, G.J., 1982. Nonsynchronous Retreat of Ice Lobes from Southeastern Massachusetts. In: Late Wisconsin Glaciation of New England, Larson, G.J., Stone, B.D., (Eds.), Kendall Hunt Publishing Co., Dubuque, Iowa, pp. 101–114.

Lavoie, M., Richard, P.J.H., 2000. Postglacial water-level changes of a small lake in southern Quebec, Canada. The Holocene 10, 621– 634.

Leathers, D., Grundstein, A.J., Ellis, A.W., 2000. Growing season moisture deficits across the northeastern United States. Climate Research 14, 43-55.

Li, Y.-X., Yu, Z., and Kodama, K.P., 2007. Sensitive moisture response to Holocene millennial-scale climate variations in the Mid-Atlantic region, USA. The Holocene 17, 3-8.

Mann, M.E., Woodruff, J.D., Donnelly, J.P., Zhang, Z., 2009. Atlantic hurricanes and climate over the past 1,500 years. Nature 460(13), 880-885.

Marsh, R., Petrie, B., Weidman, C.R., Dickson, R.R., Loder, J.W., Hannah, C.G., Frank, K., Drinkwater, K., 1999. The 1882 tilefish kill – a cold event in shelf waters off the north-eastern United States? Fisheries Oceanography 8(1), 39-49.

Masterson, J.P., Walter, D.A., 2009. Hydrogeology and Groundwater Resources of the Coastal Aquifers of Southeastern Massachusetts. United States Geological Survey Circular 1338, Reston, VA. 16 p.

Mayewski, P.A., Rohling, E.E., Stager, J.C., Karlen, W., Maasch, K.A., Meeker, L.D., Meyerson, E.A., Francoise, G., van Kreveld, S., Holmgren, K., Lee-Thorp, J., Rosqvist, G., Rack, F., Staubwasser, M., Schneider, R.R., Steig, E.J., 2004. Holocene climate variability. Quarternary Research 62, 243-255.

McCabe, G.J., Palecki, M.A., Betancourt, J.L., 2004. Pacific and Atlantic Ocean influences on multidecadal drought frequency in the United States. Proceedings of the National Academy of Sciences 101(12), 4136-4141.

McCabe, G.J., Betancourt, J.L., Gray, S.T., Palecki, M.A., Hidalgo, H.G., 2008. Associations of multi-decadal sea-surface temperature variability with US drought. Quaternary Interntional 188, 31-40.

Meeker, L.D., Mayewski, P.A., 2002. A 1400-year high-resolution record of atmospheric circulation over the North Atlantic and Asia. The Holocene 12, 257 - 266.

Moberg, A., Sonechkin, D.M., Holmgren, K., Datsenko, N.M., Karlen, W., 2005. Highly variable Northern Hemisphere temperatures reconstructed from low- and high-resolution proxy data. Nature 433, 613-617.

Newby, P.E., Donnelly, J.P., Shuman, B.N., and MacDonald, D., 2009. Evidence of centennial-scale drought from southeastern Massachusetts during the Pleistocene/Holocene transition. Quaternary Science Reviews 28**,** 1675-1692.

Nigam, S., Barlow, M., Bery, E.H., 1999. Analysis Links Pacific Decadal Variability to Drought and Streamflow in United States. EOS 80(51), 1-8.

Norvitch, R.F., and Lamb, M.E.S., 1966. Housatonic River Basin, United States Geological Survey Massachusetts Basic-Data Report 9, Ground-Water Series, Washington D. C., 40 pp.

O'Brien, S.R., Mayewski, P.A., Meeker, L.D., Meese, M.S., Twickler, M.S., Whitlow, S.I., 1995. Complexity of Holocene Climate as Reconstructed from a Greenland Ice core. Science 270, 1962-1964.

Oldale, R.N., Barlow, R.A. 1986. Geologic Map of Cape Cod and the Islands, Massachusetts. Miscellaneous Investigations Series, Map I-1763. U.S. Geological Survey, Reston, Virginia.

Oppo, D.W., McManus, J.F., Cullen, J.L., 2003. Deepwater variability in the Holocene epoch. Nature 423, 277-278.

Pederson, D.C., Peteet, D.M., Kurdyla, D., Guilderson, T., 2005. Medieval Warming, Little Ice Age, and European impact on the environment during the last millennium in the lower Hudson Valley, New York, USA. Quaternary Research 63, 238-249.

Rayner, N.A., Parker, D.E., Horton, E.B., Folland, C.K., Alexander, L.V., Rowell, D.P., Kent, E.C., Kaplan, A., 2003. Global analyses of sea surface temperature, sea ice and night marine air temperature since the late nineteenth century. Journal of Geophysical Research 108, D14, 1–37.

Reimer, P.J. (others), 2004. IntCal04 Atmospheric radiocarbon age calibration, 26-0 ka BP, Radiocarbon 46, 1026-1058

Reimer, P.J., Baillie, M.G.L., Bard, E., Baylis, A., Beck, J.W., Bertrand, C.J.H., Blackwell, P.G., Buck, C.E., Burr, G.S., Cutler, K.B., Damon, P.E., Edwards, R.L., Fairbanks, R.G., Friedrich, M., Guilderson, T.P., Hogg, A.G., Hughen, K.A., Kromer, B., 2004. IntCal04 terrestrial radiocarbon age calibration, 0–26 cal kyr BP. Radiocarbon 46, 1029–1058.

Russell, W.B., Davis, R.B., Anderson, R.S., Rhodes, T.E., Anderson, D.S., 1993. Recent Centuries of vegetational change in the glaciated north-eastern United States. Journal of Ecology 81, 647-664.

Shuman, B., Bartlein, P., Logar, N., Newby, P., Webb III, T., 2002. Parallel Climate and Vegetation Responses to the Early-Holocene Collapse of the Laurentide Ice-Sheet. Quaternary Science Reviews 21, 1793–1805.

Shuman, B., Bravo, J., Kaye, J., Lynch, J.A., Newby, P., Webb III, T., 2001. Late-Quaternary Water-Level Variations and Vegetation History at Crooked Pond, Southeastern Massachusetts. Quaternary Research 56, 401–410.

Shuman, B., Donnelly, J.P., 2006. The influence of seasonal precipitation and temperature regimes on lake levels in the northeastern United States during the Holocene. Quaternary Research 65, 44-56.

Shuman, B.N., Newby, P.E., and Donnelly, J.P., 2009. Abrupt climate change as an important agent of ecological change in the Northeast U.S. throughout the past 15,000 years. Quaternary Science Reviews 28, 1693-1709.

Wandle Jr., W.S., 1991. Massachusetts Floods and Droughts. In: Paulson, R.W., Chase, E.B., Roberts, R.S., Moody, D.W. National Water Summary 1988-1989:

hydrologic events and floods and droughts. U.S. Geological Survey Water-Supply Paper 2375, pp. 327–334.

Webb III, T., Bartlein, P.J., Harrison, S., Anderson, K.H., 1993. Vegetation, lake level, and climate change in eastern North America. In: Wright Jr., H.E., Kutzbach, J.E., Webb III, T., Ruddiman, W.F., Street-Perrott, A., Bartlein, P.J. (Eds.), Global Climates since the Last Glacial Maximum. University of Minnesota Press, Minneapolis, MN.

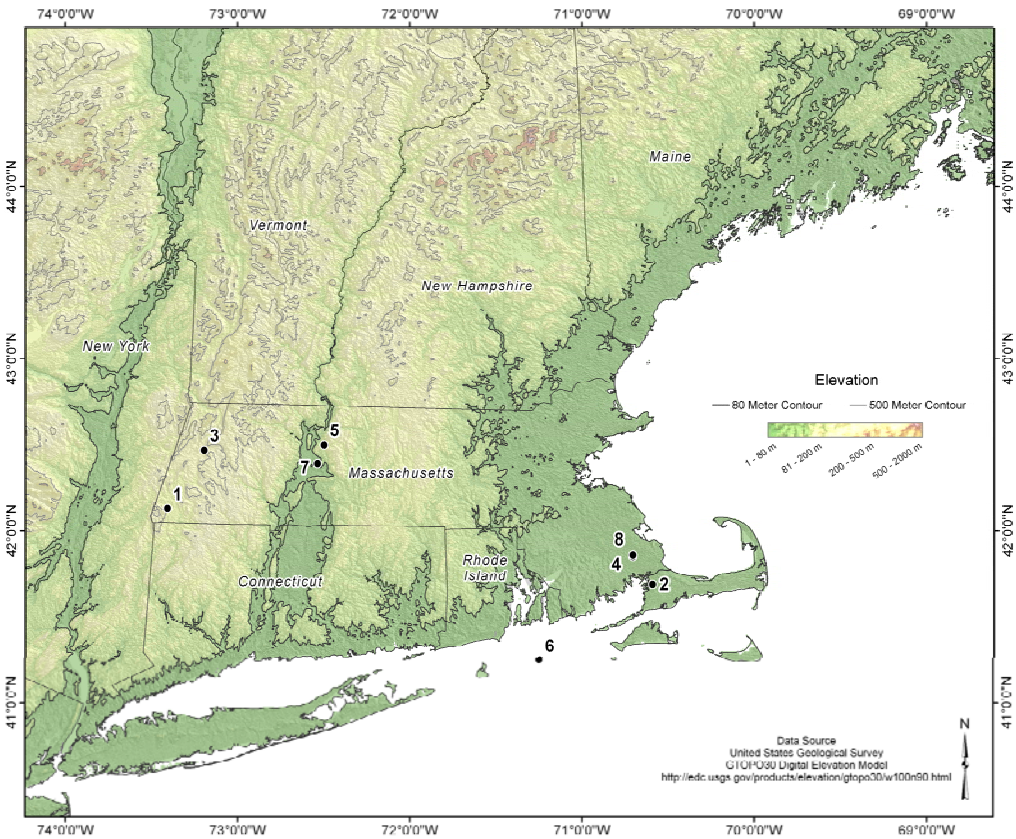

Figure 4-1. Sites and locations of data series referred to in text: 1-Davis Pond; 2-Flax Pond, 3-USGS 01197000, East Branch Housatonic River, Coltsville, Massachusetts, drainage area 149.18 km^2, 302.8 m asl (NCVD29); 4-New Long Pond; 5-Gridpoint 267 from the North American Summer PDSI Reconstructions, actual PDSI from AD 1900-2003, reconstructed PDSI AD 481-2003, (Cook et al., 2004a, b); 6-PDSI gridpoint from global grid 75.0N-60.0 S, 1.25E-358.75 E (2.5^o x 2.5^o; Dai et al., 2004a,b); 7-Datapoint 190120, 45.7 m asl, Amherst, Masschusetts, precipitation data from United States Historical Climatology Network, (Easterling et al., 1999), http://cdiac.ornl.gov/epubs/ndp/ushcn/ushcn.html; 8-Round Pond.

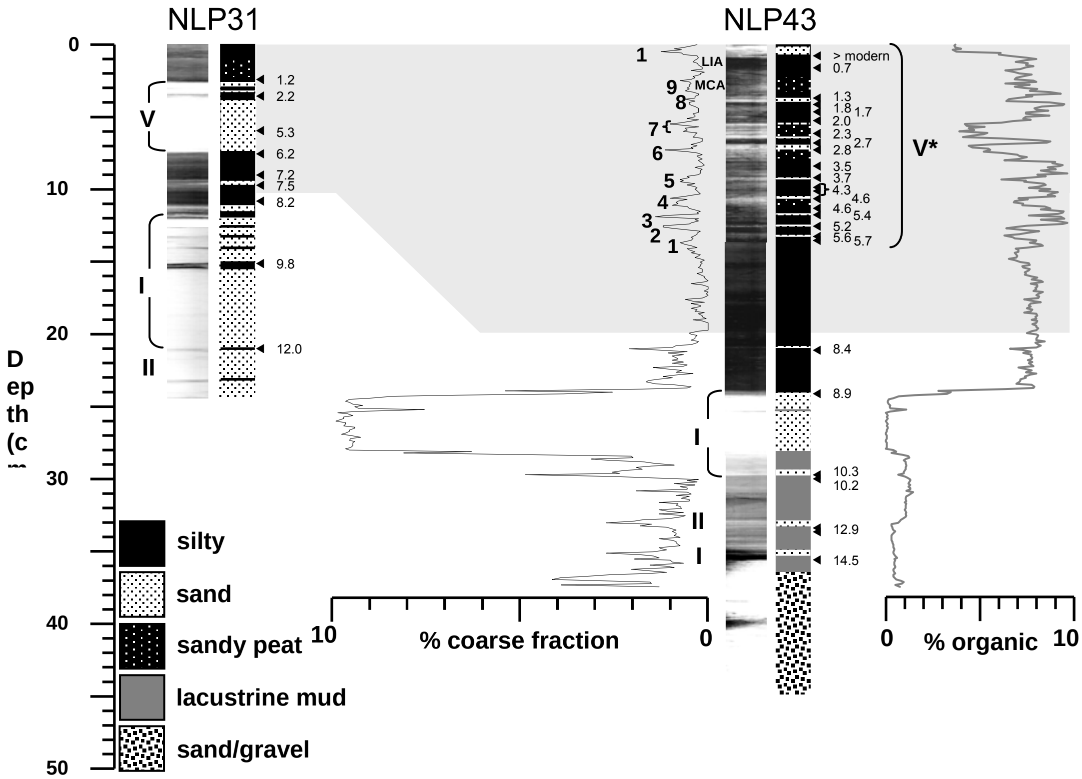

Figure 4-2. Radiographs with calibrated median radiocarbon ages for NLP31 and NLP43. Percent coarse fraction and percent organic matter (1/2 scale of %CF) are from NLP43. The Holocene-age droughts are numbered 1-10 and the interval from 8.0 ka to present is shaded (gray); *V is the unit for this packet of sediments in Newby et al. (2009).

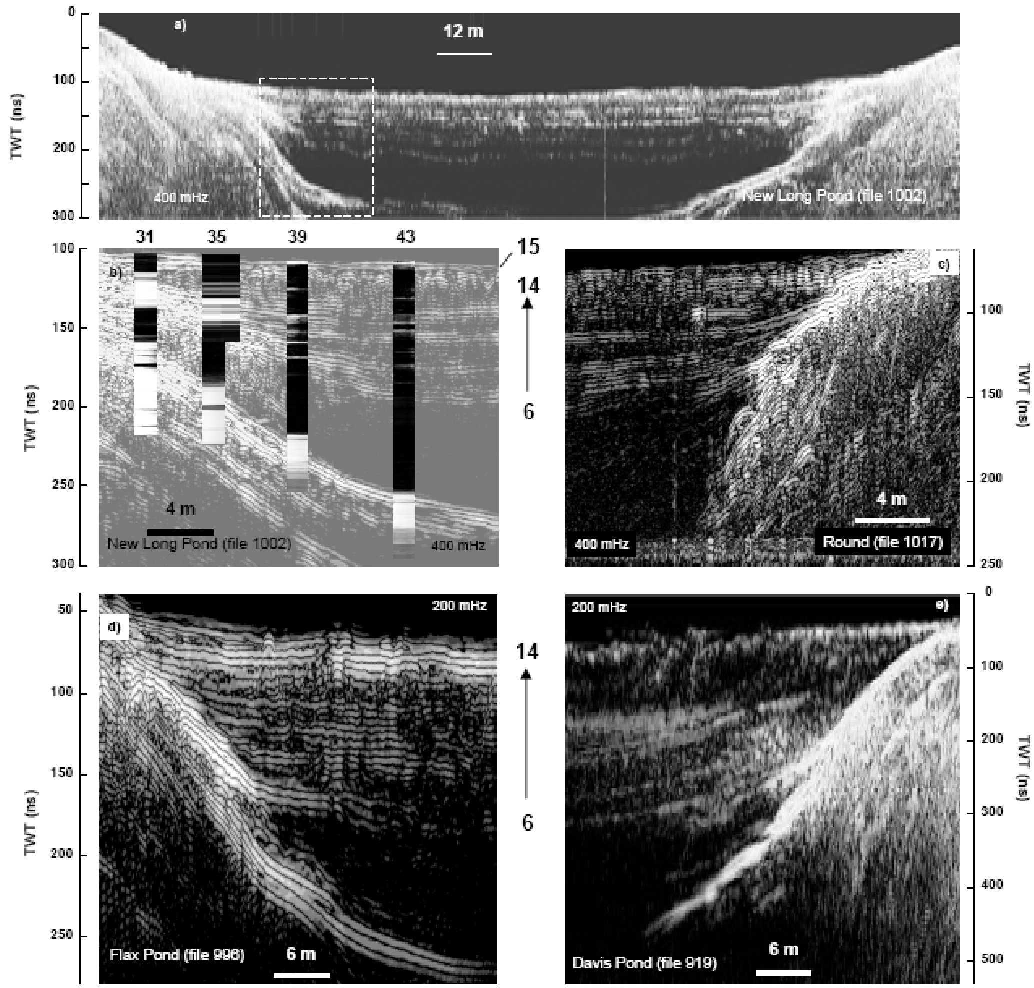

Figure 4-3. a. Ground penetrating radar profile from west shore to east shore across New Long Pond, MA. Below the sediment-water interface, multiple, closely-spaced bright reflectors extend laterally across the pond; these correspond to layers with low percent organic and sand. The image in b is enlarged from the white box on the profile. b. Radiographs from four of thirteen cores collected from the pond; numbers above cores indicate the distance in meters from the shore. NLP31 and NLP 43 are also shown in Fig. 2 with median radiocarbon ages. The contrast between the bright reflectors in the uppermost portion of the GPR profile and the dark area below distinguishes the Holocene-age sequence (events 6-15) of droughts described in this paper from the

interval below, when water levels were higher. c-e. Three additional GPR profiles from Round Pond, Flax Pond, and Davis Pond illustrate the most shoreward portion of each basin, and reveal a similar stratigraphy to that recorded in New Long Pond.

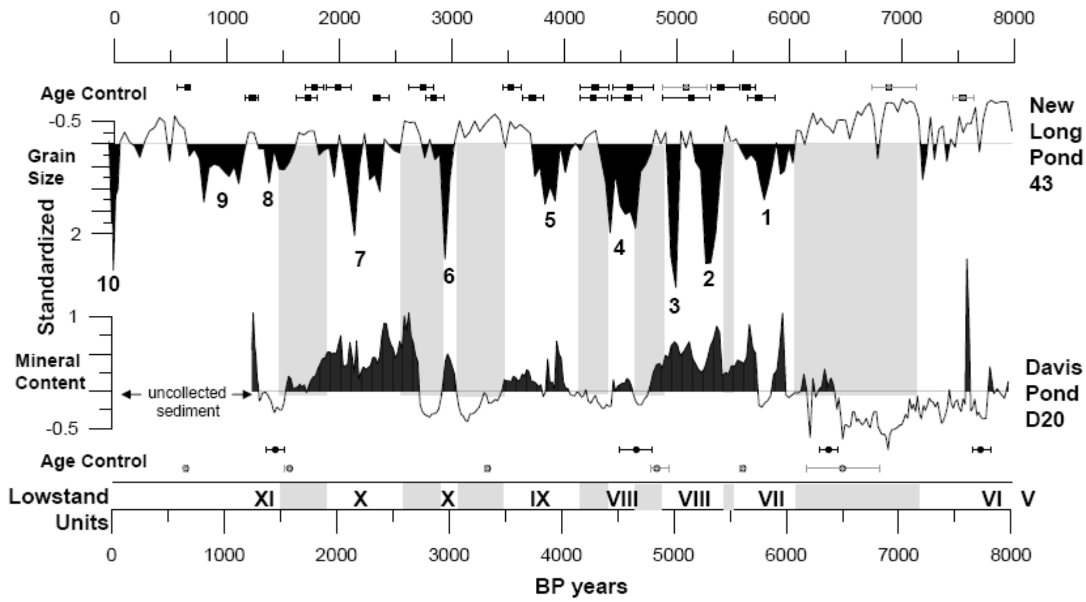

Figure 4-4. Timing of changes (BP years) in the standardized coarse fraction from New Long Pond 43 and the standardized mineral content from Davis Pond D20; drought events 1-10 are described in the text. Positive values (black) represent intervals with high coarse fraction or mineral content, and are plotted facing each other; shaded (gray) bars indicate coincident intervals of high water levels at each basin. Lowstand Units V-XI are from Davis Pond (Newby et al., in review). Age controls show highest and lowest age range, as well as median age, from calibrated AMS radiocarbon dates used in age model: New Long Pond 43 (black squares) and Davis Pond D20 (black circles). Other ages are from cores that show additional age control used in the multi-core lake-level reconstruction: New Long Pond 43 (gray squares) and Davis Pond D20 (gray circles).

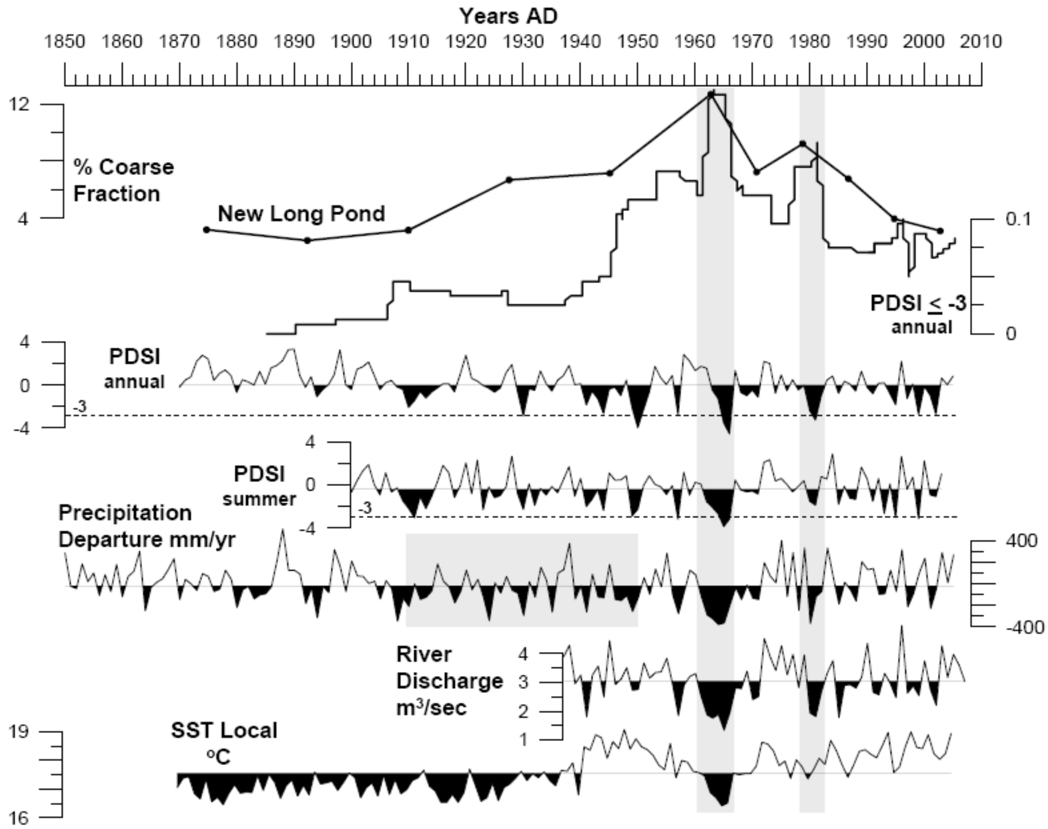

Figure 4-5. New Long Pond %CF with historic data (AD 1850-present) showing mid-20th century precipitation departure (horizontal gray-shaded area) and most recent droughts in AD1960 and 1980 (vertical gray-shaded areas) in association with regional datasets described here: from AD 1850 to present, we use instrumental records of precipitation (Amherst, MA 42° 23' 24"N, 72° 32' 24"W; Karl et al., 1990), streamflow (42° 28' 10"N, 73° 11' 49"W; USGS, 2110), sea surface temperatures (AD 1860 to 2007) off New England (39-40ºN; 65-66ºW; HadSSTs from Rayner et al., 2003), and three measures of PDSI (Cook et al., 2004; Dai et al., 2004). PDSI is a measure derived using long-term differences between moisture supply (positive values) and demand (originally by Palmer, 1965)(negative values). We selected the closest PDSI data point in southern New England (Fig. 1; 41º 15'N; 71º 15'W) from the global compilation by Dai et al.

(2004); Dai Palmer Drought Severity Index data provided by the NOAA/ OAR/ESRL PSD, Boulder, Colorado, USA, from their Web site at http://www.esrl.noaa.gov/psd/. A tree-ring derived PDSI series (AD 481-2003 and instrumental PDSI (AD 1900-2003) series are from the same site (#267, 42.5N, 72.5W) in western Massachusetts (Cook et al., 2004).

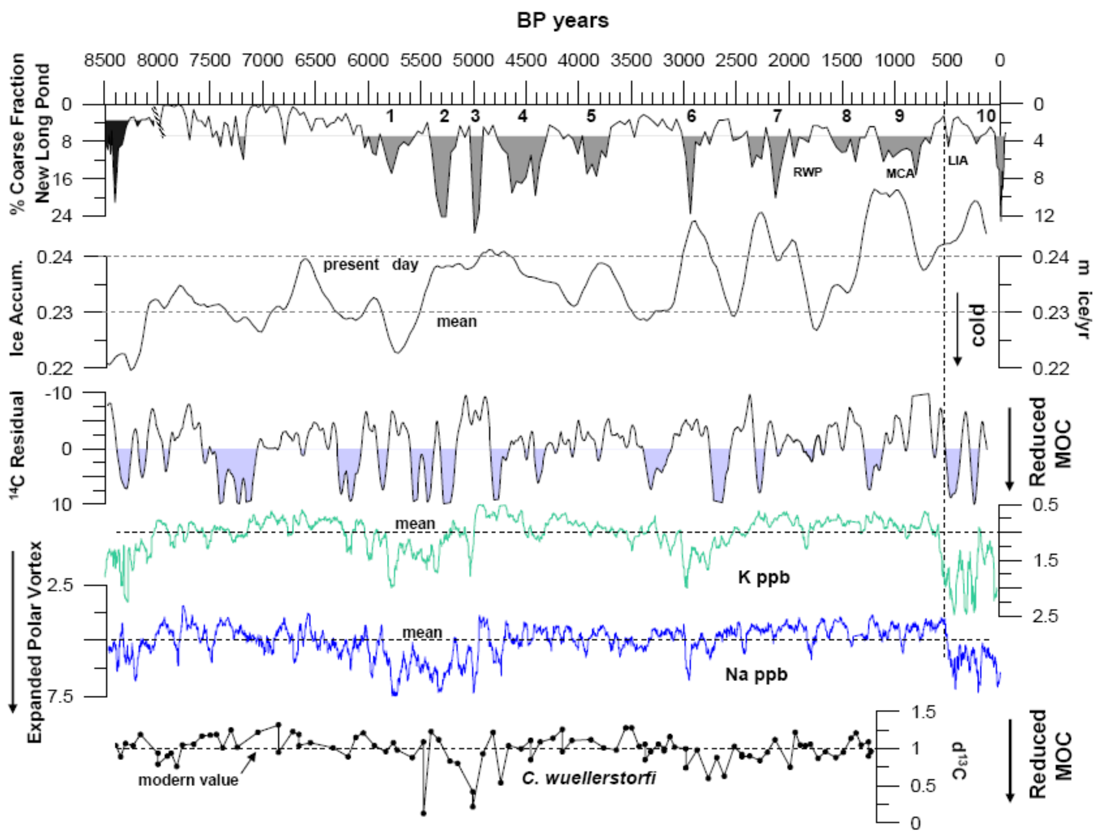

Figure 4-6. New Long Pond %CF and data proxies from 8.0 ka to present. Data from 8.5-8.0 ka have a different scale, and are included to show the contrast between pre-8.0 ka and post-8.0 ka conditions Vertical dashed line shows transition between the Medieval Climate Anomaly (MCA) and Little Ice Age (LIA) at ca. 0.55 ka (also shown in Figure 7). RWP is Roman Warm Period. For the Holocene interval, we selected high resolution (sampling, radiocarbon dates, high sediment accumulation rates) data series using proxies responsive to changes in conditions in the North Atlantic region. Two proxies for changes in MOC include residual ^{14}C anomaly data (Reimer et al., 2004b), in which low ^{14}C anomalies indicate limited sequestration of ^{14}C in the deep ocean (>MOC), and changes in the abundance of the $\delta^{13}C$ epifaunal benthic foram *Cibicidoides wuellerstorfi* from ODP core 980, in the Feni Drift of northeastern Atlantic Ocean (ca. 25 cm/yr

sediment accumulation rate; Oppo et al., 2003). Changes in the abundance $\delta^{13}C$ are a proxy for nutrient content and deep sea ventilation, with high values associated with nutrient-rich southern source water (>MOC) and low values associated with nutrient-depleted (<MOC) water. Values $<0.5^{o}/_{oo}$ $\delta^{13}O$ indicate significantly decreased MOC production in the Holocene (Keigwin et al., 2005). Proxies from GISP2 provide synchronous information about local climate in Greenland, in which cool temperatures are associated with slow ice accumulation rates, and regional climate, in which high concentrations of terrestrial-source potassium (K) and sea-salt (Na) aerosols are indicative of winter-like conditions, associated with an expanded polar vortex or enhanced meridional circulation during the Holocene (ca. 2.4 yr/sample; O'Brien et al., 1995; Alley, 2000). As a basis of comparison, rates for ice accumulation doubled (from 0.07 $\pm$ 0.01 to 0.14 $\pm$ 0.02) at the end of the Younger Dryas; modern accumulation rates are 0.24 m ice/yr (Alley, 2000).

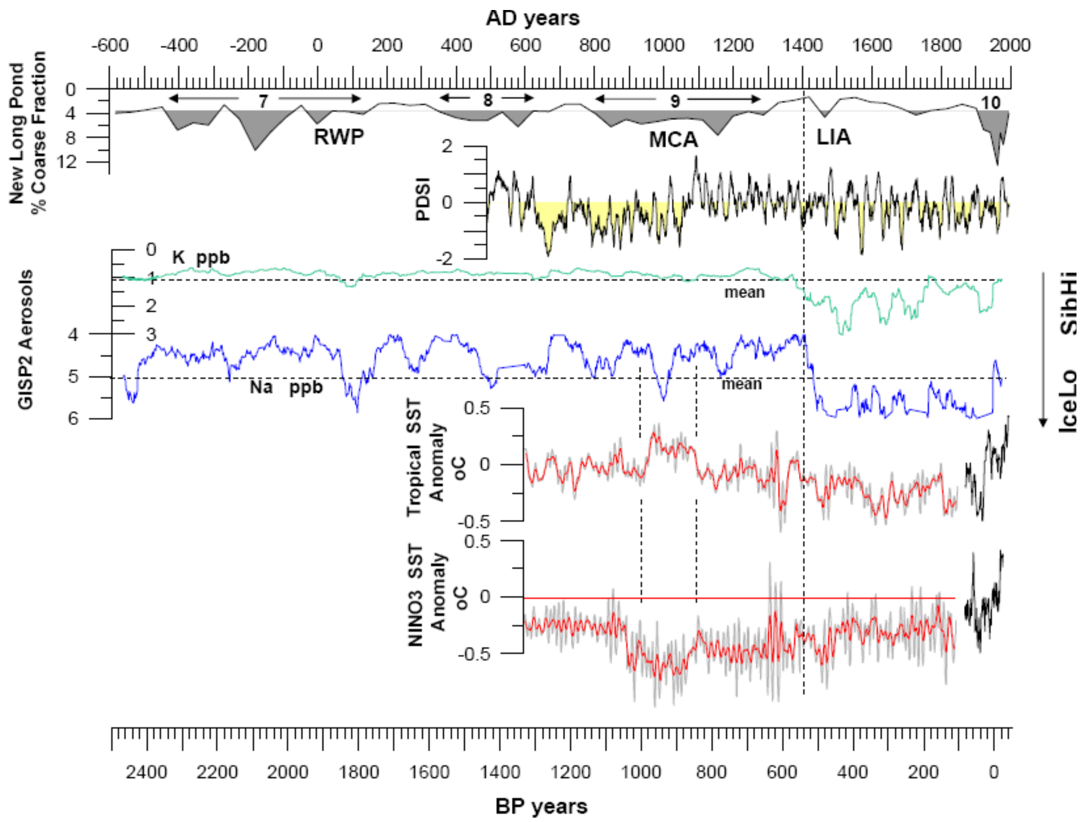

Figure 4-7. New Long Pond %CF and data proxies between 2.5 to –0.5 ka (BC 600 to AD 2000). Vertical dashed line shows transition between the Medieval Climate Anomaly (MCA) and Little Ice Age (LIA) at ca. 0.55 ka. Shorter dashed lines delineate 100-year interval during MCA with enhanced Icelandic Low, positive Tropical Atlantic SST anomaly and NINO3 SST anomaly. RWP is Roman Warm Period. For the historic interval, climate inferences are enhanced for GISP2 K and Na series by the addition of observational data for sea-level pressure and SST (AD 1879-1987), which correlate intensified winter circulation (deepening Icelandic Low) in the North Atlantic region with high concentrations of Na and spring strengthening of the Siberian High with high concentrations of K (Meeker and Mayewski, 2002). A central Asian source for wind-transported K is postulated for this time (see Meeker and Mayewski, 2002). We use

Meeker and Mayewski's (2002) inferences to interpret the interval from 2.5-1.0 ka. For this same interval, we also compare the Mann et al. (2009) time series for tropical SST and NINO3 (El Niño Southern Oscillation, ENSO), reconstructed using calibrations from instrumental data, 10^{o}-$14\,^{o}$N, $20\,^{o}$-$70\,^{o}$W.